UNIVERSIDAD COMPLUTENSE DE MADRID

FACULTAD DE PSICOLOGÍA

TESIS DOCTORAL

Caracterización del funcionamiento cerebral, su estructura y la cognición asociados al daño cerebrovascular en el envejecimiento

Characterization of brain functioning, structure and cognition associated to cerebrovascular damage in aging.

MEMORIA PARA OPTAR AL GRADO DE DOCTORA

PRESENTADA POR

Lucía Torres Simón

DIRECTORES

Fernando Maestú Unturbe
Pablo Cuesta Prieto

Universidad Complutense de Madrid
Facultad de Psicología
Programa de Doctorado en Psicología

Tesis Doctoral

Caracterización del funcionamiento cerebral, su estructura y la cognición asociados al daño cerebrovascular en el envejecimiento

Characterization of brain functioning, structure and cognition associated to cerebrovascular damage in aging.

Memoria para optar al grado de Doctora
presentada por:
Lucía Torres Simón

Directores:
Dr. Fernando Maestú Unturbe
Dr. Pablo Cuesta Prieto

2023

La sonrisa es lo último que se pierde…

Agradecimientos

En primer lugar, me gustaría resaltar la importancia de estos agradecimientos para mí. Me ha costado casi más escribir estas líneas que terminar la tesis. Me ha resultado muy complicado escribir esto porque no sabía cómo empezar a expresar lo que siento. Los años que han trascurrido desde que empecé la tesis han sido probablemente los más duros de mi vida y ojalá hubiera sido solo por el estrés que conlleva superar esta etapa académica. Los últimos años a nivel personal han incluido mudanzas, reformas, pandemias mundiales, enfermedades, fallecimientos y mucha incertidumbre y desesperanza a nivel personal. Desde este contexto es desde donde realmente me nace agradecer profundamente la compañía y apoyo incondicional de todas las personas que habéis hecho no solo que siguiera para delante, si no que haya sido capaz de hacerlo con una sonrisa en muchos momentos, y acompañando mis lágrimas en otros.

Gracias, papá, mamá y Amaro por enseñarme que tener un equipo incondicional, donde poder caerte y sentirte segura, te hace poder con cualquier cosa. Gracias a ese soporte me he sentido fuerte para terminar proyectos como la tesis e incluso empezar otros nuevos sin miedo y con ilusión.

Gracias prima María porque tu año en Madrid acompañándome es una de estas cosas que la vida organiza a nuestras espaldas haciendo parecer que lo elegíamos nosotras. Menos mal que lo hizo porque tenerte tan cerca en esos momentos hizo que no hubiera un día sin una sonrisa o un abrazo. "*La sonrisa es lo último que se pierde".*

Gracias a todos los compañeros y compañeras del laboratorio. Habéis sido mi principal apoyo social en muchos momentos. Nunca habéis hecho preguntas, simplemente habéis estado ahí para acompañarme, echarme una mano o provocar que me riera a carcajadas incluso cuando lo único que era capaz de hacer era pasarme un ratillo a medio día a comer con vosotros. Gracias a ese apoyo, cariño y compañerismo no he tirado la toalla con este proyecto, nunca dejasteis que la esperanza se fuera del todo. Muchas gracias de todo corazón.

Gracias Pablo y Bruña, por formar parte de mi vida, es tanto lo que me gustaría agradeceros que probablemente sea más fácil demostrároslo el resto de la vida.

Gracias Fernando por ese apoyo, confianza y libertad absolutos. Creo que no hubiera sido capaz de terminar la tesis sin la comprensión que me has mostrado siempre. Me has protegido y generado el espacio que necesitaba como persona para hacerme crecer como profesional. Mil gracias por confiar en mí.

Finally, I would like to thank Rik Henson for welcoming me with open arms in Cambridge, literally in his office, in the middle of the pandemic with all the mobility restrictions and regulations. Thank you for such a warm welcome to your team both personally and professionally. You are a wonderful group.

Gracias a todos por formar parte de mi vida y gracias a los que ya no están, pero me han ayudado a ser quien soy ahora.

CONTENTS

Glossary of terminology

A

AAL: Automated anatomical labeling atlas (Tzourio-Mazoyer et al., 2002)
AD: Alzheimer's Disease
ADDTC: California Alzheimer's Disease Diagnostic and Treatment Centers criteria for VaD diagnosis (Chui et al., 1992)
ADLs: Activities of daily living
APA: American Psychiatric Association
ARWMC: Age-Related White Matter Changes Scale
AHA/ASA: American Stroke Association criteria for VCI diagnosis (Gorelick et al., 2011).
Aβ: Amyloid β-peptide

B

BBB: Blood-brain barrier
BIANCA: Brain Intensity AbNormality Classification Algorithm (WMH segmentation algorithm)

C

CADASIL: Cerebral autosomal dominant arteriopathy with subcortical infarcts and leukoencephalopathy
CT: Computed tomography
CVD: Cardiovascular disease
CBVD: Cerebrovascular disease (Santos, 2017)
CNS: Central nervous system
CSF: Cerebrospinal Fluid

D

Dpss: Discrete prolate spheroidal sequences
DSM: Diagnostic and Statistical Manual of Mental Disorders (versions: DSM-IV-TR and DSM-5)
DTI: Diffusion tensor imaging
DWI: Diffusion weighted imaging
DWMH: Deep white matter hyperintensities

E

EEG: Electroencephalography
EOG: Electrooculogram

F

FA: Fractional anisotropy
FC: Functional Connectivity
FLAIR: Fluid-attenuated inversion recovery magnetic resonance sequence.
fMRI: Functional magnetic resonance image
FSL: FMRIB Software Library (FMRI, MRI and DTI brain imaging toolbox)

G

GM: Grey matter

H

HC: Healthy control
Hz: Hertz

I

IADLs: Instrumental activities of daily living
ICA: Independent component analysis
ICD: International Classification of Disease

J

K

L

Low-VI: Low vascular impairment
LST: Lesion segmentation tool (Neuroimaging toolbox)
LST-LGA: LST- Lesion Growth Algorithm (WMH segmentation algorithm)
LST-LPA: LST- Lesion Predictor Algorithm (WMH segmentation algorithm)

M

Major VCI: Major vascular cognitive impairment (traditionally known as Vascular dementia)
MCI: Mild Cognitive Impairment
MEG: Magnetoencephalography
MID: Multi-infarct dementia
MildVCI: Mild vascular cognitive impairment
Mild-VI: Mild vascular impairment
MMSE: Mini-mental State Examination
MNI: Montreal Neurological Institute brain template
MRI: Magnetic resonance imaging

N

NINDS-AIREN: Neuroepidemiology Branch of the National Institute of Neurological Disorders and Stroke – Association Internationale pour la Researche et l'Enseigment en Neurosciences criteria for VaD diagnosis (Román et al., 1993)
NINDS-CNS: National Institute of Neurological Disorders and Stroke-Canadian Stroke Network (Hachinski et al., 2006)
NVU: Neurovascular Unit

O

P

PET: Positron emission tomography
PLV: Phase lock value
PLV-st: Phase lock value, mean strength
PSD: Post-stroke dementia
PWMH: Periventricular white matter hyperintensities

Q

R

ROI: Region of interest

S

SAMSEG: Sequence Adaptive Multimodal SEGmentation (WMH segmentation algorithm)
SiVaD: Subcortical ischemic dementia
SPM: Statistical Parametric Mapping (Neuroimaging toolbox)
SVD: Small vessel disease.

T

U

V

VaD: Vascular Dementia (currently identified as Major VCI)
VASCOG: International Society for Vascular Behavioral and Cognitive Disorders criteria for VCI diagnosis (Sachdev et al., 2014)
VCI: Vascular Cognitive Impairment
VICCCS: The Vascular Impairment of Cognition Classification Consensus Study for VCI diagnosis (Skrobot, 2017)

W

WM: White matter
WMH: White Matter Hyperintensities

Y

Z

SYMBOLS

δ: Delta
θ: Theta
α: Alpha
β: Beta

Abstract

Introduction

Major vascular cognitive impairment (VCI), also referred as Vascular Dementia (VaD), is responsible for up to 20% of cases of dementia worldwide (Kalaria, 2018). Besides from pure VaD, cerebrovascular diseases are also important comorbid contributors to the progression of other dementias (Wardlaw et al., 2019). Although cerebrovascular damage, specially white matter hyperintensities (WMH) is intrinsic to ageing, the accumulation or severity of these conditions represent an important cause of cognitive decline (Zimmerman et al., 2021). Nevertheless, there is ample evidence that the progression of cerebrovascular degradation can be slowed by controlling vascular risk factors and treating underlying pathologies (Zimmerman et al., 2021). Consequently, early detection and differentiation of the vascular origin of the cognitive impairment becomes a crucial scientific and clinical goal, and the ultimate purpose of this thesis.

The study of electrophysiological brain signatures have been well established for early detection and prognosis in different neurodegenerative disorders (López-Sanz et al., 2019). The biochemical alterations that occur in VCI can modify cell membrane polarity, action potentials, and cell-to-cell communication, completely altering the electrophysiological functioning of the brain. Therefore, it seems reasonable to search for new potential electrophysiological biomarkers for the early differentiation of VCI. After an extensive systematic review of the literature, we were able to ascertain that they were not yet ready for inclusion in diagnosis criteria because the results were not robust enough to be used as clinical biomarkers. The motivation and objectives of the research project presented here arise from this scientific context, trying to offer specific solutions to the limitations perceived of the previous literature and heading towards the search for useful electrophysiological biomarkers for VCI.

Objectives

The main objective was to characterize the effect of cerebrovascular damage on brain function, structure, and cognition in a cognitively healthy and old population, searching for new possible electrophysiological biomarkers in the preclinical stages.

- ✓ To obtain a clear picture of the literature regarding neurophysiological patterns (EEG and MEG) for mild and major VCI.
- ✓ To identify the most accurate algorithm for the automatic detection of WMH according to clinicians' manual segmentations.
- ✓ To establish a possible threshold from which WMH volume in the brain could have clinical implications.
- ✓ To characterize the behavior of sociodemographic features, brain structural integrity and cognitive performance according to the WMH volume in aging.
- ✓ To find spectral power signatures associated with the WMH, and their correlation with cognitive performance and brain structure in aging.
- ✓ To recognize the functional connectivity signatures associated with the WMH, and their relationship with cognitive performance and brain structure in aging.

Methods

Participants and sample characterization

The sample consisted of 300 clinically healthy individuals (≥ 26 MMSE) older than 50 years. The protocol included MEG recordings, MRI, and a neuropsychological assessment. Cerebrovascular damage was accounted by the WMH volume, a proxy for cerebral white matter deterioration triggered by disruption of the vascular system. The WMH volume for the entire sample was computed through two automated algorithms included in a neuroscience toolbox (SPM12). After that, we calculated a specific WMH volume baseline cut-off (i.e., 1000 mm^3). Finally, we divided the sample into two subgroups according to the cut-off: low vascular impairment (Low-VI) and mild vascular impairment (Mild-VI).

Experimental variables

- Cognition: We incorporated a comprehensive neuropsychological battery including all core cognitive domains recommended by VICCCS-II for assessment in VCI.
- Brain structural integrity (MRI): In addition to the WMH volumes, we included brain volumetric measures calculated through T1 images (Freesurfer) and white matter integrity, with the DWI images (*AutoPtx).*
- Brain electrophysiological functioning (MEG): We carried out analysis in source space of spectral power and functional connectivity (through phase lock value) with the eyes-closed resting state recordings.

Statistical analysis

We performed correlational analyses to assess the progression of the vascular load in the healthy population as a continuum that grows with age. Therefore, the WMH cut-off was used to model two sequential stages of the neurodegenerative process, without calculating electrophysiological differences between groups.

Main results

After the systematic review and the two methodological studies (i.e., to better segment WMH and to set a WMH cut-off), we describe three experimental studies. The first tried to give answer to the fourth objective. In this analysis we verified the existence of significant correlations between WMH volumes and age, cognitive performance, and brain structural integrity.

Subsequently, the two other experimental studies were focused on finding robust electrophysiological markers associated with the cerebrovascular damage, trying to give response to objective 5 and 6. Furthermore, the results that emerged from these analyses were submitted to further correlational analyses with brain structural integrity and cognition in an attempt to better understand the role of these electrophysiological signatures. Below, we depict a graphical summary of the results to provide a comprehensive overview at a glance: A) main findings for the whole sample; B) main results for the low-VI subgroup; and C) main outcomes for the mild-VI subgroup.

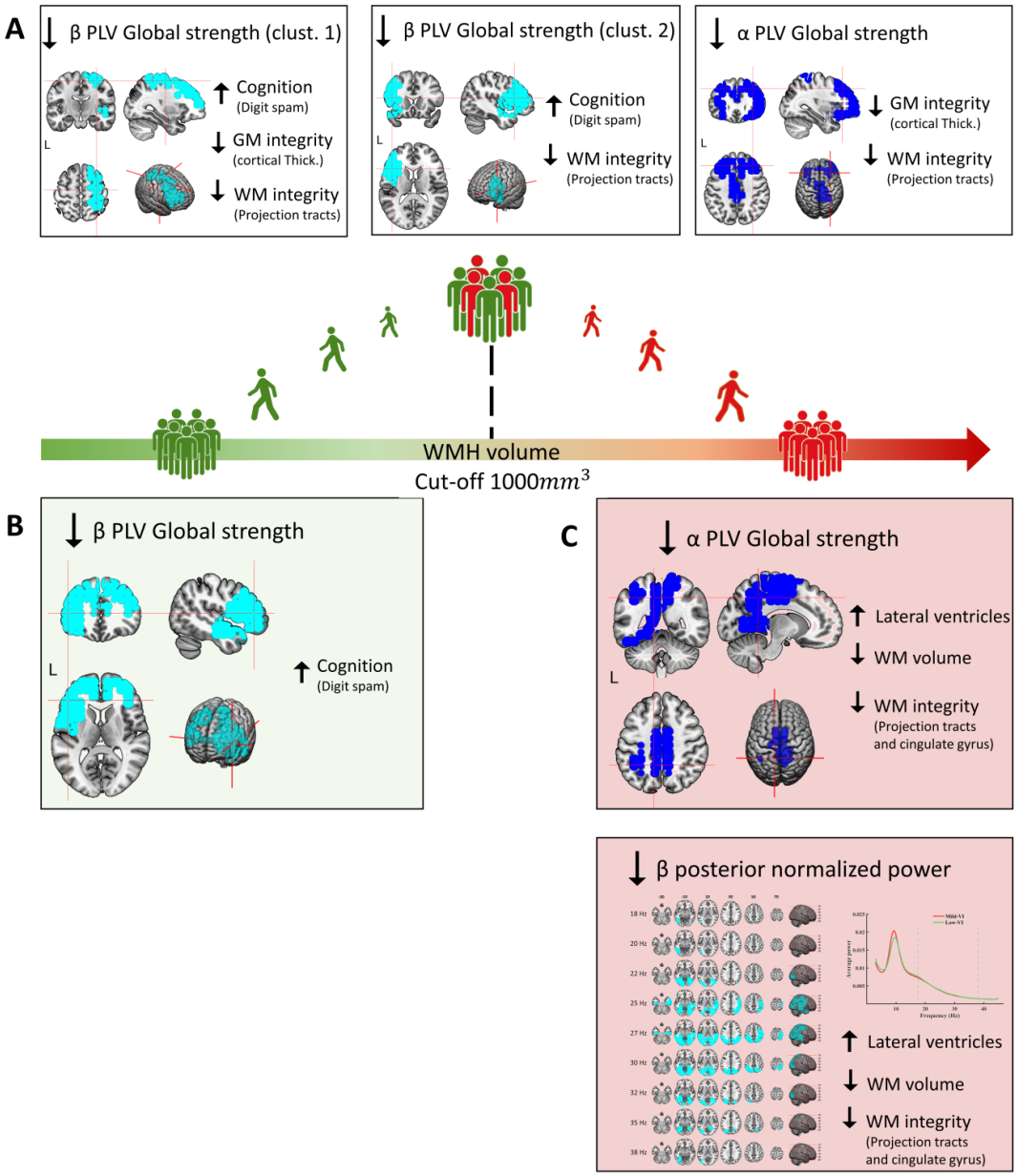

Conclusion

Firstly, we could conclude that the each of the specific objectives of the present thesis have been reasonably achieved. In general, we could say that the findings described in this manuscript are an excellent initial baseline for characterizing the effect of cerebrovascular damage on brain function, structure, and cognition in the cognitively healthy aging. We hope that the methodological study on automatic algorithms to calculate the WMH volume can facilitate early detection and close monitoring of cognitively healthy people with evidence of WMH in their brain scans. Additionally, given that nowadays the study of VCI with MEG is an unexplored field, it is expected that the findings described in this thesis can provide valuable information, establishing a solid starting point for the development of a line of interesting and necessary research. The possible transfer of the results obtained with MEG to EEG would facilitate an inexpensive and non-invasive test to provide electrophysiological markers that can act as surrogate signatures for the progression of vascular damage within healthy and pathological aging.

Resumen

Introducción

El deterioro cognitivo vascular (DCV), también denominado demencia vascular (DVa), es responsable de hasta el 20% de los casos de demencia a nivel mundial (Kalaria, 2018). Además, las enfermedades cerebrovasculares también son un factor crucial en la progresión de otras demencias (Wardlaw et al., 2019). Aunque el daño cerebrovascular, especialmente las hiperintensidades de la sustancia blanca (WMH, en inglés), es intrínseco al envejecimiento, la acumulación o gravedad de estas afecciones están asociadas al deterioro cognitivo (Zimmerman et al., 2021). No obstante, existen evidencias de que la progresión puede ralentizarse controlando los factores de riesgo vascular y tratando las patologías subyacentes (Zimmerman et al., 2021). En consecuencia, la detección precoz y la diferenciación del origen vascular del deterioro cognitivo se convierten en un objetivo científico y clínico crucial, y en el propósito último de esta tesis.

Existe mucha evidencia del del uso de la electrofisiología para la detección precoz y el pronóstico de diferentes trastornos neurodegenerativos (López-Sanz et al., 2019). Las alteraciones bioquímicas que se producen en la DCV pueden modificar la polaridad de las membranas celulares, los potenciales de acción y la comunicación célula-célula, alterando por completo el funcionamiento electrofisiológico del cerebro. Por lo tanto, parece razonable buscar nuevos biomarcadores electrofisiológicos para la diferenciación precoz de la DCV. Tras una extensa revisión sistemática, pudimos constatar que aún no estaban preparados para su inclusión en los criterios diagnósticos porque los resultados no eran lo suficientemente robustos como para ser utilizados como biomarcadores clínicos. Es en este contexto surge la motivación y los objetivos esta tesis, tratando de ofrecer soluciones específicas a las limitaciones percibidas de la literatura previa y encaminándose hacia la búsqueda de biomarcadores electrofisiológicos útiles para el DCV.

Objetivos

El objetivo principal es caracterizar el efecto del daño cerebrovascular en la función, la estructura y la cognición cerebrales en una población anciana y cognitivamente sana, buscando nuevos biomarcadores electrofisiológicos en las fases preclínicas.

- ✓ Obtener una imagen clara de la literatura relativa a los patrones neurofisiológicos (EEG-MEG) para el DCV.
- ✓ Identificar el algoritmo más preciso para la detección automática de las WMH de acuerdo con las segmentaciones manuales de los radiólogos.
- ✓ Establecer un posible umbral a partir del cual el volumen de WMH en el cerebro podría tener implicaciones clínicas.
- ✓ Caracterizar el comportamiento de las variables sociodemográficas, la integridad estructural cerebral y el rendimiento cognitivo en función del daño cerebrovascular
- ✓ Encontrar marcadores de potencia espectral en asociadas a las WMH, y su relación con el rendimiento cognitivo y la estructura.
- ✓ Reconocer los patrones de conectividad funcional asociadas a las WMH, y su relación con el rendimiento cognitivo y la estructura.

Métodos

Participantes y caracterización de la muestra

La muestra consistió en 300 individuos cognitivamente sanos (≥ 26 MMSE) mayores de 50 años. El protocolo incluía registros de MEG, RM y una evaluación neuropsicológica. El daño cerebrovascular se calculó mediante el volumen WMH, un indicador indirecto del deterioro de la sustancia blanca cerebral desencadenado por la alteración del sistema vascular. El volumen de WMH para toda la muestra se calculó mediante dos algoritmos automatizados incluidos en una toolbox de neurociencia (SPM12). Adicionalmente, se calculó un punto de corte para el volumen de WMH (i.e.,1000 mm3), en base al cual se dividió la muestra en dos subgrupos: deterioro vascular bajo (Low-VI) y deterioro vascular leve (Mild-VI).

Variables experimentales

- Cognición: Se incorporó una batería neuropsicológica que incluía todos los dominios cognitivos recomendados por VICCCS-II para la evaluación del DCV.
- Integridad estructural (RM): Además del volumen total de WMH, incluimos medidas volumétricas cerebrales calculadas mediante imágenes T1 (Freesurfer) e integridad de la sustancia blanca, con las imágenes DWI (AutoPtx).
- Funcionamiento electrofisiológico (MEG): Se realizaron análisis de potencia espectral y conectividad funcional (PLV) en el espacio de fuentes con los registros en estado de reposo con ojos cerrados.

Análisis estadístico

Realizamos análisis correlacionales para evaluar la progresión de la carga vascular en la población sana como un continuo que crece con la edad. Por lo tanto, el punto de corte se utilizó para modelar dos etapas secuenciales del proceso neurodegenerativo, sin calcular diferencias electrofisiológicas entre los grupos.

Resultados principales

Tras la revisión sistemática y los dos estudios metodológicos (segmentar mejor la WMH y establecer un punto de corte), realizamos tres estudios experimentales. El primero trató de dar respuesta al cuarto objetivo. En él pudimos comprobar la existencia de correlaciones significativas entre los volúmenes de WMH y la edad, el rendimiento cognitivo y la integridad estructural cerebral.

Posteriormente, los otros dos estudios experimentales se centraron en la búsqueda de marcadores electrofisiológicos robustos asociados al daño cerebrovascular, tratando de dar respuesta a los objetivos 5 y 6. Además, los resultados que surgieron de estos cálculos se sometieron a posteriores análisis correlacionales con la integridad estructural y la cognición, para tratar de comprender mejor el papel de estos marcadores. A continuación, presentamos un resumen gráfico de los resultados para ofrecer una visión global: A) resultados principales para toda la muestra; B) resultados para low-VI; y C) resultados para mild-VI.

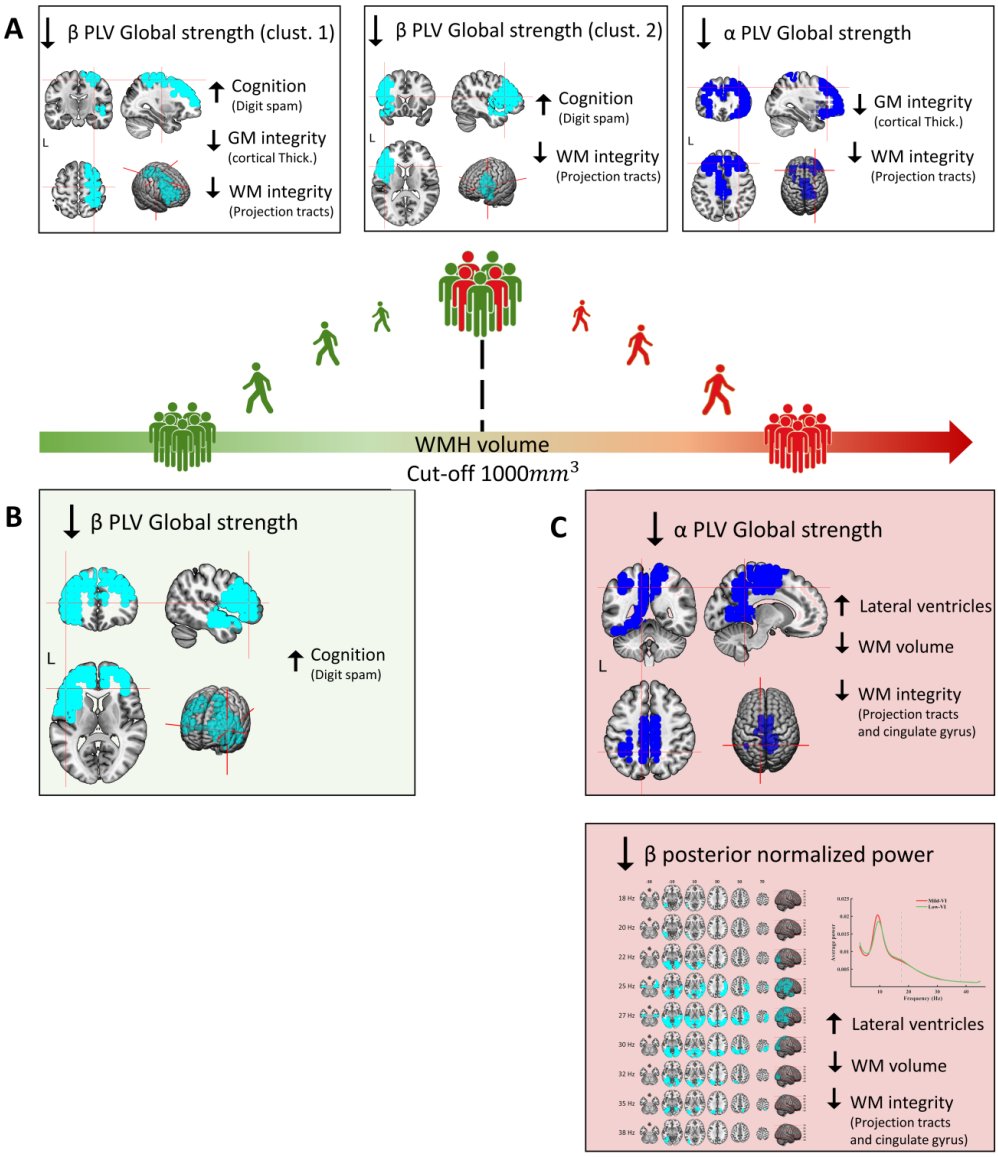

Conclusión

En primer lugar, podríamos concluir que se han alcanzado razonablemente cada uno de los objetivos de la tesis. En general, los hallazgos descritos constituyen una excelente línea de base para caracterizar el efecto del daño cerebrovascular sobre la función cerebral, la estructura y la cognición en el envejecimiento cognitivamente sano. Esperamos que el estudio metodológico sobre algoritmos para calcular el volumen de WMH pueda facilitar la detección precoz y seguimiento de personas cognitivamente sanas con evidencia de WMH en sus escáneres cerebrales. Adicionalmente, dado que en la actualidad el estudio de la DCV con MEG es un campo inexplorado, se espera que los hallazgos descritos puedan aportar información valiosa, estableciendo un punto de partida sólido para el desarrollo de una línea de investigación interesante y necesaria. La posible transferencia de los resultados obtenidos con MEG a EEG facilitaría una prueba con bajo coste y no invasiva para proporcionar marcadores electrofisiológicos que puedan actuar como biomarcadores de la progresión del daño vascular dentro del envejecimiento sano y patológico.

List of figures

List of tables

Introduction

Chapter 1: Aging

1.1. The aging of the population

In the last century, the life expectancy has increased abruptly, and predictions bode the positive tendency maintenance. People are living longer and older to the extent that a baby born in 2021 could expect to live on average almost 25 years more than a newborn from 1950 (United Nations, 2023). Nowadays, around 10% of the worldwide population is over 65 years old and this number of persons is projected to more than double in the next 30 years, from 716 million in 2021 to 1,6 billion in 2050. For people aged 80 years or over this growth is even faster (United Nations, 2023) In this context, it is important to notice that the population pyramids have been completely transformed in the last decades, establishing the aging stage in the focus of interest for the first time in history. The conjunction of a longer life expectancy, due to improvements in health and survival, with the reduction in fertility, sustains this population displacement, which is more pronounced in Europe, even more in Spain (see Figure 1), but this phenomenon is occurring rapidly in all societies of the world (United Nations, 2023).

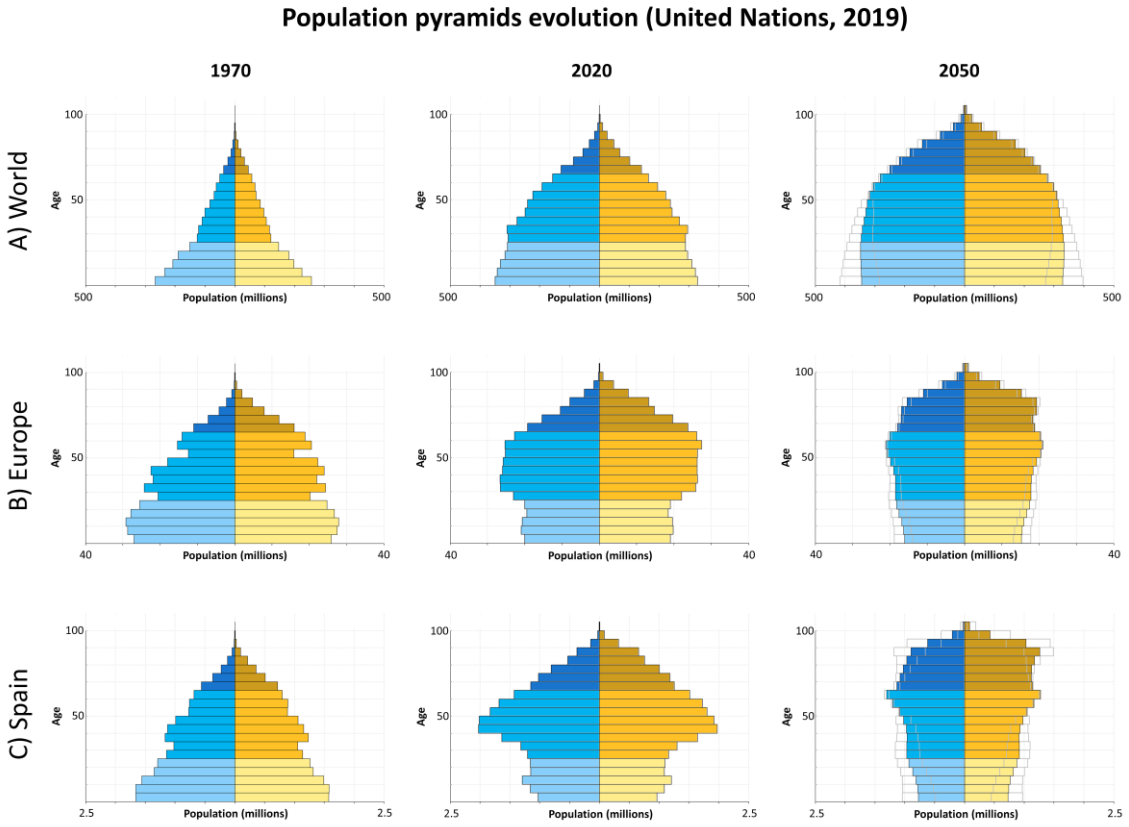

Figure 1 Population pyramids evolution. Data extracted from the United Nations web page (https://population.un.org/wpp/Graphs/).Note: data are depicted for three different history moments (first column for 1970, second for 2020 and third for 2070) and for three different territories: A) World data; B) Europe data; and C) Spanish population data. Blue for males and yellow for females.

Aging inevitably starts as early as a new life begins. It is a complex multifactorial process, through which people experience a set of molecular, structural, and functional changes, which are cumulative, progressive, endogenous, and deleterious (Sgarbieri & Pacheco, 2017). However, it is a concept that has generated controversy given the number of components that intervene in its development, such as biological variables, chronological age, socioeconomic conditions, and social and individual behavior (Cancino & Rehbein, 2016). Nevertheless, independently of the causes or contributors, healthy progress of aging is probably one of the most important goals of the 21st century (United Nations, 2023).

1.2. Aged-related pathologies: dementia.

Given the shift in the population pyramid over the course of the last century, aged-related pathologies are in the spotlight for social, clinical, and scientific efforts. Aging is a driving factor of multiple diseases, including cardiovascular pathologies, cancer, immune system disorders, and musculoskeletal disorders; but probably the first pathology that comes into our mind while talking about aging is dementia. In fact, the overall prevalence of dementia is around 7% in people older than 50 years of age (Cao et al., 2020). Dementia is a medical condition truly disabling, which carries devastating effects at social and emotional levels for the sufferers, but also for people around them. Moreover, the global cost of dementia must not be overlooked: health care, psychological support, social services, and the assistance to relatives and caregivers are, among other, expenses directly or indirectly derived from dementia. Nowadays the global cost of this pathology is estimated at around 1.14 billion euros (United Nations, 2019) which makes it exceed the market value of companies like Apple (1.13 billion euros) or Google (0.81 billion euros) in 2019.

Dementia is not a disease itself, but rather a group of symptoms caused by a number of clinical circumstances or underlying etiologies. This is a wide term that can reflect several conditions, although, in general, it involves difficulties in cognitive processes such as thinking, memory, and reasoning, which affect patients' ability for independent daily living (Cao et al., 2020). It is important to bear in mind that healthy aging is also usually associated with changes in brain functioning,(Mandal et al., 2018) structure and cognition (Oschwald et al., 2019), especially in speed processing, attention, cognitive flexibility, visuospatial skills, and memory. Therefore, distinguishing normal declines in cognitive functioning associated with healthy aging from pathological impairment is crucial. In the last version of the Diagnostic and Statistical Manual of Mental Disorders (DSM-5), the American Psychiatric Association (APA) proposed the term neurocognitive disorder, replacing the organic mental disorders of its previous version (DSM-IV-TR), which included “dementia, delirium, amnesic and other cognitive disorders”. Within this new diagnosis group three categories were included: delirium, minor neurocognitive disorder, and major neurocognitive disorder, which etiologies and severity must be specified (Regier et al., 2013). Delirium is a disturbance in attention and awareness that develops over a brief period of time (usually hours to a few days). It represents an acute change from baseline attention and awareness and tends to fluctuate in severity during the course of a day. Given the temporality associated with this pathology, delirium is out of the scope of the present thesis. The minor neurocognitive disorder contemplates a pathological stage of pre-dementia in the style of Petersen's mild cognitive impairment (MCI) (Petersen, 2004), and dementia is included in the new

concept of major neurocognitive disorder, not excluding the use of this term in the etiological subtypes. For this reason, from now on we will refer to the condition of major neurocognitive disorder either with this term or with the classic term of dementia, since it is the one that is mostly used in current research and clinical scenario.

Besides labeling changes, some diagnostic criteria have been modified from DSM-IV-TR (American Psychiatric Association, 2000) to DSM-5 (American Psychiatric Association, 2013). Most importantly, cognitive impairment as a dementia criterion is no longer necessarily limited to memory deficits. On the contrary, significant deficits in any of the proposed cognitive domains (i.e., learning and memory, language, executive functions, complex attention, perceptual-motor capacities, and/or social cognition) are now sufficient to fulfill the first criterion for major neurocognitive disorder diagnosis. This amplification of the diagnosis criteria to other cognitive domains has driven the clinicians' and researchers' attention to less common dementia etiologies and highlights the importance of considering the possible pathological comorbidities that could trigger impairment on other psychological functions before memory. Consequently, it allows different treatment approaches from the very early stages of the disease. The DSM-5 diagnostic criteria for minor neurocognitive disorder and major neurocognitive disorder and the specific subtypes according to the etiology are described in Table 1.

Table 1 Diagnosis Criteria for mild and major Neurocognitive Disorder according to DSM-5

Mild Neurocognitive Disorder	Mayor Neurocognitive Disorder
A. Evidence of modest cognitive decline from a previous level of performance in one or more cognitive domains (complex attention, executive function, learning and memory, language, perceptual motor, or social cognition) based on: I. Concern of the individual, a knowledgeable informant, or the clinician that there has been a mild decline in cognitive function; and II. A modest impairment in cognitive performance, preferably documented by standardized neuropsychological testing or, in its absence, another quantified clinical assessment.	A. Evidence of significant cognitive decline from a previous level of performance in one or more cognitive domains (complex attention, executive function, learning and memory, language, perceptual-motor, or social cognition) based on: I. Concern of the individual, a knowledgeable informant, or the clinician that there has been a significant decline in cognitive function; and II. A substantial impairment in cognitive performance, preferably documented by standardized neuropsychological testing or, in its absence, another quantified clinical assessment.
B. The cognitive deficits do not interfere with capacity for independence in everyday activities (i.e., complex instrumental activities of daily living such as paying bills or managing medications are preserved, but greater effort, compensatory strategies, or accommodation may be required).	B. The cognitive deficits interfere with independence in everyday activities (i.e., at a minimum, requiring assistance with complex instrumental activities of daily living such as paying bills or managing medications).
C. The cognitive deficits do not occur exclusively in the context of a delirium.	C. The cognitive deficits do not occur exclusively in the context of a delirium.
D. The cognitive deficits are not better explained by another mental disorder (e.g., major depressive disorder, schizophrenia).	D. The cognitive deficits are not better explained by another mental disorder (e.g., major depressive disorder, schizophrenia).
Etiological subtypes	
1. Alzheimer´s disease 2. Frontotemporal lobar degeneration 3. Lewy body disease 4. Vascular disease 5. Traumatic brain injury 6. Substance/medication use 7. Human immunodeficiency virus (HIV) infection 8. Prion disease 9. Parkinson´s disease 10. Huntington´s disease 11. Another medical condition 12. Multiple etiologies 13. Unspecified	

Notably, DSM-5 continues to support neuropsychological evaluations as key measures for the diagnosis of neurocognitive disorders, mainly in its minor condition. However, the need to specify the etiological subtype in the diagnosis force to discuss the role of additional markers. This highlights the importance of neuroimaging studies, especially those developed with magnetic resonance imaging (MRI) and positron emission tomography (PET). Only some biological markers for dementia are included in DSM-5 criteria because, as they report, many of them are not fully validated yet. As mentioned before, there are multiple underlying etiologies for dementia and early accurate differentiation allows better management of the pathology.

A good example of the importance of biomarkers in dementia is that nowadays Alzheimer Disease (AD) is known as the most common subtype of dementia, accounting for 60 to 80% of cases globally (Alzheimer´s Association, 2020). AD is mainly characterized by a prominent, but not isolated, episodic memory impairment. The codification of new memories is especially compromised in the early stages, although it can also produce confusion, mood disorders, and spatial-temporal disorientation. The quintessential biomarker for AD pathophysiology involves the progressive accumulation of beta-amyloid plaques outside neurons and twisted tangles of protein tau inside neurons (Blennow et al., 2015; Hampel et al., 2010; Vlassenko et al., 2012). Nevertheless, only half of patients diagnosed with AD showed pure AD physiopathology in postmortem examinations, the rest fulfilling the criteria for a mixed dementia diagnosis, as can observed in Figure 2 (Azarpazhooh et al., 2017). This hints the existence of other comorbid pathologies usually present, but not detected in clinical assessment. The insertion of biomarkers in the rutinary clinical and research practice for dementia diagnosis could be a crucial point for differentiation and classification of its subtypes, and to understand the load of each pathophysiological sign on the severity and progression of their symptoms.

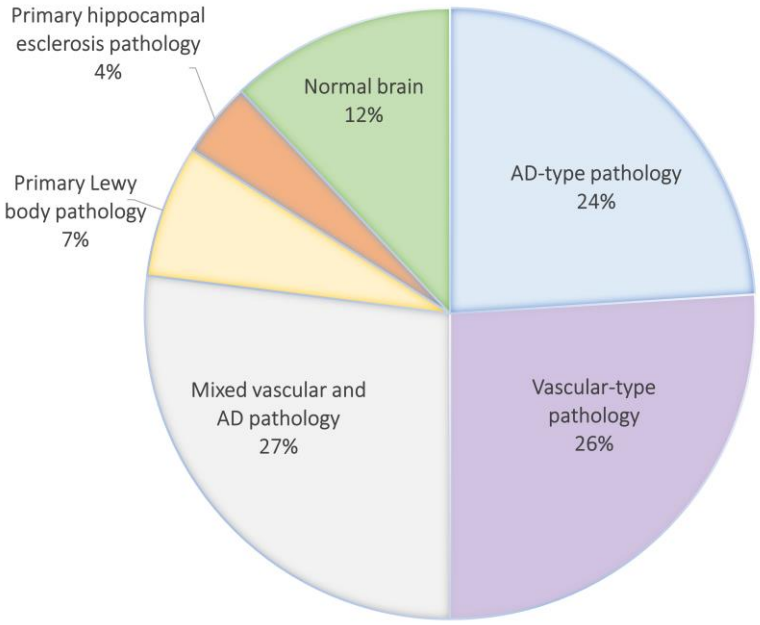

Figure 2 Dementia subtypes prevalence in post-mortem studies. Data extracted from: "Concomitant vascular and neurodegenerative pathologies double the risk of dementia". Azarpazhooh, M. R., Avan, A., Cipriano, L. E., Munoz, D. G., Sposato, L. A., & Hachinski, V., 2017. Alzheimer's and Dementia.

Looking at these data, it seems crucial to pay attention to the vascular function. Aging has an important effect on the heart and vascular system, leading to an increased prevalence of cardiovascular diseases (CVD), such as atherosclerosis, hypertension, myocardial infarction, and stroke (Donato et al., 2018). In fact, cardiovascular diseases remain the leading cause of disease burden in the world (Roth et al., 2020) and they have direct consequences to cerebral vasculature functioning (Zimmerman et al., 2021). Cerebrovascular diseases (CBVD) involves a variety of medical conditions or changes in the cerebral or systemic vasculature with brain impact, including a huge number of pathologies and etiologies (i.e., arterial stiffening, weakening or inflammation, hypoperfusion, strategic infarct, multi-infarct, small vessel disease (SVD), microbleeds, hemorrhages, cerebral autosomal dominant arteriopathy with sub-cortical infarcts and leukoencephalopathy (CADASIL), or cerebral amyloid angiopathy among others) (Iadecola, 2013). This heterogeneity is critical to analyze general prevalence, but it is known that many of these conditions are inherent to the ageing process. In fact, cerebrovascular decline starts early in life (i.e., arterial inflammation or stiffening around 20-30 years old) and worsen with age (Zimmerman et al., 2021). Although cerebrovascular damage is intrinsic to healthy ageing, accumulation or severity of these conditions represent a significant cause of cognitive decline (Bos et al., 2018; Dey et al., 2016; Zimmerman et al., 2021). The aforementioned heterogeneity triggers many different cognitive symptoms making difficult the identification of its effects in the patient's behavior only by means of the neuropsychological profile. Nevertheless, neuroimaging evidence of cerebrovascular damage could help clinicians in the early identification and differentiation of cognitive decline due to vascular impairment.

Vascular Dementia (VaD), when existing alone, is responsible for up to 20% of cases of dementia worldwide, being the second most prevalent after AD (Catindig et al., 2012; Kalaria, 2018; O'Brien & Thomas, 2015; Rizzi et al., 2014). Besides from pure VaD, CBVD are also major comorbid contributors to the progression of other neurodegenerative diseases, it can be observed in 50%–90% of AD patients (Iadecola, 2013; Santos et al., 2017), and about 50% of dementias worldwide (Schneider et al., 2007; Wardlaw et al., 2019). It has been described that the risk of dementia is higher when appearing cerebrovascular neuropathology that when having neuropathological evidence of AD; skyrocketing the risk when happening concomitant pathologies (see Figure 3) (Azarpazhooh et al., 2017; Schneider et al., 2007).

Given the high presence of cerebrovascular problems in healthy and pathological aging, it is pertinent to highlight the potential prevention and modification opportunities that CBVD confer. There is ample evidence that most of these types of damage are somewhat preventable, or even reversible, and that their progression can be slowed by controlling vascular risk factors (i.e., as tobacco use, unhealthy diet and obesity, physical inactivity, and harmful use of alcohol) and treating vascular underlying pathologies (Erkinjuntti et al., 2004; Zimmerman et al., 2021). Precisely, the existence of approaches to tackle CBVD, understanding its effects in both brain function and cognition is especially important from the clinical perspective to slow down the patients' deterioration and modify the course of the process.

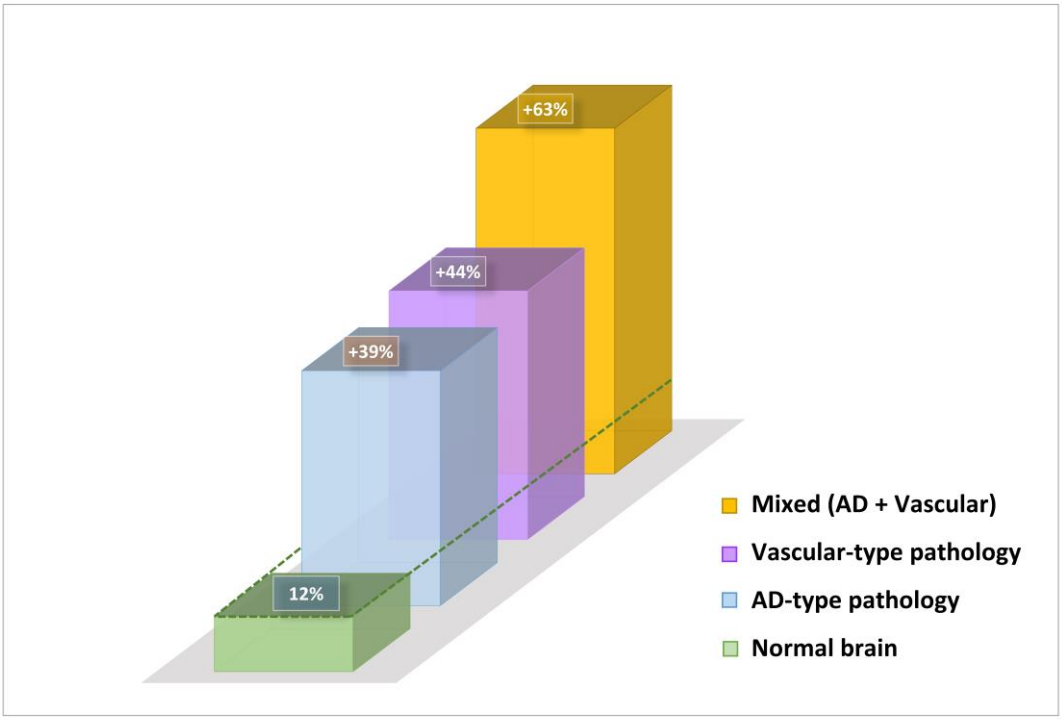

Figure 3 Risk of developing dementia or major neurocognitive disorder symptoms based on the neuropathology evidenced in the brain in post-mortem studies. Data extracted from: "Concomitant vascular and neurodegenerative pathologies double the risk of dementia". Azarpazhooh, M. R., Avan, A., Cipriano, L. E., Munoz, D. G., Sposato, L. A., & Hachinski, V., 2017. Alzheimer's and Dementia.

Following this perspective, the DSM-5 stated the important role of structural neuroimaging for major and minor neurocognitive disorder of vascular origin through Magnetic resonance image (MRI) and Computed tomography (CT); whereas acknowledges that no other biomarker has enough evidence to be included yet. The present thesis aims to characterize the effect of cerebrovascular damage on brain function, structure, and cognition in the old population, by looking for new possible biomarkers in the preclinical stages. To achieve this goal, the first step is to comprehend the terminology, subtype's classification, diagnosis criteria, and underlying pathophysiology around these diseases.

1.3. Vascular cognitive impairment

Evolution of the terminology and diagnosis criteria

The heterogeneity of cerebrovascular diseases has led to a lack of consensus in the definition, classification, and diagnosis criteria of the cognitive impairment of vascular origin in both research and clinical fields over the years (going from arteriosclerotic dementia to vascular cognitive impairment -VCI- or Vascular dementia -VaD-). Lack of clarity over the years, has impeded sharing and comparison of data on a larger scale, leading to different specialties conducting narrow focused research (Skrobot et al., 2017)To date, all diagnostic criteria for characterizing cognitive syndromes associated with vascular disease are based on three conditions: 1) demonstration of

the presence of a cognitive disorder by neuropsychological testing, 2) a history of clinical stroke or presence of vascular disease by neuroimaging, and 3) a link between the cognitive impairment and the vascular lesions (Gorelick et al., 2011). However, specific criteria have undergone important transformations over the years.

Approximately 50 years ago, the classical term "arteriosclerotic or atherosclerotic dementia" was refused and replaced by multi-infarct dementia (MID), giving importance to the occurrence of multiple small or large cerebral infarcts as main cause of dementia, instead of atherosclerosis of the cerebral arteries themselves (Hachinski et al., 1974)This approach was very influential, and subsequent classification systems for vascular dementia, including the International Classification of Disease (ICD) and Diagnostic and Statistical Manual of Mental Disorders (DSM) were largely based on this notion. In this line, in 1992, the California Alzheimer's Disease Diagnostic and Treatment Centers (ADDTC) criteria were developed for the diagnosis of VaD caused exclusively by ischemic cerebrovascular lesions (Chui et al., 1992)

From this time, numerous successive proposals have tried to capture the clinical and etiologic complexity of cognitive impairment caused by heterogeneous cerebrovascular pathologies, highlighting the agreement that it extends beyond the traditional concept of multi-infarct dementia. One of the most used diagnostic criteria in research for the last twenty years were established in 1993 by the Neuroepidemiology Branch of the National Institute of Neurological Disorders and Stroke – Association Internationale pour la Researche et l'Enseigment en Neurosciences (NINDS-AIREN). In this agreement, it was adopted the definition of dementia from the 10th revision of The Neurological Adaptation of the International Classification of Diseases (ICD-10NA) (van Drimmelen-Krabbe, 1995), where the presence of a decline in memory and intellectual abilities that causes impaired functioning in daily living was required to fulfill the criteria. Cognitive decline should be demonstrated by loss of memory and deficits in at least two other domains, including orientation, attention, language-verbal skills, visuospatial abilities, calculations, executive functions, motor control, praxis, abstraction, or judgment. Moreover, radiologic lesions for this pathology included the presence of large-vessel strokes and/or small vessel disease in specific locations. A key point to be highlighted is the suggestion to avoid the term "mixed dementia", advising the use of AD with CBVD (Román et al., 1993)

In 2002, neuroimaging evidence of any cerebrovascular disease without specific localization and cognitive decline associated was accepted as sufficient to document VaD (Rockwood, 2002). This evolution on the consideration of cognitive impairment of vascular origin as a continuum led to broader criteria for the early stages of disease development. In this line, one of the most significant contributions in this time was the introduction of the terms **vascular cognitive impairment (VCI)** and mild vascular cognitive impairment (MildVCI), giving importance to the spectrum condition of these pathologies (O'Brien et al., 2003).

With the purpose of establishing a standardized baseline and clarifying the concepts, classification, and descriptive terminology surrounding cerebrovascular-related cognitive impairment, international research groups have invested a great deal of resources to reach a consensus. In 2006, specific neuroimaging standards and neuropsychological tests, more sensitive to earlier stages, were also developed by international consensus at the National

Institute of Neurological Disorders and Stroke-Canadian Stroke Network (NINDS-CNS) (Hachinski et al., 2006). In 2011, the American Stroke Association (AHA/ASA) included and recommended the clarification of probable or possible VCI, depending on the level of evidence of vascular damage in neuroimaging, and they promoted the use of the term vascular mild cognitive impairment (VaMCI) (Gorelick et al., 2011). Furthermore, different expert groups tried to deeper define neuropathological, comorbidity, demographic, familial aspects, as well as lifestyle and risk factors related to vascular cognitive impairment as a spectrum (Gorelick et al., 2011; Hachinski et al., 2006).

Years later, in 2014 the VASCOG diagnostic criteria was published, including the latest advances in dementia definition depicted in the DSM-5 (described in previous section). It gives great importance to the co-occurrence of different neurocognitive pathologies interacting with cerebrovascular diseases, reviving the concept of "mixed dementias" (Sachdev et al., 2014).

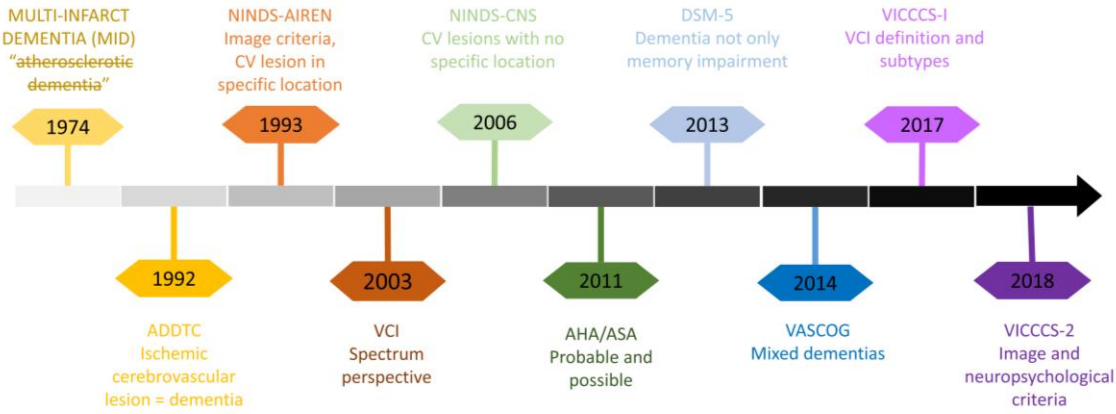

Figure 4 Diagram of most relevant milestones in the evolution of terminology and diagnosis criteria for cognitive impairment of vascular origin

Updated classification and diagnosis criteria for VCI

In this thesis we will use the definitions that the Vascular Impairment of Cognition Classification Consensus Study (VICCCS) published in 2017 (Skrobot et al., 2017). The VICCCS stated the concept of VCI (O'Brien et al., 2003), referring to all forms of mild to severe cognitive impairment associated with, and presumed to be caused by, cerebrovascular disease (Skrobot et al., 2017). This concept includes from mild forms of vascular cognitive impairment (MildVCI) to major VCI, also called vascular dementia). This international agreement defined 4 types of dementia or major forms of VCI (see Table 2): post-stroke dementia (PSD), multi-infarct dementia (MID), subcortical ischemic dementia (SiVaD), and mixed dementias. Finally, descriptive terms for either the "mechanism" or "location" of damage were also approved: familial/ sporadic, strategic infarct, hypoperfusion, hemorrhagic, specific arteriopathies (including genetic, hereditary, and developmental anomalies), and vasculitis.

Table 2 Summary of Vascular Cognitive Impairment definition and classification according to VICCCS (Skrobot et al., 2017, Skrobot et al., 2018).

Mild VCI: Impairment of at least one cognitive domain with mild to no impairment in instrumental activities of daily living (IADLs)/activities of daily living (ADLs), respectively (independent of the motor/sensory sequelae of the vascular event).		
Major VCI or VaD: Clinically significant deficits of sufficient severity in at least one cognitive domain (deficits may be present in multiple domains) and severe disruption to IADLs/ADLs (independent of the motor/sensory sequelae of the vascular event).	**Subcortical Ischemic Dementia (SiVaD)**	Small-vessel disease and white matter lesions are the primary cause of SiVaD. Lacunar infarcts are the most common vascular lesions identified and are located predominantly in subcortical grey and white matter. This diagnosis incorporates the overlapping clinical entities of Binswanger's disease and the lacunar state.
	Multi-Infarct dementia (MID)	MID indicates the presence of multiple large cortical infarcts.
	Post-Stroke Dementia (PSD)	PSD encompasses dementia that develops within six months of a stroke. There can be multiple cortical-subcortical infarcts or a single strategic lesion. The temporal relationship between cognitive decline and stroke differentiates PSD from other forms of major VCI (VaD).
	Mixed dementias (VCI-another dementia)	Mixed dementia includes phenotypes representing combinations of vascular and neurodegenerative disease. The most prevalent combination is VCI-AD. This term, describing the pathologies, is now preferred to the previously used but less-specific term "mixed dementia."
*"Probable" and "possible" VCI	***Probable*** mild VCI or major VCI (VaD) is the appropriate diagnostic category if computed tomography imaging is the only imaging available. ***Possible*** mild VCI or major VCI (VaD) is diagnosed when neither MRI nor computed tomography imaging is available.	

In 2018, a second report (VICCCS-II) set down updated neuropsychological and neuroimaging protocols for the diagnosis of VCI (Skrobot et al., 2018), based on the recommendations suggested in the NINDS-CNS (Hachinski et al., 2006), to promote scientific collaboration in the field. A remarkable fact of this consensus was that, while in VICCCS the temporal relationship between the cognitive impairment and vascular lesion was defined only for the PSD subtype, requiring that cognitive decline developed within 6 months of stroke, VICCCS-II additionally indicated that a clear temporal relationship between a vascular event and the onset of cognitive deficits should not be an essential component for diagnosis of mild VCI, SiVaD, mixed dementias, or MID (Skrobot et al., 2018). Details of these diagnosis guidelines for VCI can be found below.

Guidelines for VCI neuropsychological assessment

According to VICCS-II guidelines, the core cognitive domains for assessment in VCI should be executive function, attention, memory, language, and visuospatial function. The domains of learning, neuropsychiatry, and social cognition should be treated as optional, outside of the core assessment, unless and until there is stronger evidence for their inclusion.

It was agreed that a neuropsychological assessment protocol for use in a typical clinical diagnostic setting, noting time pressures and patient group capabilities, should take at most 60 minutes, although optional assessments could take additional time for particular cases. The inclusion of all core and supplementary items proposed by the NINDS-CSN 60-minute and 30-minute protocols were supported for use in VICCCS-II guidelines. The specific neuropsychological scores included in these protocols are depicted in Table 3.

Table 3 Neuropsychological assessment 30- and 60-minutes protocols for VCI diagnosis according to VICCCS-II guidelines

Cognitive domain	Neuropsychological tool	60- min	30-min
Executive function	Animal naming (semantic fluency)	X	X
	Controlled Oral Word Association (phonemic fluency)	X	X
	WAIS-III Digit Symbol-Coding (processing speed and activation)	X	X
	Trail Making Test (processing speed and activation)	X	supp
	Simple and choice reaction time tasks	X	
Memory/ learning	Revised Hopkins Verbal Learning Test (HVLT-R)	X	X
Language	Boston Naming Test 2nd Edition, Short Form	X	
Visuospatial function	Rey-Osterrieth Complex	X	
Neuropsychiatric/ depressive symptoms	Neuropsychiatric Inventory, questionnaire Version (NPI-Q)	X	X
	Center for Epidemiological Studies-Depression Scale (CES-D) Short form	X	X
Premorbid status	Mini-Mental State Examination (MMSE)	supp	supp

Guidelines for VCI neuroimaging assessment

The VICCCS-II consensus stated that imaging evidence of CBVD was essential for diagnosis of major VCI (VaD) and mild VCI. Moreover, MRI must be the gold-standard imaging for VCI, and CT could be used only if MRI were not available or in patients where MRI is contraindicated. According to the type of image available for diagnosis, it was settled the use of the term “possible” together with mild or major VCI if neither MRI nor CT imaging were available, and “probable” was the appropriate diagnostic category if only CT imaging were available.

Table 4 depicts the imaging measures specifications, depending on the neuroimaging technology used and the type of vascular damage. Additionally, it is important to note that VICCCS-II guidelines support that no other neuroimaging technique or application was yet ready for inclusion in clinical diagnosis, as they require further research. In this consensus, four vascular damages were described as the observable signatures of cerebrovascular pathologies underlying the cognitive impairment evidenced in the neuropsychological assessment.

Brain atrophy (Figure 5): refers to a lower brain volume that is not related to a specific macroscopic focal injury such as trauma or infarction. Brain atrophy can be general or focal (affecting only particular lobes or specific brain regions—e.g., the hippocampus), symmetrical or asymmetrical, or tissue selective (affecting a certain tissue class—e.g., white matter), and occurs in many neurodegenerative disorders. The pathological changes of atrophy are heterogeneous and not necessarily indicative of neuronal loss. Brain atrophy occurs with the usual ageing process, but the extent varies between individuals and pathologies. In the context of vascular disease and dementia, neuropathological substrates of atrophy include neuronal loss, cortical thinning, subcortical vascular pathology with white matter rarefaction and shrinkage, arteriolosclerosis, venous collagenosis, and secondary neurodegenerative changes. (Wardlaw et al., 2013).

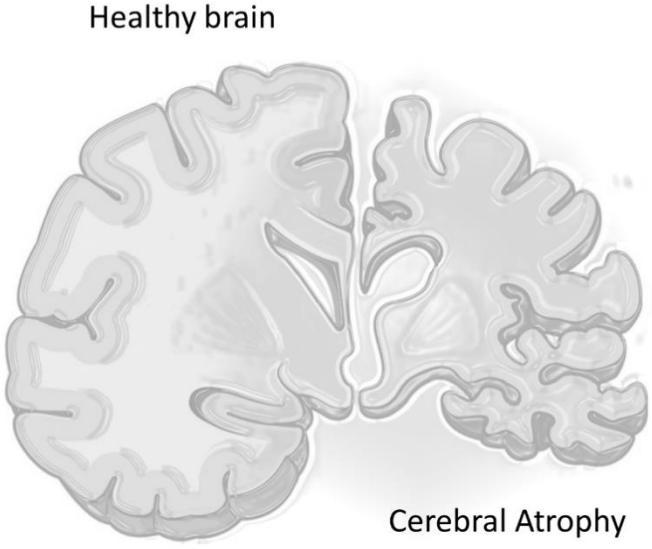

Figure 5 Morphological differences between a healthy brain and a brain with atrophy. Modified from : "The extended scope of neuroimaging and prospects in brain atrophy mitigation: A systematic review". Sungura, R., Onyambu, C., Mpolya, E., Sauli, E., & Vianney, J. M. , 2021. Interdisciplinary Neurosurgery: Advanced Techniques and Case Management.

*White Matter Hyperintensities (WMHs) (*Figure 6*):* characterized by bilateral, mostly symmetrical diffuse areas of high signal intensity (hence, "hyperintense") on T2-weighted or fluid-attenuated inversion recovery (FLAIR) MRI sequences (Wardlaw et al., 2013). By far, the most prevalent vascular lesions associated with VCI are related to alterations in small vessels in the hemispheric white matter (Jellinger, 2013). Small vessel disease (SVD) is the most common vascular cause of dementia, a major contributor to mixed dementia, and the cause of about a fifth of all strokes worldwide. (Norrving, 2008; Pantoni, 2010).

Neuroimaging signs for SVD include WMH, along with recent small subcortical infarcts, lacunes, prominent perivascular spaces, cerebral microbleeds, and brain atrophy, according to the standards for research into small vessel disease criteria (STandards for ReportIng Vascular changes on nEuroimaging - STRIVE) (for specific information about SVD MRI markers see Wardlaw et al, 2013). Additionally, WMHs are common accompaniment of aging, not only in dementia patients, but also in healthy populations; more than 90% of the general population older than 80 years of age has some degree of WMH (Kloppenborg et al., 2014)The vascular pathologies underlying these lesions consist of atherosclerotic plaques affecting small cerebral vessels, depositions of a hyaline substance in the vascular wall, fibrotic changes in the vessel wall resulting in stiffening and microvascular distortion (arteriolosclerosis), and total loss of integrity of the vascular wall (fibrinoid necrosis) (Thal et al., 2012).

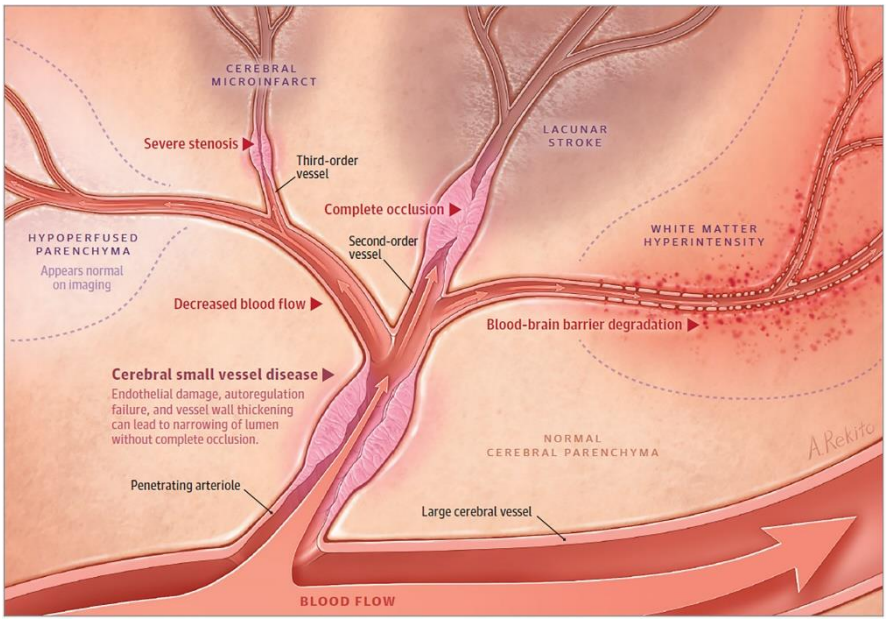

Figure 6 Graphical explanation of cerebral small vessel disease (specially, WMH). Image from: "Advances in Lacunar Stroke Pathophysiology: A Review". Regenhardt, R. W., Das, A. S., Lo, E. H., & Caplan, L. R., 2018. JAMA Neurology

Infarction (Figure 7): refers to neuroimaging evidence of recent or old infarction in the territory of one cerebral vessel. It is also called ischemic stroke and occurs as a result of disrupted blood flow to the brain due to an obstruction of one of the blood vessels that supply it (i.e., arterial thrombosis, embolization, or critical hypoperfusion). A lack of adequate blood supply to brain cells deprives them of oxygen and vital nutrients (i.e., glucose) (Iadecola, 2013). This initiates a cascade of events at a cellular level which, if circulation is not re-established in time, will lead to cell death. Stroke doubles the risk for dementia (poststroke dementia), and approximately 30% of stroke patients go on to develop cognitive dysfunction within 3 years (Allan et al., 2011; Pendlebury & Rothwell, 2009). Additionally, multiple infarcts, caused by multiple arterial occlusions over time, are well known to impair cognition (multi-infarct dementia) (Iadecola, 2013). However, ischemic strokes are often associated with many of the vascular pathologies, which also contribute to the total vascular burden.

Hemorrhage (Figure 7): indicates the consequence of a recent rupture of an artery of the brain causing that brain cells and tissues do not get oxygen and nutrients. In addition, pressure builds up in surrounding tissues and irritation and swelling occur, which can lead to further brain damage. When the hemorrhage become chronic the consequence observed in imaging is similar to the one derived from an old infarct.

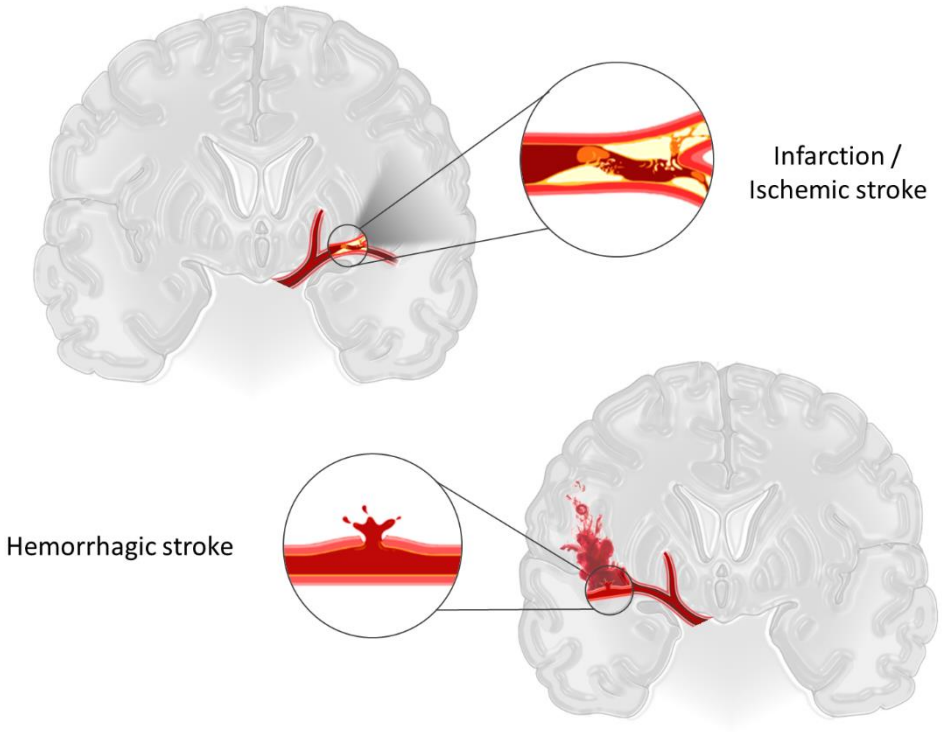

Figure 7 Schematic difference between brain infarction or ischemic stroke and hemorrhage.

Table 4 Imaging measurement specifications for VCI diagnosis according to VICCCS-II

	Core MRI measures	Additional MRI measures	CT measures
Brain atrophy	- Estimates of atrophy & ventricular size using the Cardiovascular Health Study - CHS Scale - Estimates of medial temporal lobe atrophy using Scheltens Scale	- Quantitative measurement of brain volume normalized for head size	- Ventricular size - Hippocampus: medial temporal atrophy
WMHs	- Preferred: ARWMC scale - Acceptable: CHS WMH Scale	- Quantitative measurement of WMH volume normalized for head size. - Anatomical mapping also encouraged (CHS Scale)	- Diffuse white matter: ARWMC scale
Infarction	- Number and size at specified locations: *Size (largest diameter): large.> 1cm// small = 3–10 mm - Location (encourage use of Talairach Atlas for precision - Supratentorial - Hemisphere - Cortical (may include subcortical) - Exclusively subcortical white matter - Exclusively subcortical gray matter - Infratentorial	- All infarcts localized using a standard approach to generate quantitative measures of volume and location. Ideally, identified infarcts would also be mapped to a common stereotactic space (CHS) - All infarcts should be differentiated from perivascular spaces (Virchow-Robin spaces) by CHS criteria	- Discrete hypodensities (Cerebrospinal fluid (CFS) density; consistent with infarction or old hemorrhage): Small = 3–10 mm Large. > 1 cm - Number, volume, and location—as core MRI
Hemorrhage	- Number and size in each location * Size (largest diameter): Large > 1 cm // Microhemorrhage < 1 cm, susceptibility on gradient echo Must report lower size limit cutoff, field strength. - Location—as infarcts	- All lesions localized using a standard approach to generate quantitative measures of volume and location. - Ideally, identified lesions would also be mapped to a common stereotactic space (CHS)	- Acute hemorrhage - Number, volume, and location—as core MRI
Other		Mass lesions, arteriovenous malformations, extra-axial fluid collections, malformations, dysplasia, or any other lesion that might complicate assessment of cerebrovascular disease	

References: ARWMC, age-related white matter change (Wahlund et al., 2001); CHS Scale, Cardiovascular Health Study Scale (Arnold et al., 1997); Scheltens scale (Scheltens et al., 1992);Medial temporal atrophy scale (Frisoni et al., 2002); Talairach Atlas (Talairach & Tournoux, 1988). *Abbreviations: AVMs, arteriovenous malformations

Vascular pathophysiology underlying VCI.

In order to fully understand the background surrounding the cognitive impairment of vascular origin, we should look into the pathophysiology underlying VCI. Far from simplifying the scenario, embracing the complexity and heterogeneity of the pathophysiological processes associated with cerebrovascular dysfunction would help us to understand the confusion and lack of consensus in the terminology and diagnosis of this pathology.

To address the effect of vascular pathology on brain function, we must first consider the Neurovascular Unit (NVU), where the coupling between neural activity and blood flow takes place. The NVU refers to a union of cells of both vascular and neural origin that work together to maintain the homeostatic equilibrium of the brain's physiological function through autoregulation and hyperemia. The NVU comprises neurons, glial cells (oligodendrocytes, microglia, and astrocytes), vascular cells (endothelial cells, pericytes and smooth muscle cells) and the basal lamina matrix within the vasculature.

Over time, NVU elements undergo multiple aging-related changes, increasing the brain's vulnerability to ischemia and predisposing it to neurovascular disease (Cai et al., 2017; T. Yang et al., 2017). Due to aging, there is a progressive failure of the endogenous DNA repair mechanisms in neurons, cytoplasm, and mitochondria-derived proteins, which triggers neuronal oxidative stress and accumulation of toxic proteins such as Amyloid β-peptide (Aβ) (Mattson & Magnus, 2006). Microglia function also declines, dramatically increasing the production of pro-inflammatory molecules and cytokines in response to noxious stimuli (Leovsky et al., 2015; Lourbopoulos et al., 2015). Moreover, damage to myelin and oligodendrocytes exceeds their capacity for repair and renewal, resulting in slower axonal conduction velocity (Peters, 2009). At the same time, astrocytes show decreased supportive capacity, limiting their regulation of inter-synaptic glutamate concentration, which triggers neuronal excitotoxicity and turns their phenotype into a pro-inflammatory one, inducing blood-brain barrier (BBB) disruption and contributing to brain inflammation. Finally, aging-associated mitochondrial failure affects substance exchange mechanisms and the ability of endothelial cells to regulate cerebral blood flow (Seals et al., 2011), and reduces endothelium-derived vasodilators, which ultimately results in the decrement of the vasodilation capacity (Nicholson et al., 2009; Prisby et al., 2006).

It is proposed that dysregulation or augmentation of these metabolic changes leads to the pathophysiological conditions causative of VCI (see Figure 8): increased BBB permeability, contributing to neurodegeneration, apoptosis, and functional disruption (Farrall & Wardlaw, 2009; Schreiber et al., 2013; Zlokovic, 2008); white matter injuries with axonal damage and even diffuse demyelination (Hase et al., 2018; Jang et al., 2017; Venkat et al., 2017); dysregulation of neurotransmitter systems, such as the cholinergic system (Caruso et al., 2019; Wallin et al., 2003); and alterations of cerebral blood flow and chronic hypoperfusion (Tak et al., 2011; D. W. Yang et al., 2002).

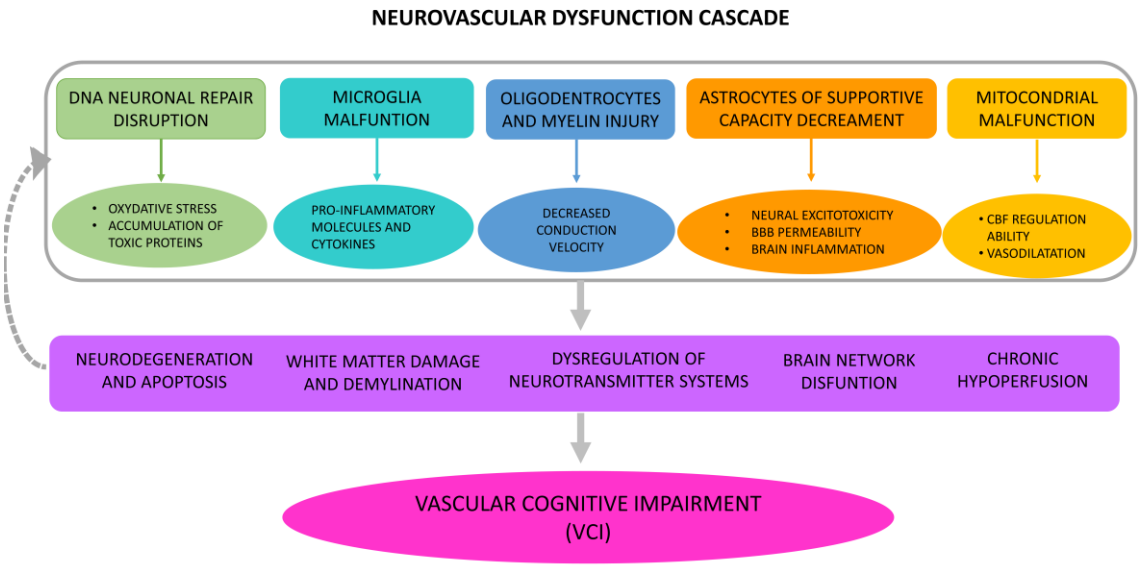

Figure 8 Vascular pathophysiology underlying VCI.

Biomarkers can be defined as body signatures that act as reliable predictors and indicators of a disease process, allowing the identification of the disease even before its clinical manifestation. Biochemical alterations occurring during VCI progression triggers structural and functional changes in the brain, that could serve as early biomarkers, even before the onset of the cognitive decline (Banerjee et al., 2020). These signatures can be captured by different neuroimaging techniques, which is precisely the principal aim of the present thesis. Once we have done an in-depth review about the terminology, subtype's classification, diagnosis criteria, and underlying pathophysiology, it is important to understand the neuroimaging techniques that could be used for the VCI research. The following chapter is dedicated to the clarification of the most representative neuroimaging techniques in research and clinical context for VCI characterization.

Chapter 2: Neuroimaging

Neuroimaging is the medical discipline that deals with the *in vivo* depiction of anatomy and function of the central nervous system (CNS) in health and disease (Fulham et al., 2004). It has become increasingly important in the clinical assessment and diagnosis of many neurological diseases, including dementia, due to the ability of aid in the differential diagnosis, early detection, tracking of progression over the time, and monitoring the effects of treatment.

In this chapter we show a brief introduction to the basic features and the information that can be obtained through the structural neuroimaging techniques (MRI and CT) that are recommended by the guidelines for VCI diagnosis for clinical and research practice (Hachinski et al., 2006; Skrobot et al., 2018). Furthermore, to the scope of the present thesis, information of the functional neuroimaging techniques is also offered, with a detailed description for the electrophysiological ones has they will be used on the further analysis (i.e., electroencephalography (EEG) and magnetoencephalography (MEG))

2.1. Structural neuroimaging techniques

Structural brain imaging can provide information about the shape, position, and, more importantly, volume of brain tissue, which can reveal certain patterns of atrophy, vascular pathology, or inflammatory changes (Wattjes, 2011). These techniques help to understand and analyze the morphological alterations induced on the brain tissues (i.e., white, and grey matter, cerebrospinal fluid, cerebral vessels) and on the skull.

According to current international diagnosis guidelines, neuroimaging, preferably MRI, should be performed at least once during the diagnostic work-up of patients with suspected or definite dementia (Wattjes, 2011) and specially for CBVD identification and differentiation ((Skrobot et al., 2018; Wardlaw et al., 2013). In fact, imaging evidence of certain cerebrovascular events is one of the requirements for VCI diagnosis. Remember that if no imaging data is available, only a diagnosis of "possible" VCI can be made. As mentioned before, VCI includes a great number of cerebrovascular damages (i.e., ischemic, and hemorrhagic strokes in different brain vessel's location and with diverse etiologies, sizes, and number of lesions) that finally produce a brain structural injury. Thanks to the neuroimaging advances, all these brain lesions of presumed vascular origin can be captured and identified for early diagnosis, and especially for accurate differentiation of cerebrovascular pathologies from other subtypes of dementia. Introduction, physical features, and clinical utilities of both structural neuroimaging techniques recommended for VCI diagnosis in the DSM-5 and VICCCS-II are described below:

Computerized tomography (CT)

Computerized (or computed) tomography, also referred to as computerized axial tomography (CAT), is an X-ray procedure that combines many X-ray projections with the aid of a computer to generate cross-sectional views and, if needed, three-dimensional images of the internal organs

and structures of the body. It was one of the earliest techniques to determine brain structure, and it is used to define normal and abnormal structures in the body and to assist in procedures by helping to accurately guide the placement of medical devices or treatments. CT is a non-invasive technique, although the patient is exposed to a low amount of X-ray radiation. Due to its physical properties, it is especially suited for the visualization of high-density tissues, such as bones, but not as good for the differentiation of low-density organs. Furthermore, it offers a good spatial resolution, well under 1 mm.

Cerebral CT is still widely used for routine management of patients with neurologic and neurosurgical conditions. It can rapidly identify cerebral edema, atrophy, hydrocephalus, cerebral infarction, and hemorrhage, as well as mass lesions (i.e., infections or tumors). Moreover, CT is the technique used in the evaluation of the skull in the context of traumatic head injury (Fulham et al., 2004). Limitations of CT include the radiation exposure (as X-rays are ionizing radiation), artifacts caused by patient motion, and low contrast resolution for soft tissue. CT has a limited use in VCI research because it measures only acute vascular lesions or severe disease, and the findings are difficult to quantify due to the low contrast resolution (see Figure 9). Because of this limitation, in VCI diagnosis when only CT imaging is available, "probable" VCI is the appropriate diagnostic category (Skrobot et al., 2018)

Magnetic resonance image (MRI)

MRI is a non-invasive medical imaging technique used to generate images of the anatomy and the physiological processes of any part of the body. MRI scanners generate a powerful, uniform magnetic field which aligns the protons that are normally randomly oriented, including those within the hydrogen nuclei in water molecules of the tissue being examined. This alignment (or magnetization) is then perturbed or disrupted by the introduction of external radio frequency energy. The nuclei return to their resting alignment through various relaxation processes, and in so emit a radio frequency signal that is captured by an array of sensors in the scanner. Depending on the tissue properties, the relaxation times will vary. These differences in tissue relaxation times are the main determinants of image contrast. By varying the sequence (i.e., the nature and duration) of radio frequency pulses applied, different types of images can be obtained, allowing to better detect different brain tissues of interest:

- T1 (longitudinal relaxation time) is the characteristic time that takes the excited protons to return to equilibrium. T1-weighted images have high contrast between white matter (bright), gray matter (darker gray), and cerebrospinal fluid (darkest), allowing the detection of morphology-related pathologies. Furthermore, abnormal low signal (i.e., darker areas) on T1 images is related to loss of fatty tissue and increase in water content, which frequently indicates a pathological process such as trauma, infection, or cancer.
- T2 (transverse relaxation time) is the characteristic time that takes the excited protons to go out of phase with each other. In T2-weighted images, white matter (darkest), gray matter (dark), and cerebrospinal fluid (bright) can be differentiated, and it is especially suited for detecting soft tissue pathologies. Abnormal brightness (i.e., whiter areas) on a T2 image indicates increased water content, which is related to certain lesions, for example those referred as white matter hyperintensities.

- A third commonly used sequence is the Fluid Attenuated Inversion Recovery (**FLAIR**). It is a sequence that is usually employed to achieve a T2-weighted image, with the particularity that the times in the sequence of radio frequency pulses are very long. By doing so, abnormalities remain bright but normal cerebrospinal fluid (CSF) fluid is attenuated (thus the name) and made dark. This means that the lesions are still bright while the surrounding fluid is not, making this sequence very sensitive to pathology, and the differentiation between CSF and an abnormality much easier.
- The diffusion weighted image (**DWI**) is inherently a series of T2-weighted sequences specially targeted to detect random movement of protons in water molecules (i.e., Brownian motion) along a magnetic field gradient, and induces signal attenuation quantified by a diffusion coefficient (mm^2/s). If there is no net movement of molecules (i.e., tightly confined molecules), their underlying T2 signal intensity is preserved, resulting in a hyperintense DWI signal. On the contrary, a net movement of water molecules along the direction of the gradient (i.e., free movement of molecules in that direction) causes dephasing with underlying T2 signal loss, resulting in hypointense DWI signal. DWI is usually characterized in several directions and allows to identify and characterize compact matter (no net movement), free water (movement in any direction), and tubular structures like axons (movement only in one direction). It is a sensitive marker for evaluating alterations in tumor composition and a helpful aid in the determination of acute ischemic stroke. DWI is widely used to characterize brain white matter (WM), particularly through the use of the method named diffusion tensor imaging (DTI).

MRI is a highly used technique in the clinical setting in oncology, soft tissue damage assessment, and especially in neurology and neuroscience. Brain MRI shows great contrast to the different tissues (gray matter, white matter, CSF etc.) allowing for the segmentation (identification of tissues), and even to determine the volume of individual structures to compare the size across subjects or groups of subjects. It also offers a good spatial resolution; both in clinical and research practice it is common to find images with a spatial resolution around 1 mm.

According to current VCI diagnosis guidelines, MRI is the gold standard for imaging (Hachinski et al., 2006; Skrobot et al., 2018; Wardlaw et al., 2013). The MRI sequences explained before are able to detect specific brain lesions of vascular origin: 1) T1 is used to study brain atrophy, discern gray from white matter and discriminate some SVD signs, specially lacunes from dilated perivascular spaces; 2) T2 is able to characterize brain structure, identify old infarcts and differentiate lacunes from WMH and perivascular space; 3) FLAIR is, as T2, also able to identify WMH and established cortical or large subcortical infarcts, but more adequate to differentiate white matter lesions from perivascular spaces and lacunes due to the darkening of CSF, allowing an easier differentiation between these and CSF in the ventricles; and 4) DWI is very useful in the detection of acute ischemic or hemorrhagic infarction, and the study of the effect of vascular lesions (i.e., small vessel disease) in white matter integrity. The correct use of the different sequences according to the vascular damage may be crucial for a correct detection and quantification, as can be appreciated in Figure 9.

Given the advantages of MRI versus CT, and the international consensus recommendations for VCI diagnosis, T1, FLAIR and DWI images will be employed in the experimental studies developed in the present thesis.

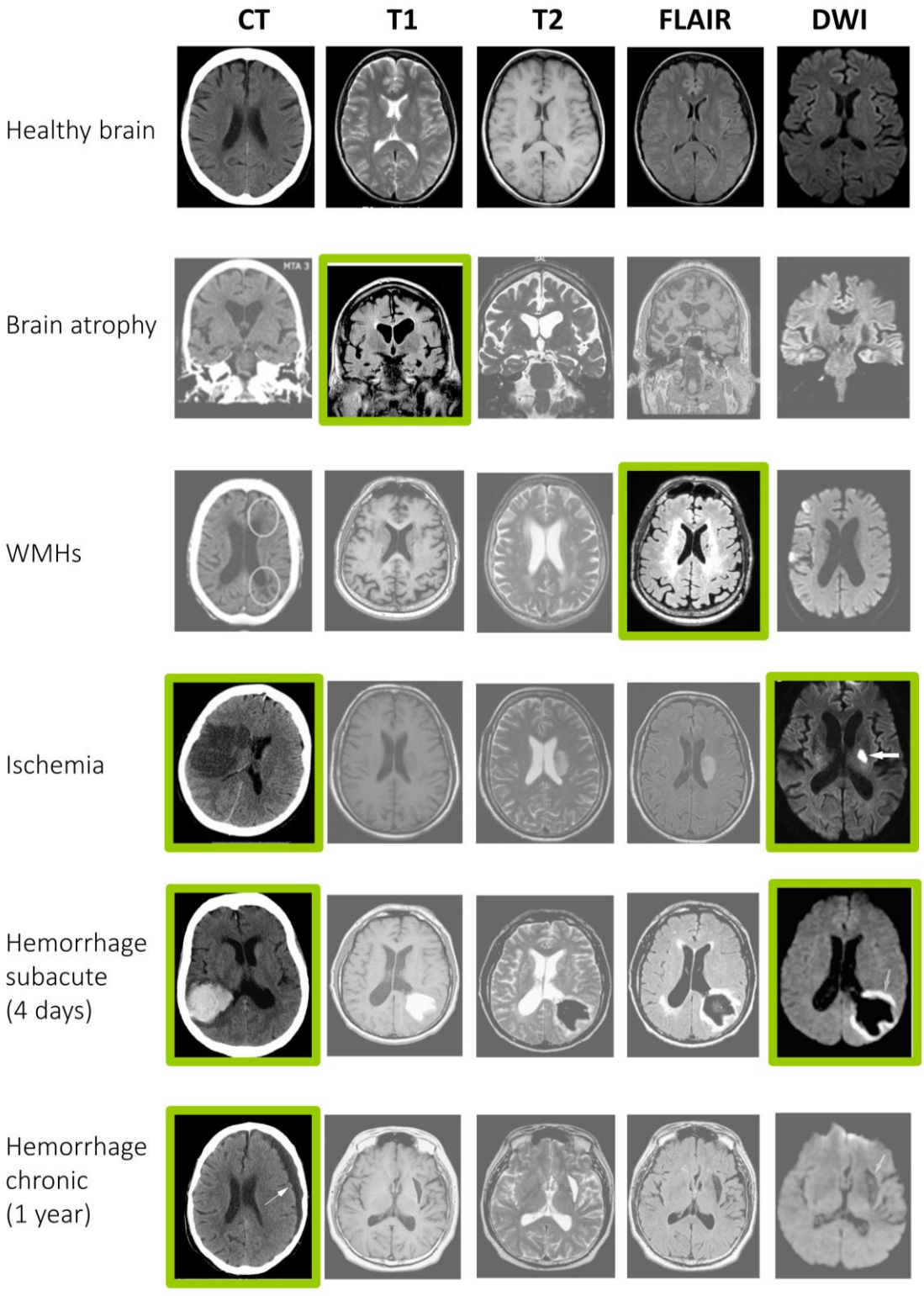

Figure 9 Structural neuroimaging overview of the main type of vascular damages described in the VICCCS-II neuroimaging guideline for VCI diagnosis. These damages are showed for the main structural neuroimaging techniques described before. Rows from left to right: computerized tomography (CT) and magnetic resonance imaging in four sequences (T1, T2, Flair and DWI). The green squares indicate the most appropriate technique for detecting each vascular damage.

2.2. Functional neuroimaging techniques

Functional brain imaging reveals how cells in various brain regions are working together in a certain brain state (e.g., in resting state or during some behavioral task). Although structural neuroimaging is included within the diagnostic criteria for different dementias, they only partially account for the heterogeneity of behavioral outcomes. For instance, in AD dementia metabolic alterations occurring years before the onset of clinically evident symptoms may induce functional changes that can be captured using functional techniques (Dubois et al., 2016; Jiang et al., 2017; Nakamura et al., 2018).

Brain functioning imaging started with the development of EEG in the 1920s to assess the bioelectrical basis of human brain function (Hans Berger, 1929; Millet, 2022) After that, many functional neuroimage techniques have been developed, and they can be divided in three broad categories depending on what physiological phenomena occurring in the brain are able to capture:

- *Measuring neural metabolism.* The central nervous system consumes around ten times more energy than the average of the peripheral tissue and relies almost exclusively on glucose to fuel its neural activity (Lundgaard et al., 2015). Positron emission tomography (PET) imaging can be used to measure the mentioned metabolic function. This technique is based on a radio-labeled (radioactive biocompatible) compound that is injected into the patient. Depending on the administered compound, either brain structure or function can be measured. Specifically, 2-fluoro-2-deoxy-D-glucose (18FDG), a radioactive molecule that mimics glucose, is routinely employed to identify activity-dependent increases in local metabolic function in the human brain. The modified glucose is taken up by nerve cells, and when radioactive atoms decays, high-energy particles are emitted. The tomography scan can detect these particles and quantify the amount and location where they are generated, indicating the areas of high glucose consumption (Aguirre, 2014).

- *Measuring neurovascular changes.* Local changes in neural activity give rise to local changes in blood flow and blood oxygenation—thus the term "neurovascular coupling." When the load of neural processing of information increases, so does the need for fuel, in the form of oxygen and glucose. Correspondingly, when neurons increase their activity, local blood vessels increase in size, allowing more blood to flow to the active areas, increasing their local concentration of oxygen. Measurement of this increase in tissue oxygenation following neural activity is the basis of blood-oxygen-level-dependent (BOLD) functional magnetic resonance imaging (fMRI). The way in which an MRI scanner ultimately measures this proxy of neural activity—oxygen levels in the blood—is the consequence of a chain of associations that allows fMRI to make indirect measurements of neural activity (Aguirre, 2014).

- *Measuring electrical activity in the brain.* The main form of information transfer in the nervous system is the movement of ions across the cell membrane of neurons. This movement produces electrical currents and changes the electrical potential (voltage) of the neurons. The change of the electrical properties of the neuron is termed primary current, as it is allocated inside the neurons. As the charged particles are exchanged with the extracellular fluid, a secondary current also appears outside of the neuron and, because it is not confined to the interior of a cell, diffuses throughout the extracellular space (Baillet et al.,

2001), reaching distance areas. Additionally, both electrical currents generate related magnetic fields perpendicular to them. These phenomena are depicted in Figure 10. "Electrophysiologic" neuroimaging techniques are able to capture this electrical brain activity (Aguirre, 2014). Specifically, the measurement of electrical potential differences generated by secondary currents is the basis of EEG, while MEG primarily measures the magnetic field produced by the spatial and temporal distribution of the primary currents in the brain (Lopes da Silva, 2013).

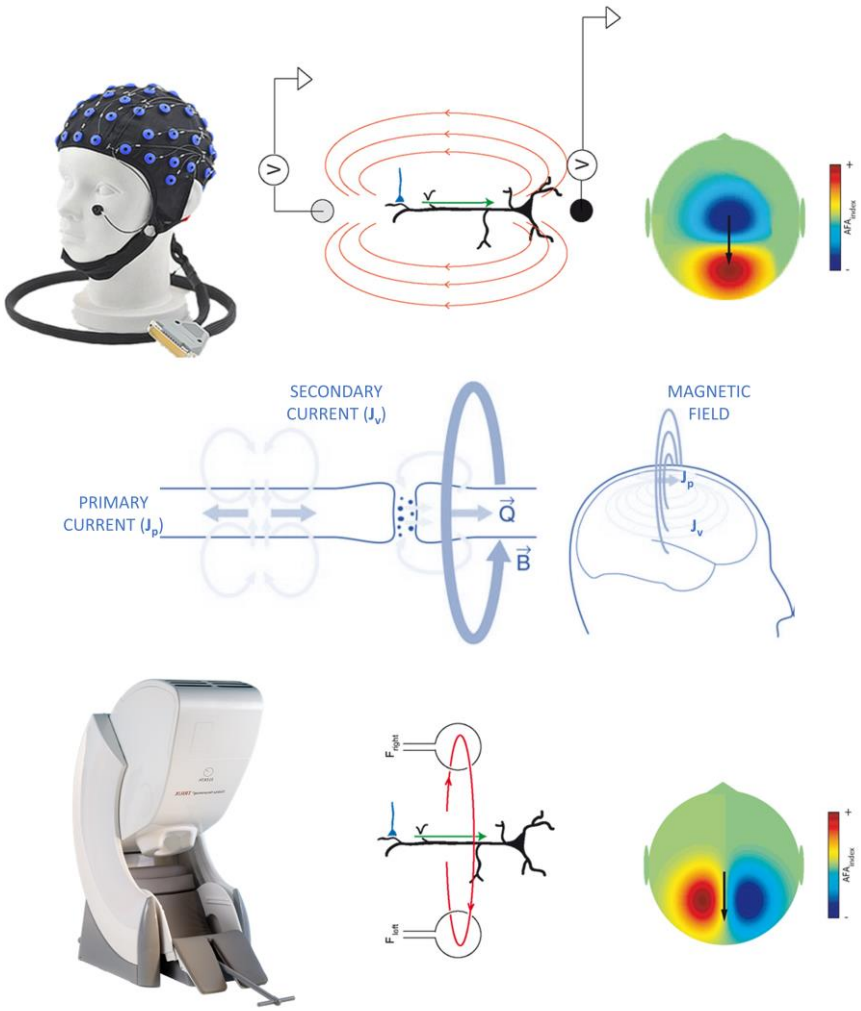

Figure 10 Origin of EEG and MEG signals. EEG measures the electrical potentials that are generated by the flow of current through the extracellular fluid surrounding neurons (secondary currents). MEG registers the magnetic field generated by the flow of primary currents through the neurons in the brain.

The different neuroimaging techniques make different trade-offs in spatial and temporal resolution. Although the electrically based measures (EEG and MEG) provide lower spatial resolution —they are not that good at detecting **where** in the brain the activity is occurring—, they provide high temporal resolution —this is, they are good at specifying **when** a given neural activity of interest begins and ends. With the metabolic and neurovascular techniques, such as BOLD fMRI and PET, the situation is the opposite: they have better spatial resolution but poorer temporal resolution, as the metabolic changes that they detect occur many seconds after the

changes in brain activity of interest (Aguirre, 2014). A comparison of spatial and temporal resolution between the techniques described above is represented in Figure 11.

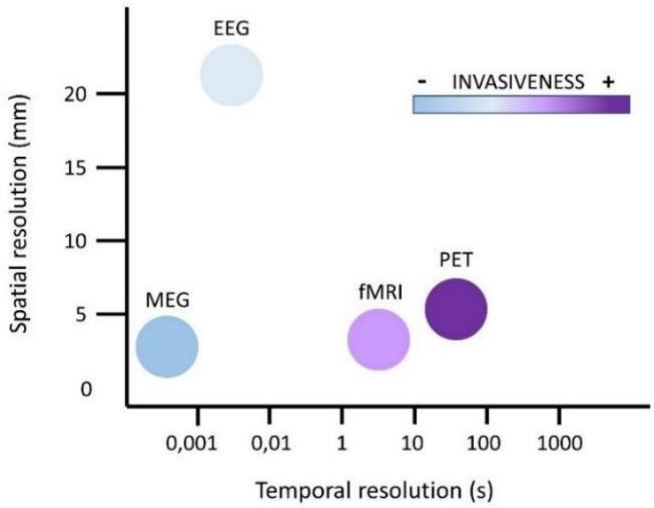

Figure 11 Relative spatial and temporal resolution of functional neuroimaging. Adapted from: "Magnetoencephalography as a putative biomarker for Alzheimer's disease". Zamrini, E., Maestu, F., Pekkonen, E., Funke, M., Makela, J., Riley, M., Bajo, R., Sudre, G., Fernandez, A., Castellanos, N., Del Pozo, F., Stam, C. J., van Dijk, B. W., Bagic, A., & Becker, J. T., 2011. International Journal of Alzheimer's Disease

Electrophysiologic techniques are of special interest for the present thesis, as they bring useful information for assessing brain function and network dynamics, revealing changes inaccessible to standard structural imaging techniques. Besides from the benefit of the millisecond resolution, electrophysiologic techniques are capable to measure the neural activation directly, instead of doing it by means of indirect measures such as blood flow or metabolism and allow repeated measurements without any risk for the subjects, since are the most ecological techniques for the participants.

Electrophysiological brain activity

The main generator of the signals recorded outside the scalp by EEG/MEG is the synchronized electrophysiological activity of thousands of pyramidal neurons. This type of neurons, excitatory in nature, make up 80% of the neocortex, the remaining 20% being inhibitory neurons. The particularity of pyramidal neurons is that they are arranged in the cortex in the form of a palisade (see FIGURE 3X), with their apical dendrites parallel to each other and perpendicular to the cortical surface (Lopes da Silva, 2013). This spatial symmetry allows thousands of synchronously activated pyramidal neurons to aggregate the longitudinal components of their postsynaptic potential currents (called principal currents). The sum of all these currents is strong enough (≈ 10 nA) to generate an electromagnetic field that can extend over long distances and be measured by EEG/MEG systems (M. Hämäläinen et al., 1993). Action potentials contribute little to EEG/MEG signals because they are too fast (1-2ms) to facilitate their synchronization. Furthermore, they

decay much faster due to their quadripolar nature ($1/r^4$), as opposed to the dipolar nature of postsynaptic potentials ($1/r^3$). Consequently, EEG/MEG signals are mostly generated by the interaction between inhibitory interneurons and excitatory pyramidal cells that create an alternating balance between states of excitation and inhibition (Buzsáki, 2006; Cohen, 2014).

The resulting electromagnetic activity recorded by EEG/MEG outside the scalp reflects a rhythmic pattern associated with the degree of synchronization of large populations of neurons in the brain. The more synchronized the activity of the neural assemblies, the greater the signal that reaches the scalp surface. The synchronization can occur, often simultaneously, on many spatial and temporal scales (Varela et al., 2001): at the local level (sort-range synchronization), or between distant neuronal ensembles (long-range synchronization); it can last only a few milliseconds (for example, an epileptic spike) or extend over several seconds (e.g., alpha trains). This complexity has generally been addressed by compartmentalizing the dimensionality of the data, focusing on studying certain fragments of the information contained in the electrophysiological signals, while controlling the others. One of the main approaches is the creation of frameworks to study the spatial activation of the brain: from the quantification of brain activity in a certain brain region, to the evaluation of communication patterns between different areas of the brain. On one hand, regional brain activity is commonly analyzed by either evaluating the amplitude of the electromagnetic fields in the time domain, or performing spectral analysis, using the Fourier transform, to quantify the energy of each brain rhythm in frequency space. On the other hand, the evaluation of interregional communication patterns is a relatively recent approach that uses mathematical methods to calculate the statistical interdependence, the connectivity, between EEG/MEG signals, providing information at the network level. In this framework, the sensors/sources that originate the electrophysiological signals act as network nodes and the connectivity values are considered measures of the link between each pair of nodes (Cohen, 2014; Fornito et al., 2016; Maestú, Pereda, et al., 2015).

In addition to temporal and spatial dimensions, electrophysiological cerebral oscillations are waves, which means that they can be characterized by three parameters: 1) frequency, defined as the number of cycles per unit of time; 2) power, calculated as the square of the amplitude of the oscillation; and 3) phase, the relative position of the wave at an instant of time. Although the brain's electrophysiological signals are intricate multidimensional oscillations, in practice they are broken down, usually using the Fast Fourier Transform (FFT), into a few frequency bands, generally referred to as "classical". These classical frequency bands are electrophysiological oscillations, defined by characteristic frequency ranges and topographic locations, which have been extensively studied and are considered useful for studying the neural mechanisms underlying different cognitive and behavioral states, and for developing diagnostic and therapeutic tools. for neurological and psychiatric disorders. The most prominent are: 1) Delta waves (0.5-4 Hz), typically observed during deep sleep and also appear in epileptic seizures and loss of consciousness. These waves are commonly located in frontal regions and can be considered an inhibitory rhythm; 2) Theta waves (4-8 Hz), are associated with a variety of cognitive processes, including memory formation and spatial navigation. Its location informs about the attentional state of the individual: a low attentional state is associated with generalized theta oscillations distributed throughout the scalp, whereas focused attention can be inferred when theta is located in the frontal midline of the scalp (Schacter, 1977); 3) Alpha waves (8-12 Hz), are the most prominent during the resting state of the brain, especially with the eyes closed,

reaching their maximum power in the posterior-occipital region (Lopes da Silva, 2013). 4) Beta waves (12-30 Hz), are associated with a variety of cognitive processes (Engel & Fries, 2010), including motor control, attention, and working memory. They are commonly found in the central frontal regions of the brain; and 5) Gamma waves (30-100 Hz), are believed to reflect complex integration and association processes that require high temporal and spatial precision (Binding hypothesis) (Buzsáki et al., 2012).

Magnetoencephalography

At the macroscopic level, beyond the underlying complexity, the emerging information consists of values over time of voltage (EEG) or magnetic field (MEG), which create the waves that constitute electrophysiological oscillations. In the case of EEG, the voltage is a relative measure, usually in microvolts (μV), that corresponds to changes in electrical potential between each electrode and the reference. A typical EEG system uses a set of electrodes placed directly on the surface of the scalp, that could vary from the tens to few hundred sensors (Klem et al., 1999). On the other hand, MEG directly records the magnetic field, commonly femtotesla (fT), which emerges perpendicular to the scalp surface, originated by those neurons whose dendrites are oriented at right angles to the sulcus walls (the cortical folds) (M. S. Hämäläinen & Ilmoniemi, 1994; Lopes da Silva, 2013) (See Figure 12, right).

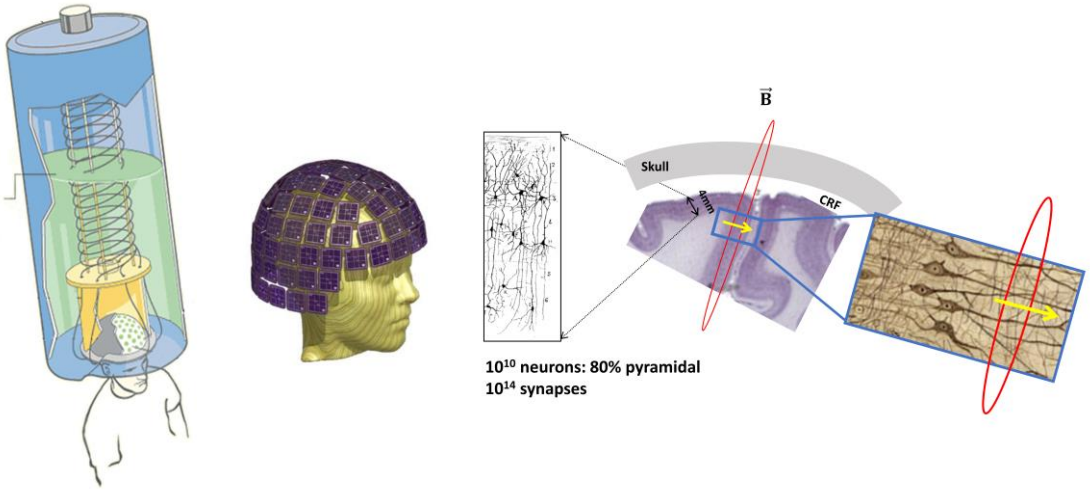

Figure 12 Left, schematic representation of the MEG system. Center, Elekta MEG helmet with 102 sensors. Right, origin of the MEG signals.

The MEG is a non-invasive and completely silent system capable of detecting the weak magnetic activity generated by the brain. The participant can be sitting or lying down, while their head is placed inside a helmet where the sensors are located (see Figure 10 and Figure 13, B). Modern MEG systems typically have hundreds of sensors, and the MEG studies described in this thesis use a 306-channel Vectorview system (Elekta Neuromag), consisting of 102 magnetometers and 204 planar gradiometers (see Figure 12, center). The MEG is 20 to 40 times more expensive than an EEG because the brain's magnetic fields range from 1 fT to 100 pT (M. Hämäläinen et al., 1993), which are 100 million times lower than the Earth's magnetic field. In order to do so, a MEG system requires three components: 1) a magnetically shielded room (see Figure 13, A & B) that is

composed of different layers of aluminum and a material, called μ-metal, with a very high permeability, which protects against static or low-frequency magnetic fields; 2) sensors composed of extremely sensitive devices called Superconducting Quantum Interference Devices or SQUIDs, which allow the detection of magnetic activity in the brain, and flow transducers that act as antennas to project the magnetic flux onto the SQUID (M. Hämäläinen et al., 1993) (see Figure 13, E); and 3) a Dewar flask, filled with liquid helium at its boiling temperature (4.2 K) and thermally insulated to keep the exterior of the MEG helmet at room temperature. The Dewar flask is needed to maintain the MEG sensors in a superconductor state (see Figure 12, left and Figure 13, E).

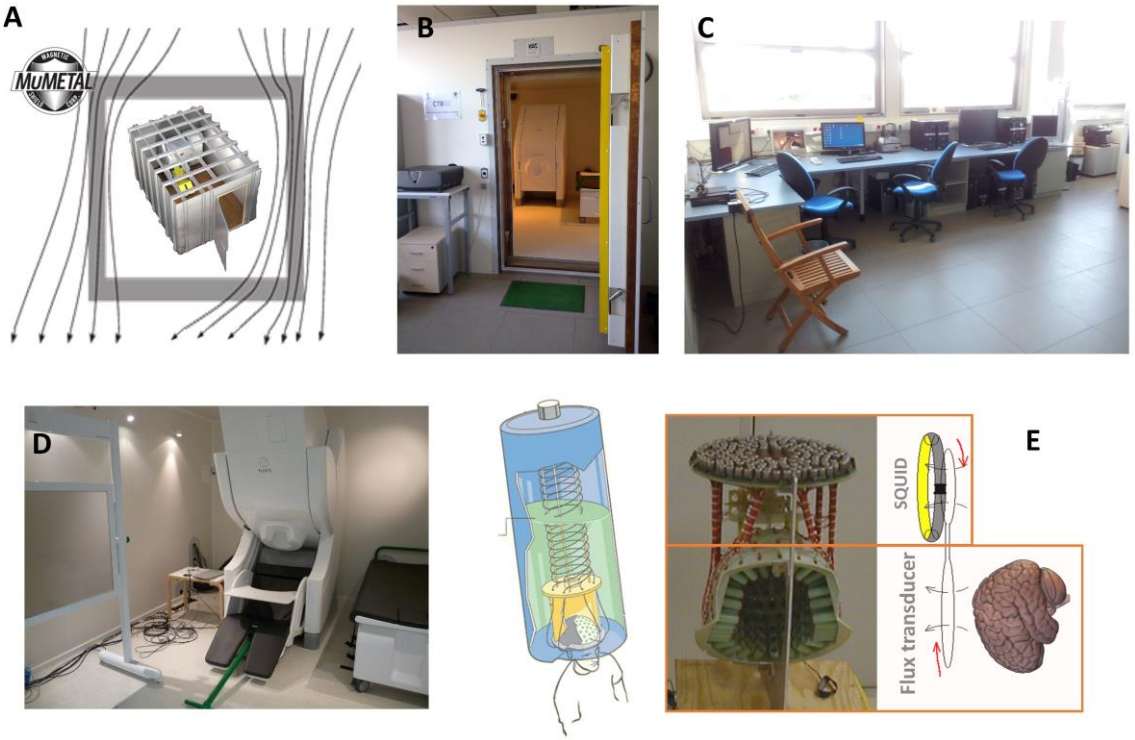

Figure 13 MEG system. ***A*** *Sketch of a magnetically shielded room (MSR) reflecting magnetic noise.* ***B****, MSR gate giving entry to the MEG system.* ***C****, MEG operating room.* ***D****, MSR interior: MEG system stimulus screen, recording chair, and recording bed.* ***E****, main electronic devices required to detect brain biomagnetic activity. All images correspond to the MEG system installed in the Center for Biomedical Technology in Madrid*

Comparison between MEG and EEG

EEG and MEG can essentially measure the same underlying electromagnetic brain activity, but the origin and biophysical mechanisms of their signals are different, which determines their limitations. Therefore, the selection of the most appropriate technique would depend on the purpose (e.g., clinical use or research). For example, the main limitation of EEG is the difficulty to estimate the true origin of its electrophysiological signals. Currents recorded at the scalp are generated in the brain, travel through the brain, diffuse through the cerebrospinal fluid, and travel through the skull, always following the path of least resistance. The signal acquired at the scalp is affected by the electrical properties of the head, and the estimation of the path followed

is a complicated task. On the contrary, magnetic fields are very little disturbed as they pass through the different tissues of the head since they all have the same magnetic permeability. This disadvantage of EEG in assessing brain activity in source space can be ameliorated by using structural 3D MR imaging to create individualized 3-layer patient head models, although MEG works very well with 1-layer head models.

In this context, it could be concluded that MEG presents some technical advantages over the EEG as for example: 1) a better disposition for the estimation of neural sources, since the solution of the inverse problem in MEG is easier than in EEG; and 2) a better signal to noise ratio for higher frequency bands (> 45Hz). However, EEG is a much cheaper medical device, and it is frequently available in the clinical setting throughout the world. It can be easily transported, and its recordings can be made in all types of settings, while the MEG is confined to the interior of the MSR.

Electrophysiological signatures of cerebrovascular damage

The study of electrophysiological brain signatures (i.e., EEG and MEG) have been well established for early detection and prognosis in neurodegenerative disorders (David López-Sanz et al., 2019; Stam, 2010) like Alzheimer's disease (David López-Sanz et al., 2018; Nakamura et al., 2017, 2018), Parkinson's disease (Olde Dubbelink et al., 2014; Stoffers et al., 2008), Lewis body dementia (Matar et al., 2019), and mild cognitive impairment (David López-Sanz et al., 2017; Maestú, Peña, et al., 2015; Nakamura et al., 2018; Pusil et al., 2019).

Biochemical alterations occurring in VCI (see Chapter 1, section Vascular pathophysiology underlying VCI.) are able to modify cell membrane polarity, action potentials, and cell-to-cell communication, altogether disturbing brain electrophysiological functioning. Cortical activity depends on a complex balance among different systems of neurotransmitters within cholinergic pathways. As explained before, the failure in the NVU triggers alteration of neurotransmitters' functioning. Furthermore, spike timing is vital for proper communication between neurons, and the loss of myelin found in CBVD is known to cause reduction of the speed conduction and may disrupt connectivity at a microscopic scale. These pathological mechanisms are predominantly involved in white matter alterations present in VCI, in which EEG indications of failure in macroscopic scale timing have been previously reported (van Straaten et al., 2015). Therefore, MEG and EEG quantitative analysis provide the opportunity to study disruption of brain functioning due to changes in synaptic potentials produced by vascular-related pathophysiological alterations in a direct and non-invasive way, with millisecond precision.

In this context, in order to find new biomarkers, specially based on brain electrophysiological information, for early differentiation of cognitive impairment of vascular origin it is important to have a clear picture of the previous knowledge in the field. With this purpose, the next chapter is focused on the exposition and analysis of the state-of-art electrophysiological signatures, measured with EEG and MEG, which characterized the VCI.

Chapter 3: Electrophysiology (M-EEG) as a biomarker for VCI: systematic review

Electrophysiological signatures are yet not included in standardized guidelines for VCI diagnosis. However, EEG and MEG are non-invasive techniques with the ability to detect changes in brain functioning, suggesting its use to seek biomarkers for early detection and longitudinal tracking of VCI. In particular, EEG is a low-cost technology widely distributed in the clinical context that can be used as a first-level scan for brain pathology, whereas MEG offers higher frequency and spatial resolution (Hedrich et al., 2017), that increase its ability to detect specific vascular-associated pathology. The high prevalence of cerebrovascular disease, along with its modifiable risk factors, support the need for a research effort to study electrophysiological methods that could be useful to detect and differentiate early cognitive impairment, specially trying to reinforce electrophysiological or neurophysiological VCI research to include it as complementary diagnosis criteria (Babiloni et al., 2021). In this context, the first study of the present thesis involved an exhaustive systematic review to obtain a clear picture of the literature regarding neurophysiological patterns for mild and major VCI, before trying to look for specific biomarkers in the experimental studies. This study has been already published in a JCR indexed journal:

Torres-Simon, L., Doval, S., Nebreda, A., Llinas, S. J., Marsh. E. B., & Maestu, F. (2022) Understanding brain functioning in Vascular Cognitive Impairment and Dementia with EEG and MEG: a systematic review. ***Neuroimage: Clinical. https://doi.org/10.1016/j.nicl.2022.103040***

The review included all studies carried out with EEG and MEG that assessed all the subtypes of VCI described by the VICCCS. No exclusion was performed by the specific signal analysis executed in the studies (i.e., visual, spectral, connectivity, event-related potentials, or entropy).

3.1. Methods

Literature search

A systematic search of literature was conducted in September 2020 using the PubMed, Cochrane, Web of Science and PsycInfo databases utilizing the PICO search strategy ((Miller & Forrest, 2001). Keywords included “vascular dementia" OR “vascular cognitive impairment" OR “vascular cognitive disorder" OR “cerebrovascular disease" OR “cerebrovascular disorder" OR “multi-infarct dementia" OR “subcortical ischemic dementia” OR “post-stroke dementia” OR “mixed dementias'' OR “mild vascular cognitive impairment”) AND (“EEG” OR “electrophysiology” OR electroencephalogra* OR “MEG” OR magnetoencephalogra* OR “neural oscillation” OR “brain oscillation” but NOT epilep* [Title/Abstract].

Article's inclusion and exclusion criteria

Articles meeting the following criteria were included: 1) articles must be written in English and 2) they must be peer-reviewed and published in journals indexed in journal citations reports (JCR) since January 2000 (for a review that includes older papers see Babiloni et al., 2021). Study participants included patients 60 years of age or greater who were diagnosed with vascular cognitive impairment (either mild or major VCI). In order not to be too restrictive, we accepted any diagnostic criteria indicative of VCI. Studies also had to report EEG or MEG data and include neuropsychological assessment or/and MRI as diagnostic criteria. Since epilepsy events might affect establishing an accurate criterion for VCI diagnosis, those articles focused on epilepsy were excluded and those focused on treatment evaluation. Familial pathologies were excluded as they were not the scope of this review. Finally, according to the DSM-5 (American Psychiatric Association, 2013) and VICCCS-2 guidelines (Skrobot et al., 2018), the diagnosis of PSD should be within six months of the stroke. Articles reporting post-stroke patients in the acute phase were excluded as the focus of this review is to characterize diagnosis criteria for VCI and its subtypes.

Screening protocol

The review was registered in PROSPERO CRD42020152953 to avoid duplication and followed a systematic review protocol to ensure the reliability of the process (Moher et al., 2014; Stewart et al., 2012). Articles were imported into COVIDENCE (Veritas Health Innovation). Two reviewers (SD and LT) conducted the review process as recommended in the Preferred Reporting Items for Systematic Reviews and Meta-Analyses (PRISMA) guidelines for systematic reviews (Moher et al., 2010). In the first stage, the article's abstracts were independently screened according to the established inclusion and exclusion criteria. The full texts of the selected articles were obtained and subsequently reviewed. Disagreements were resolved by expert's meetings (screening and final selection protocols are depicted in Figure 14).

Quality assessment

Three reviewers (LT, SD and AN) independently assessed the quality of the articles selected using the Tool for cross-sectional studies using biomarker data - BIOCROSS (Wirsching et al., 2018). The specific evaluation of the items was adapted, as some items could not be easily applied due to the nature of the research field and electrophysiological biomarkers. These specifications did not modify the structure of the scale or the aim of study for each item. The changes only attempted to clarify the quality standards in agreement with the study population (i.e., VCI diagnosis criteria) and neurophysiology technical specifications, research protocol or data processing and modeling (For more details, see supplementary material included in Torres-Simon, et al., 2022). The review was conducted in two rounds. After the first evaluation, the reviewers met to discuss their scoring and addressed potential discrepancies. However, the results were nearly identical across the two rounds. The analysis of both rounds (pre and post) with intra class correlation coefficient (ICC) across the 3 reviewers found significant (p value $<< 0.05$) high ICC scores. Originally, inter-reviewer consistency reached an ICC = 0,811 (95% CI: 0.692-0.895). After discussing the differences and reaching consensus, the ICC raised up to 0,969 (95% CI: 0.946-0.984). No articles were excluded based on the quality assessment. Final scores for the 32 articles in each quality item and for the three reviewers in the second round are reported in the supplementary material included in Torres-Simón et al., 2022.

3.2. Brief results and Discussion

A total of 586 articles were imported for screening after conducting a literature search in the specified datasets. After removing those duplicates and those irrelevant for the aim of this systematic review, a total of 74 studies were assessed for eligibility. Based on the exclusion criteria, 42 studies were excluded: nine of them were not JCR; thirteen did not include a vascular cognitive impairment diagnosis; eight did not use MEG or EEG; six were systematic reviews; four included a vascular dementia diagnosis less than six months after stroke; one did not use neuropsychological or MRI assessment; and one focused only on treatment evaluation. 32 studies were finally included in this systematic review (Figure 14).

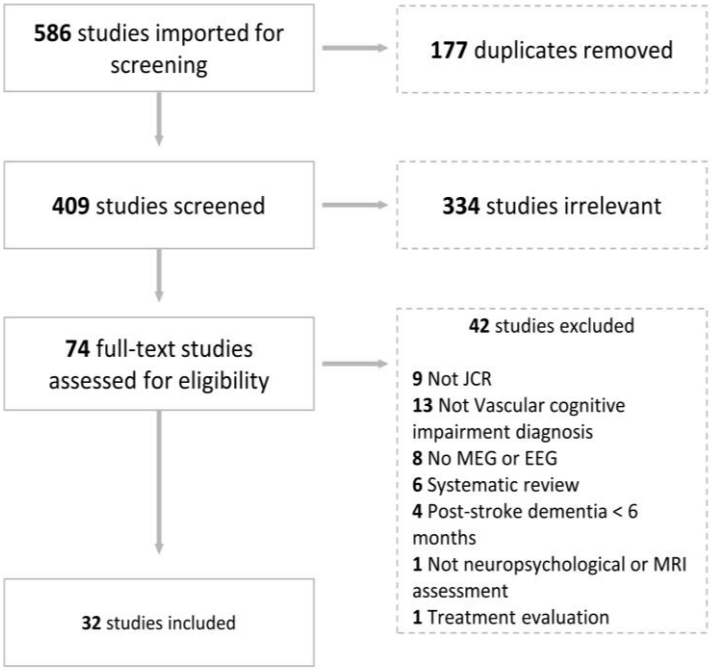

Figure 14 Flowchart of included and excluded articles through the screening process following the PRISMA presentation guidelines.

Frequently in systematic reviews, meta-analysis is not possible or appropriate due to incompletely reported effects or characteristics of the studies selected (design, population, experimental condition, or data analyses). In these situations, to be clear and rigorous, alternative synthesis methods may be adopted. Due to the diversity in subtypes of dementia, severity, recording conditions, and research and analysis methods, there was no simple way to aggregate the results found in the present systematic review. We, therefore, employed specific guidelines for data extraction and synthesis following a structured method called synthesis without meta-analysis (SWiM) (Campbell et al., 2020). First, results were divided attending to the type of analysis: visual, spectral, functional connectivity, event-related potentials (ERPs), and entropy and complexity. For each type of analysis, they were segregated in terms of the groups that were compared: 1) studies comparing VCI vs. healthy controls (HC); 2) and studies that included comparisons between VCI and AD. Finally, when it was possible the precise subtype of vascular

dementia was specified according to VICCCS (Skrobot et al., 2017, 2018). For further details about data extraction and synthesis see (Torres-Simón et al., 2022).

The most impressive information revealed by this systematic review was that only one study out of the 32 included in the final selection was performed with MEG. Regarding the type of method applied, considering that some articles use more than one, three articles performed a direct visual analysis; thirteen used spectral analysis; five measured connectivity; eight developed ERPs; and six described entropy or complexity measures. Of the articles included, sixteen compared VaD with AD and seven compared groups of VaD with different severities. Furthermore, despite not including between-group comparisons, various articles included correlation measures with cognitive or neuropsychological tests, related with the severity of the disease. Regarding the subtype of dementia, of the 32 articles that were finally included in the review, nine did not specify the subtype that was being studied, nor did they give enough details about the diagnostic criteria to allow us to classify them in one specific subtype; sixteen could be classified as studying subcortical ischemic vascular dementia; seven as post-stroke vascular dementia; and one as mixed dementia (VaD-AD).

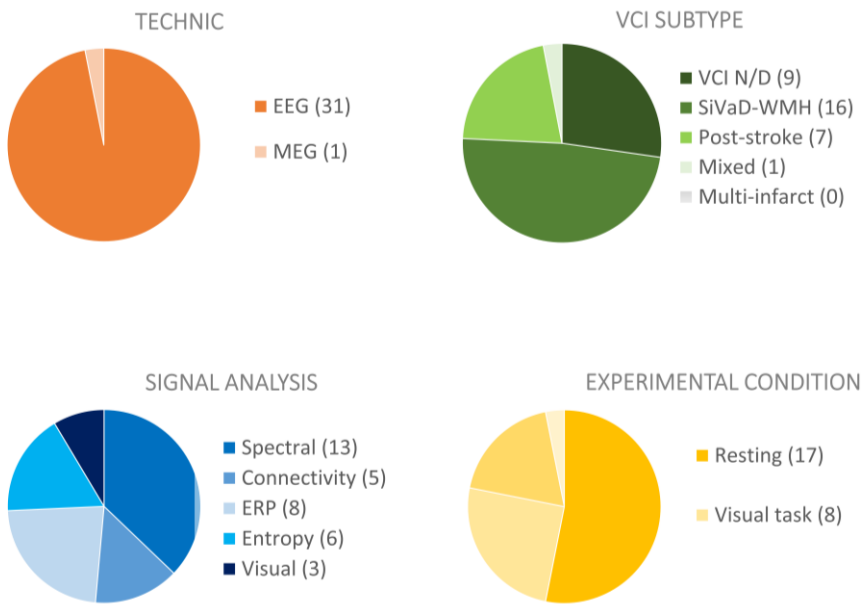

Figure 15 Classification and number of studies included in the systematic review.

The heterogeneity within the existing literature with respect to both the study population and methods of analysis makes the generalization of conclusions difficult. In most cases it is not possible to differentiate between VCI subtypes, or to assess the degree of comorbidity in mixed dementia patients. Most of the papers included in this systematic review do not report objective MRI measures to estimate structural vascular damage, or neuropsychological batteries beyond MMSE scores. This illustrates a significant knowledge gap in VCI literature, likely secondary to changes in terminology and the inclusion criteria over time. This heterogeneity, along with relatively small sample sizes, may explain the seemingly contradictory results. The lack of a clear definition of VCI and its subtypes precludes accurately assessing potential differences in

electrophysiological signatures between groups. Nonetheless, significant progress has been made, and we are hopeful that similar to the framework developed by international consortiums for AD (Albert et al., 2011; Dubois et al., 2016; McKhann et al., 2011; R. A. Sperling et al., 2011), VICCCS will allow for significant future progress and collaboration.

Along with the need for consensus definitions, standard methodologies are also required to advance the field further. This literature review reveals little consistency or replication of results. The different approaches in data analysis hinders the reliability, repeatability, and reproducibility of the results. In addition to the standardization of signal analysis methods, we recommend the incorporation of modern analyses, which could overcome many of the difficulties encountered when using classical methods. In this regard, the novel spectral analysis method proposed by Donoghue et al., (2020), which consists in the parameterization of the neural power spectra into periodic and aperiodic components, deserves special mention. This method has already provided promising results, showing that aperiodic activity changes are strongly associated with aging (Brady & Bardouille, 2022; Thuwal et al., 2021), and with Alzheimer's dementia (Wiesman et al., 2022). Moreover, most of the studies incorporated in this review report data from resting state conditions. While this can be useful for clinical practice (e.g., to identify the patient's disease), the study of brain function during specific cognitive tasks could also provide meaningful knowledge and warrants further investigation. We encourage investigation of electrophysiological function during resting state to obtain reliable and replicable data that could be used as biomarkers (Colclough et al., 2016b; Garces et al., 2016)as well as during cognitive tasks typically impaired in VCI patients, including executive function and processing speed in order to evaluate the evolution of the disease.

Despite the limitations, by analyzing the outcomes of the papers selected for this systematic review, specific patterns did emerge for patients with VCI compared to HC and those with AD (see Table 5).

a) The typical dementia profile known as "slowness" is found for VCI patients with increased power in slow bands: delta and theta; and decreased power in the beta band, related to disease severity compared to healthy controls. This pattern seems stronger for VCI than AD with similar cognitive profiles, and VCI patients present a more abnormal source distribution in these bands.

b) A significant parieto-frontal disconnection and reduction in interhemispheric connectivity in slow bands (delta, theta, and low alpha) is described for VCI patients compared to healthy controls. There was not robust evidence found for differences in connectivity between VCI and AD.

c) Longer latencies in brain responses and decreased amplitudes in the evoked responses of VCI patients is seen compared to controls across different tasks (visual and auditory).

Unfortunately, we lacked sufficient evidence to make generalizations pertaining to specific VCI subtypes. To find a highly detailed description of results divided by type of electrophysiological analysis and experimental populations comprising all the manuscripts included in the present systematic review, as well as three tables with the main findings of each paper see (Torres-Simón et al., 2022).

Table 5 Main electrophysiological signatures for VCI population against healthy control and AD.

Type of analysis	VCI vs. HC	VCI vs. AD
Spectral analysis (13)	● "Slowness" in electrophysiological pattern. Higher power in the δ, θ, and lower in β band associated with the severity of the vascular disease. ● Lower α power.	● The "slowness" pattern is stronger for VCI with a similar cognitive profile. ● VCI exhibits an abnormal distribution of sources in slow bands. ● No definite conclusion for α band, highly sensitive for dementia, but not specific to this pathology.
Connectivity analysis (5)	● Parieto-frontal and interhemispheric disconnection in slow bands (δ, θ, and low α)	● Not robust evidence could be drawn as there is only one paper.
Evoked response (8)	● Slower brain response, accompanied in general with smaller amplitudes, in the responses evoked in visual and auditory tasks.	● No significant differences were found in the literature.
Entropy/ complexity (6)	No definitive conclusion can be drawn for VCI because of the diversity of analysis used.	

3.3. Conclusion

After this systematic review of the literature about electrophysiological (M-EEG) patterns related to VCI, it can be concluded that electrophysiology signatures are not ready yet to be included in the diagnosis criteria because results are not robust, repeatable, and reliable enough to be use as clinical biomarkers. MEG and EEG quantitative analysis are precise, non-invasive tools with high temporal resolution that directly reflect changes in bioelectrical activity of the brain. These tools provide the opportunity to study brain function and network disruption due to changes in synaptic potentials produced by vascular alterations before structural changes and/or cognitive decline are evidenced, as well as the ability to serve as a prognostic tool for disease severity. Nevertheless, there is a critical need to accurately classify VCI and its subtypes to allow for future research efforts regarding its underlying pathophysiologic cause and prognosis. The results described in the Table 5 depict a general pattern that demonstrate the utility of functional analysis to augment structural imaging studies. However, these same results have low specificity for VCI diagnosis, for differentiate its subtypes or for understanding the effect of CBVD in brain function and cognition. Out of this scientific context emerges the motivation and objectives of the research project presented here, trying to offer specific solutions to the described limitations and heading towards the finding of useful electrophysiological biomarkers for VCI.

Research motivation, rationalization, and main objectives

Given the aging population trend, the understanding, prevention, and treatment of dementia are at the forefront of social, clinical, and scientific efforts. The high incidence and contribution of CBVD to cognitive impairment, added to its treatable condition, give special importance to the study of robust biomarkers related to cerebrovascular pathologies in the old population. As described in previous chapters, the electrophysiological functioning of the brain has been widely studied in the prodromal phases of other neurodegenerative diseases. Nevertheless, the heterogeneity of existing literature regarding the study populations and analysis performed with the electrophysiological signals, meticulously described in the systematic review, helped to highlight some crucial improvements for future research in this field. In order to establish MEG and EEG signatures as useful biomarkers: 1) there will need to be a clear definition of VCI and its subtypes; and 2) it will be necessary to standardize the methodology, which will allow commitment between the groups and the consolidation of multicenter efforts.

The main objective of the present thesis is to characterize the effect of cerebrovascular damage on brain function, structure, and cognition in the old population, searching for new possible biomarkers in the preclinical stages. Within the framework of this general objective, the methodological specifications and subsequently the specific objectives were built trying to fulfill some of the limitations highlighted in the systematic review.

Study population election

The first notable point is the lack of consensus in the criteria and definition of VCI. As explained above, CBVD involves a variety of medical conditions or changes in the cerebral or systemic vasculature with brain impact, including a large number of pathologies and etiologies. In this sense, trying to find biomarkers generalizable to all of them is practically impossible. The proposal for further investigation is to focus the research on identification of specific electrophysiological signatures related to specific cerebrovascular damage rather than diagnostic groups.

To face this limitation, the present thesis focuses on the study of White Matter Hyperintensities (WMH). As described in chapter 1, WMH is one of the imaging markers specified in the VICCCS diagnosis criteria for VCI. They are the neuroimaging-observable consequence of the degradation of the blood-brain barrier that occurs in Small Vessel Disease (SVD) (Regenhardt et al., 2018). The selection of this cerebrovascular damage was driven by its occurrence and clinical importance. WMH are the most prevalent vascular damage associated with VCI (Jellinger, 2013). Their presence increased the risk of incidence of all types of dementia, being also a major contributor to mixed dementia and the cause of approximately one fifth of all strokes worldwide (Chutinet & Rost, 2014; Drebette & Markus, 2010; Norrving, 2008; Pantoni, 2010).

Furthermore, with the purpose of finding robust electrophysiological biomarkers related to WMH and its effect on cognition and brain structure in the old population, for the experimental studies of the present research project, only clinically healthy individuals older than 50 years were recruited. WMH is a common accompaniment of aging, not only in patients diagnosed with dementia, but also in healthy population. In fact, WMH are present at neuroimaging in practically every individual over 60 years, ranging from 11-12% in adults, to 64 - 94% at the age of 82 (Drebette & Markus, 2010; Kloppenborg et al., 2014) and its prevalence increases with age (Alber et al., 2019; Van Leijsen et al., 2017).

The inclusion of a pathological population, either mild or major VCI or mixed dementias, would have involved the presence of many clinical covariables that are difficult to control. Given the lack of repeatable information found in electrophysiological VCI literature, these experiments have been designed to find specific electrophysiological signatures related to this specific cerebrovascular damage, reducing the incidence of other possible pathological variables, and trying to establish a solid and precise baseline for VCI research. This reductionist approach could help to understand and try to palliate particular symptoms in mixed dementias, where WMH damage is a comorbid contributor to the progression of other neurodegenerative diseases. In addition, it could help in the early identification and differentiation of VCI between subtypes among themselves and with other pure dementias. Finally, it could help in prognosis and treatment evaluation for patients in more advanced stages of VCI.

Materials election

According to the selection of materials and methodological concerns, it is important to differentiate between 1) the variables used for characterization of the sample; and 2) the experimental variables themselves.

1) Variables for sample characterization (independent variables)

One of the main limitations found in the literature was the characterization of the population with VCI included in the electrophysiological studies, not only due to the lack of consensus on the criteria and definition of VCI, but also due to the lack of standardized and objective report of patients' neuropsychological performance and imaging data. In this concern, we meticulously defined the inclusion criteria for our sample as described below.

Cognitive status

The experiments reported in the present thesis focus on a cognitively healthy population over 50 years old. Consequently, we used Mini mental State Examination (MMSE) to ensure the minimum general cognitive performance of our sample, taking 26 out of 30 as the cut-off score (Kukull et al., 1994). This test is widely used in clinical and research settings to measure cognitive impairment and screen for dementia among the elderly. In this sense, it is a good neuropsychological score to ensure that our results will be more generalizable and aggregable for other researchers and clinicians.

Vascular damage

Currently, the most widely used method to detect and assess the severity of WMH are clinical scales based on visual assessment, but these scales do not offer quantitative information, making it difficult to assess progression. Quantitative information can be approached through the manual segmentation of physicians, but this process is extremely time-consuming and presents a high inter and intra evaluator variability, which makes its application in routine protocols unfeasible. Therefore, to clarify the sample included in the studies and facilitate the combination of results in relation to cognitive impairment of vascular origin, our proposal is to report objective neuroimaging analyses, trying to avoid clinical scales for the characterization of experimental groups, which would imply a certain degree of subjectivity and inter-rater variability. To overcome these methodological limitations, we employed the WMH total volume calculated with an automatic segmentation toolbox using MRI FLAIR sequences (see Research Methods chapter).

2) Experimental variables (dependent variables)

Cognition

The selection of the experimental variables in which one might expect to find some influence of the aforementioned vascular damage was based on well-established scientific knowledge, specially, the clinical importance of WMH. This neuroimaging marker appears to be strongly related to the incidence of all types of dementia and long-life risk of stroke (Chutinet & Rost, 2014; Drebette & Markus, 2010). Furthermore, the presence and progression of WMH in the brain have been associated with general cognitive impairment, most pronounced in attention and executive functioning, with small but robust effects, in the healthy old population (Arvanitakis, Fleischman, et al., 2016; Kloppenborg et al., 2014), and in dementia patients (Arvanitakis, Capuano, et al., 2016; Lam et al., 2021; Mortamais et al., 2014; Prins & Scheltens, 2015; Van Den Berg et al., 2018). In this context, we incorporated a comprehensive neuropsychological battery that includes all the core cognitive domains recommended by VICCCS-II for assessment in VCI in 30 mins (i.e., executive function, memory, neuropsychiatric and depressive symptoms, and premorbid status).

Brain structural integrity

Additionally, WMH have been extensively linked to structural pathophysiological signatures of the brain such as grey matter degeneration (Gaubert et al., 2021; Jang et al., 2017), cortical thickness (Duering et al., 2012), ventricular dilatation (Bjerke et al., 2014), hippocampal volume (Porcu et al., 2020), and white matter integrity disruption studied with diffusion tensor imaging (DTI) (Veldsman et al., 2020). In this concern, for our studies we included brain volumetric measures calculated through T1 images and white matter integrity data extracted from the DTI analysis.

Brain functioning (power and connectivity)

Finally, as reported in the systematic review, general electrophysiological patterns for VCI have already emerged, demonstrating the utility of functional analysis to augment structural imaging studies, but only one study out of 32 used MEG. We decided to include MEG-based studies because of its better frequency and spatial resolution compared to EEG, especially when evaluating the electrophysiological function of the brain in source space. The use of this technique will allow us to increase our potential to detect specific vascular-associated pathology.

The MEG studies described in this thesis were performed with a 306-channel Vectorview system (Elekta Neuromag), which comprised 102 magnetometers and 204 planar gradiometers. We restricted our data to eyes-closed-resting state recordings, as we encourage investigation of brain electrophysiological function in this condition to obtain reliable and replicable data, both in clinical and research settings, that could be used as biomarkers (Colclough et al., 2016b; Garcés et al., 2016). In this sense, we opted to carry out analysis of spectral power and functional connectivity because they are two of the most widely used techniques in electrophysiology, and because in both cases exist previous studies with minimally consistent results. This was not the case for the studies with complexity/entropy, so we decided to leave them out in this first attempt.

The statistical methodology used in our studies was designed to find patterns of electrophysiological activity that were associated with the burden of cerebrovascular damage in a healthy population, where all patients presented cognition and structure without objective damage. We avoid making comparisons between groups because we believe that the progression of the vascular load in the healthy population is a continuum that grows with age, so that, whatever groups we could have done, we would have had a lot of intragroup variability. In relation to the latter, a recent systematic review described that, at present, data on WMH volume in healthy adults appear not to be comparable between studies, probably due to the characterization of the samples (e.g., cardiovascular risk factors, demographic features), and technical issues (e.g., different scan fields, WMH segmentation methods) (Melazzini et al., 2021). In this context, we believe that the correlational analysis would be the most appropriate to achieve the main objective of the thesis. Finally, as part of the analysis, we used a methodology designed for defining imaging biomarker cut points to determine the minimum WMH volume that can be interpreted as significant in cognitively healthy elderly. This threshold was used in our studies to model two sequential stages of the neurodegenerative process.

Objectives

With all the background clarified and the experimental variables carefully selected, the main objective is to characterize the effect of cerebrovascular damage on brain function, structure, and cognition in the population, searching for new possible electrophysiological biomarkers in the preclinical stages.

- ✓ To obtain a clear picture of the literature regarding neurophysiological patterns (EEG and MEG) for mild and major VCI.
- ✓ To identify the most accurate software for the automatic detection of white matter hyperintensities according to clinicians' manual segmentations (gold standard)
- ✓ To establish a possible threshold from which WMH volume in the brain could have clinical implications.
- ✓ To characterize the behavior of sociodemographic features, brain structural integrity and cognitive performance according to the cerebrovascular damage (WMH volume) in aging.
- ✓ To find spectral power signatures in resting-state electrophysiological signal (MEG) associated with cerebrovascular damage (WMH), and their association with cognitive performance and brain structure (i.e., grey, and white matter integrity) in aging.
- ✓ To recognize the functional connectivity signatures (resting-state MEG) associated with cerebrovascular damage (WMH), and their relationship with cognitive performance and brain structure (i.e., grey, and white matter integrity) in aging.

Research methods

Chapter 4: Participants description and cognitive assessment

4.1. Participants

The sample of the present thesis was recruited under the framework of three Spanish national projects (PSI2009-14415-C03-01, PSI2012-38375-C03-01 and PSI2015-68793-C3-1-R) focused on research and early detection of dementia. Data were collected between 2010 and 2018 in collaboration with three different clinical centers located in Madrid (Spain): the Neurology Department in "Hospital Universitario Clinico San Carlos," the "Center for Prevention of Cognitive Impairment," and the "Seniors Center of Chamartín District". The research protocol included MEG recordings, MR imaging (T1, FLAIR and DWI), a neuropsychological assessment, and genetic profiling. The initial sample enrolled 520 cognitively healthy individuals, all native Spanish speakers. The enrollment was based on the results in the following set of screening questionnaires were: the Mini Mental State Examination (MMSE) (Lobo et al., 1979), the Global Deterioration Scale (Reisberg et al., 1982), the Geriatric Depression Scale–Short Form (GDS; Yesavage et al., 1982); and the Functional Assessment Questionnaire (FAQ; Pfeffer et al., 1982), and the questionnaire for Instrumental Activities of Daily Living (Lawton & Brody, 1969). Exclusion criteria included: (1) a history of psychiatric or neurological disease; and (2) psychoactive drugs consumption or chronic use of medication, such as anxiolytics. In addition, we performed on every participant complementary exploration (class II evidence level) to rule out possible causes of cognitive decline, such as B12 vitamin deficit, diabetes mellitus, thyroid problems, syphilis, or human immunodeficiency virus. All participants signed an informed consent. This study was approved by the "Hospital Universitario Clinico San Carlos" ethics committee and the procedure was performed in accordance with approved guidelines and regulations.

The original sample (N = 520) was filtered based on data availability and quality to facilitate future reproducibility of the experimental studies contained in the present thesis. We dismissed, sequentially, participants (number in brackets) based on the following criteria: 1) be younger than 50 years old (26); 2) have a MMSE < 26 (22); 3) not having a clean report from the radiology team: evidence of any brain abnormality, different to WMH (24); 4) not having 3D MRI or having failed brain segmentation (100); 5) not having MEG recording (16); 6) having noisy MEG recording (28); and 7) have total WMH volume greater than 3 standard deviations above the mean of the remaining sample (4). In total 220 participants were dismissed ending up with a sample of 300 participants (Age = 66 ± 8; 68% females). This sample will be used for all the studies included in this thesis, using different subgroups depending on the purpose. A detailed description of each subsample can be found in each study (for general overview of whole sample division and utilization see Figure 16).

4.2. Neuropsychological assessment

All participants underwent an exhaustive neuropsychological assessment to generate detailed cognitive profiles including: Direct and Inverse Digit Span Test (Wechsler Memory Scale, WMS-III; Wechsler, 1997), Immediate and Delayed Recall (WMS-III; Wechsler, 1997), Phonemic and Semantic Fluency (Controlled oral Word Association Test, COWAT; Benton and Hamsher, 1989), and Trail Making Test A and B (TMTA and TMTB; Reitan, 1958).

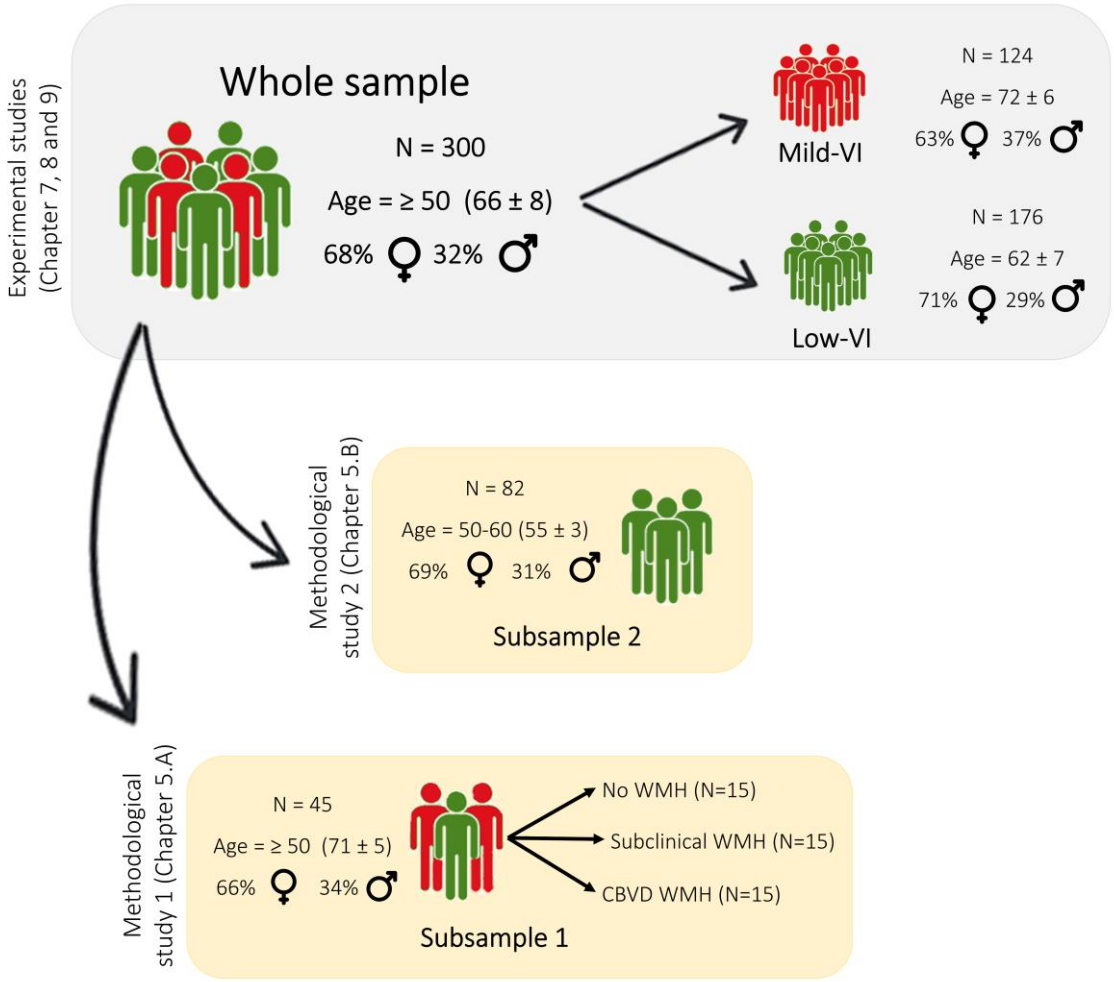

Figure 16 Sample description and subdivision for every study included in the project. Note Age= (mean ± sd).

Chapter 5: MRI recordings and measures

5.1. Magnetic resonance recordings

T1-weighted and T2-weighted 3D FLAIR and DWI MRI sequences were available for each subject. These images were acquired in a General Electric 1.5 Tesla magnetic resonance scanner in the Hospital Universitario Clinico San Carlos, using a high-resolution antenna and a homogenization PURE filter (Fast Spoiled Gradient Echo sequence). The following acquisition parameters were followed for:

- The T1-weighted imaging: repetition time (TR) = 11.2 ms, echo time (TE) = 4.2 ms, inversion time (TI) = 450 ms, Field of View (FOV) = 25 cm, flip angle (FA) = 12°, 252 coronal slices (in-plain resolution: 256×256), voxel size: 0.98 x 0.98 x 1 mm3 and acquisition time ≃ 8:00 min.
- The T2-weighted 3D FLAIR: TR = 7000 ms, TE = 101 ms, TI = 2112 ms, FOV = 24 cm, 252 coronal slices (in-plain resolution: 256×112), voxel size: 0.94 x 0.94 x 1.6 mm3 and acquisition time ≃ 4:57 min.
- The DWI: TE/TR 96.1/12,000 ms; NEX 3 for increasing the SNR; 2.4 mm slice thickness, 128 × 128 matrix, and 30.7 cm FOV yielding an isotropic voxel of 2.4 mm; 1 image with no diffusion sensitization (i.e., T2-weighted b0 images); and 25 DWI (b = 900 s/mm2). Data were recorded with a single shot echo planar imaging sequence.

5.2. Magnetic resonance measures (WMH and brain grey and white integrity)

With the available MR images, we calculated three different structural measures, as explained before: WMH volume, gray and white matter integrity.

First, we calculated the WMH volume in each participant with T1 and Flair sequences to characterize our sample in terms of cerebrovascular damage. For this, we developed two methodological studies which are described in detail below: 1) what is the best tool to calculate the total volume of WMH and how we evaluate it in our sample (section A); and 2) we work on a WMH volume cut - off point to generate potential subgroups in our sample based on their burden of vascular damage (section B)

In addition, we calculated markers of cerebral gray matter integrity by processing the T1 MR image (section C), and we computed white matter tracts integrity indicators through the DTI analysis (section D).

A. White matter hyperintensities total volume calculation
B. Sample sub-groups according WMH volume cut point.
C. Brain grey matter integrity (T1)
D. Brain white matter integrity (DTI)

A. White matter hyperintensities total volume calculation

Before the calculation of the **WMH volume** for each participant included in our sample, we developed a methodological study to identify the most accurate software for the automatic detection and quantification of WMH in neuroimaging compared to clinicians' manual segmentation and Fazekas report. This manuscript is already submitted to a journal indexed in JCR. Simultaneously, we have uploaded a preprint in medRxiv.org, to provide all data and results to the readers of this thesis.

Torres-Simón, L.†, del Cerro, A.†, Yus, M., Bruña, R., Gil-Martinez, L., Dolado, A., Maestú, F., Arrazola-Garcia and Cuesta, P (2023). Comparison between tools for automatic segmentation of white matter hyperintensities of presumed vascular origin in aging: which one, how and why to choose the most suitable for your purpose? medRxiv. https://doi.org/10.1101/2023.03.30.23287946

In this piece of work, we aimed to evaluate the performance and usability of 4 freely available WMH segmentation tools included in three of the most widely used neuroimaging toolkits used both in clinical and research settings: 1) for the SPM12 toolbox, we employed the algorithm Lesion Segmentation Tool (LST), with two different procedures: Lesion Predictor Algorithm (LST-LPA) (Schmidt, 2016) and with Lesion Growth Algorithm (LST-LGA) (Schmidt et al., 2012) for the FreeSurfer toolbox, we used the Sequence Adaptive Multimodal SEGmentation (SAMSEG) (Cerri et al., 2021) and 3) for FSL, we computed the WMH segmentation through the Brain Intensity AbNormality Classification Algorithm (BIANCA) (Griffanti et al., 2016).

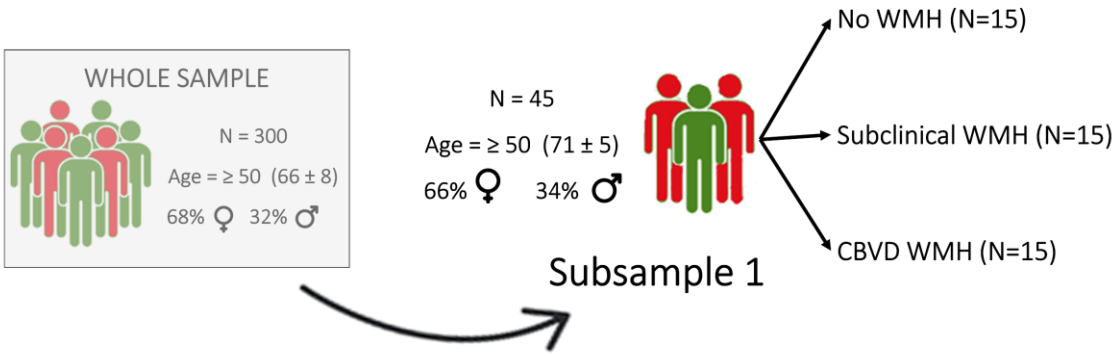

Figure 17 Subsample 1 description and segregation according to WMH load described in clinical reports

For this purpose, T1 and FLAIR images of a subsample of the total sample (N= 300) of 45 cognitively healthy participants from 50 years old with a broad distribution of WMH load were included, from our total sample (See Figure 17). The participants classification in groups was performed according to corresponding clinical reports: 15 with no alterations in their MRI, 15 with subclinical WMH, and 15 with WMH presumably associated with cerebrovascular disease (CBVD), to ensure that the images of the selected participants included a mixed range of WMH loads, covering a broad spectrum. The demographic and clinical data at baseline evaluation for each participant are described in Table 6.

Table 6 Demographic and clinical data.

	N	Age	Sex	Education	MMSE	Fazekas	Volume WMH
Whole subsample 1	45	71 ± 5	30/15	14 ± 6	29 ± 1	0.9 ± 0.8	$(5 \pm 7) \cdot 10^3$
No WMH	15	69 ± 5	11/4	12 ± 5	28 ± 1	0.2 ± 0.4	$(1 \pm 2) \cdot 10^3$
Subclinical WMH	15	71 ± 5	11/4	13 ± 6	29 ± 1	0.7 ± 0.5	$(2 \pm 1) \cdot 10^3$
CBVD WMH	15	72 ± 4	8/7	15 ± 6	28 ± 2	1.8 ± 0.6	$(13 \pm 8) \cdot 10^3$

Values are presented as mean ± standard deviation. Sex (female/male), age (in years), education (expressed in years of education). MMSE: Mini Mental State Examination. WMH volume (in mm3) corresponded with the volumes obtained with the radiologist's manual segmentation. Demographics are displayed for the whole sample and for each subsample of interest.

Methods

The FLAIR images of each participant were co-registered with their respective T1 images to define a single space per participant (Figure 19.1). On the one hand, the radiology team of the *Hospital Universitario San Carlos* used the FLAIR images to manually segment the WMH of each subject, relying on the T1 image when necessary. Simultaneously, the clinicians assigned a Fazekas score (0-3) to each participant (Figure 18). On the other hand, we calculated the WMH burden for each participant by mean of the four automatic tools. In all cases, and before starting the assessment of the performance, we analyzed the execution of each tool across their different parameters. For LST-LPA, LST-LGA and SAMSEG, we evaluated their performance at different thresholds (minimum probability criterion to accept a given voxel as lesion), and in the case of BIANCA we tested the algorithm with different training sets (for more details see Supplementary materials 1 and 2 in the preprint). Additionally, as previous studies (Hotz et al., 2021) recommended FreeSurfer's automatic segmentation of WMH over the T1 image, we also included it in the Supplementary material 4 in the preprint.

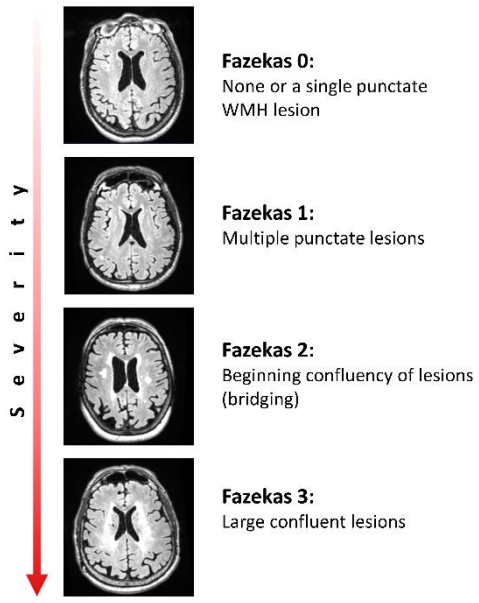

Figure 18 Fazekas scale examples for each score

With this clinical and automatic information, we performed an exhaustive and detailed analysis with the aim to understand which automatic tool could definitely give us the most accurate results compared to clinician's manual segmentation (Gold standard) before calculating the WMH for our entire sample. We did it by the correlation and performance analysis (Figure 19.3 and Figure 19.4). Additionally, we performed two extra analysis to understand in a deeper way the performance of these tools under more complex parameters: the total amount of WMH volume, the individual lesion size and finally the performance in a real world scenario (Figure 19.6). Finally, in the original study we developed user-friendliness analysis with the aim of help other researchers and clinicians to understand all the variables to consider when selecting one or another algorithm (Figure 19.2).

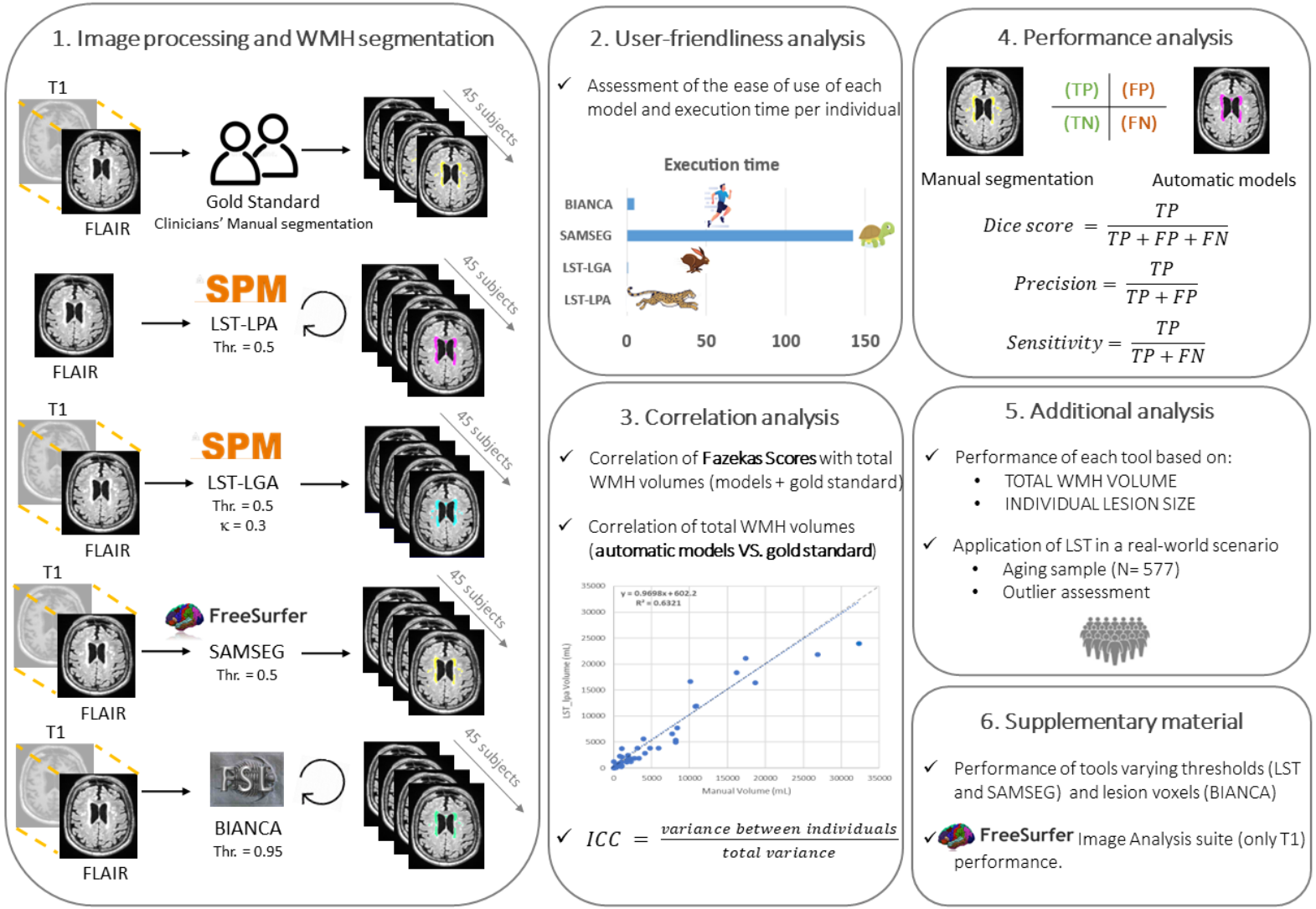

Figure 19 Methodological pipeline. From left to right: ***1:*** *3D T1 weighted and 3D FLAIR images co-registration, when required. Optimization of each algorithm performance and computation of the WMH masks of each participant. The circular arrows represent the algorithms that needs a training set.* ***2:*** *Assessment of User-friendliness by means of three expert neuroscientists.* ***3:*** *Battery of comparison based on performance and clinical relevance.* ***4:*** *comparison of the WMH masks computed by each algorithm with the corresponding of the gold standard.* ***5:*** *Evaluation of the models' performance based on different WMH volumes, when evaluating at the individual lesion level and when testing the algorithm in a large dataset* ***6****: Supplementary analysis concerning the check about the initial thresholds and lesion voxel for the algorithms analyzed and the results of the FreeSurfer Image analysis performance. The standard WMH segmentation obtained by Freesurfer recon all is described in the supplementary materials.*

Brief results

The results showed that all the metrics achieved acceptable results, useful for clinical practice, since they showed a high correlation with the Fazekas clinical scale and with the gold standard. Overall, the best algorithms in terms of performance were LST-LPA and BIANCA, but taking all the analysis into account, we decided to dig deeper into the large data set (N=577) with both LST tools, which we found to be complementary. This data set included our 300 participants and 277 extra subjects of other databases from our laboratory as in this point we only want to study the algorithms performance in a big dataset, without regard of the age or cognitive status, before relying on this metric of WMH volume for the experimental studies included in this thesis.

Below the reader can find some graphs depicting the main results obtained in this methodological study about user-friendliness, correlation, and performance analysis (for detailed description of these and the other results see *https://doi.org/10.1101/2023.03.30.23287946*).

User-friendliness results

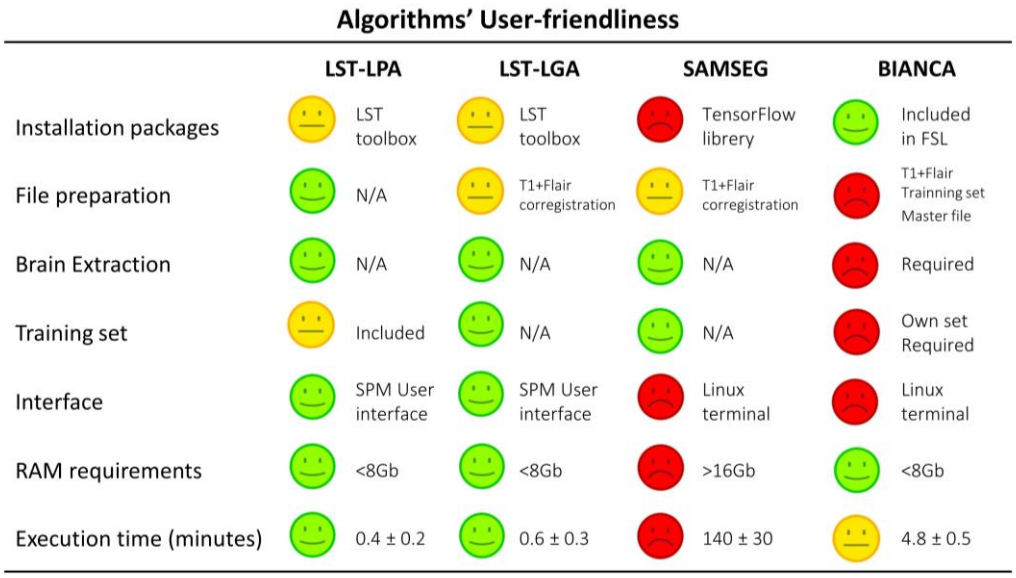

Figure 20 Difficulty of using each tool in terms of: 1) installation packages (if the algorithm is included or it requires one or more additional packages); 2) file preparation (it makes reference to the images pre-processing required before the segmentation); 3) brain extraction (if it is required before segmentation process); 4) training set (if it is required for the algorithms and when it is, if this set is included or the user should provide its own); 5) interface (if there is an user-friendly interface or the user should work in the terminal environment); 6) RAM requirements (amount of available RAM required to run the algorithms); and 7) execution time (it was calculated for each algorithm as the corresponding time (in minutes) expended for the computation of the WMH masks, without considering the images or dataset preparations and/or preprocessing).

Correlation analysis results

Table 7 Correlation analysis values

	LST-LPA	LST-LGA	SAMSEG	BIANCA	Gold Standard
Fazekas	0.78	0.78	0.79	0.80	0.84
Gold Standard	0.62	0.89	0.86	0.91	N/A
ICC	0.91	0.88	0.99	0.93	N/A

Fazekas: R^2 values of the Spearman correlation between the total WMH volumes measured by each tool and the one corresponding to the gold standard with the Fazekas scale. Gold Standard: R^2 values of the Spearman correlation between the total WMH volumes measured by each tool with the one corresponding to the gold standard. ICC: intra class correlation coefficient per each tool.

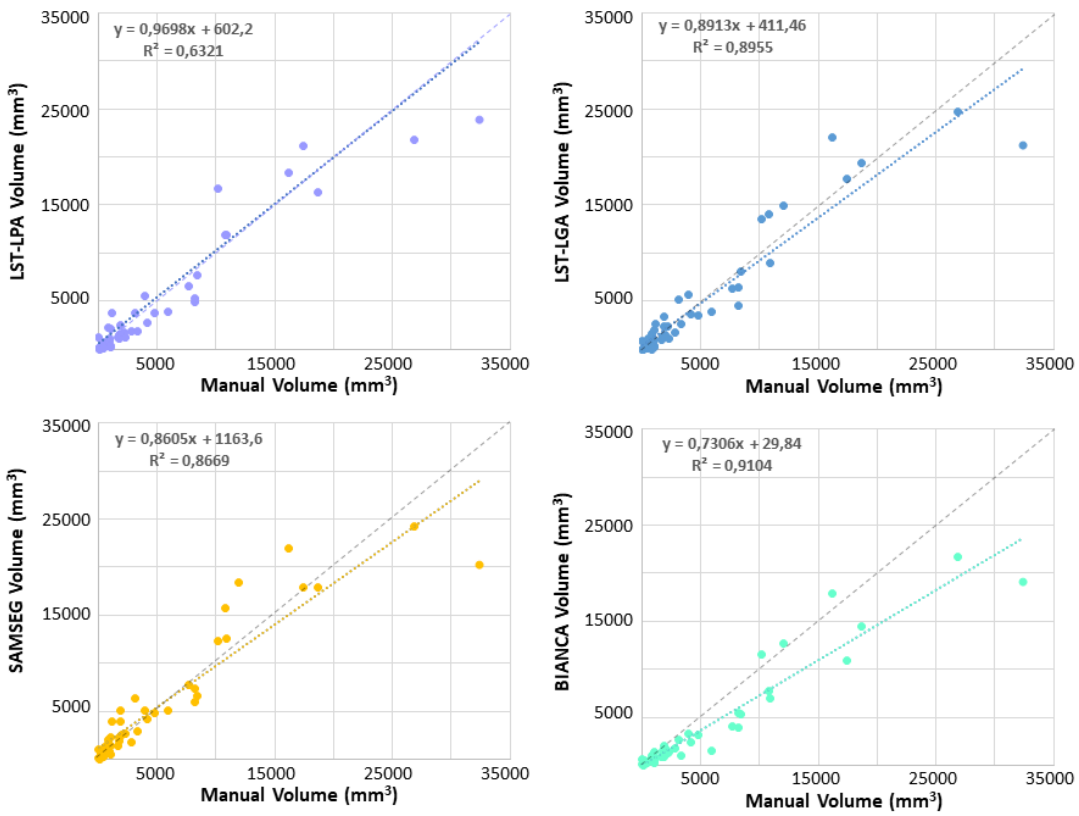

Figure 21 Correlation between the total volume of WMH from the gold standard and those obtained with each automatic segmentation. The graph shows the dispersion of the results, the equation of the trend line and its R2 value. Each colored graph represents an algorithm, and the gray dashed line represents the function y = x (slope of 1).

Performance analysis results

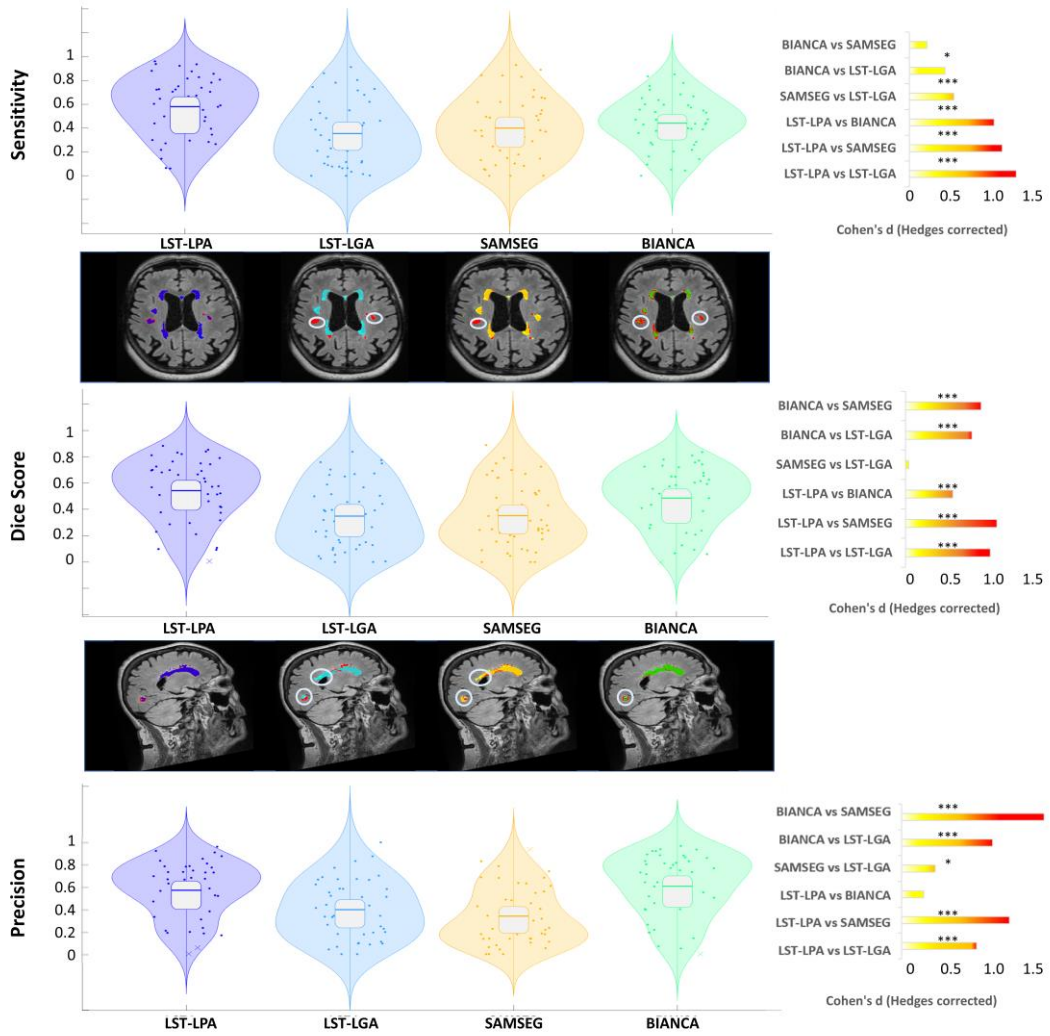

Figure 22 Lesion segmentation performance in terms of precision, sensitivity, and Dice score for the proposed methods (from left to right: LST-lpa, LST-lga, SAMSEG and BIANCA). The distribution of the values obtained in each tool LST_lpa (dark blue), LST_lga (light blue), SAMSEG (yellow) and BIANCA (green) is shown. Within each distribution the boxplot of each sample is represented indicating where the quartiles and median are located. Examples of the segmentations carried out by the different tools are shown between the measures. The gold standard lesion is shown in red, LST_lpa in dark blue, LST_lga in light blue, SAMSEG in yellow and BIANCA in green. The gray circles on the MRI images mark the main differences between the various tools. To the right of each measure, the effect size of the comparisons (repeated-measures t.test) between the different tools are represented using the Hedges-corrected Cohen's d (small (yellow), medium (orange) or high (red)) as well as the level of significance obtained (= p<0.05 and *** = p<0.001).*

Conclusion

In our experience, the LST package includes two promising and complementary methods that are widely available, easy to use, and have short execution times. Combining the results of LST-LPA (supervised) and LST-LGA (unsupervised) is a feasible procedure with the ability to be used as a useful proxy for WMH segmentation.

Therefore, according to our conclusion we calculated the **WMH total volume** for each participant included in the whole sample (N = 300) assessed with **LST-LPA** controlling the possible errors with **LST-LGA** automatic algorithm in order to report accurate, objective, quantifiable and reproducible data.

B. Sample sub-groups according to a WMH volume cut point.

As explained earlier in the introduction, a minimal WMH burden is present in virtually all individuals older than 60 years. However, the amount and progression of this vascular marker has been closely related to an increased risk of stroke and dementia and cognitive dysfunction In this context, although each biomarker exists on a continuum, such as WMH, dichotomizing biomarker values according to a cut-off point could be valuable in certain situations, for instance when dividing the sample to determine eligibility for treatment (Hampel et al., 2014; R. a Sperling et al., 2014). In order to establish a possible threshold from which the volume of WMH in the brain could have clinical implications, we computed a specificity-based cut-off point, for the volume of WMH damage, following the guideline for defining imaging cut points (Jack et al., 2017). As this study recommend only young and clinically normal people should be included to calculate the potential biomarkers. For this purpose, we used the WMH volumes obtained though the automatic segmentations of those participants from our whole sample between 50 and 60 years of age with no evidence of brain damage, including vascular disease, based on the radiological report, ending up with a subsample of 82 participants (See Figure 23).

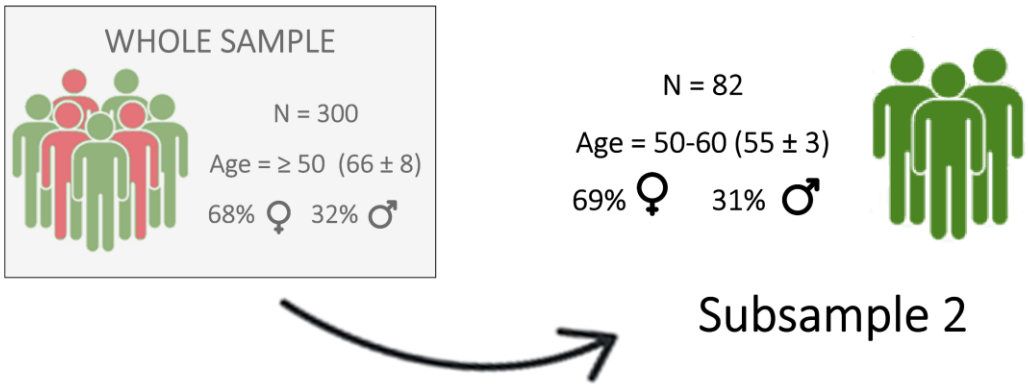

Figure 23 Subsample 2 description

The cut point calculated corresponded to the 95th percentile of the WMH volume distribution among the individuals aged 50-60 years (average 55 ± 3). The obtained cut point corresponded to a WMH volume of 960 mm^3 (Figure 24). For the studies of the present thesis, the WMH volume cut point was fixed to 1000 mm^3.

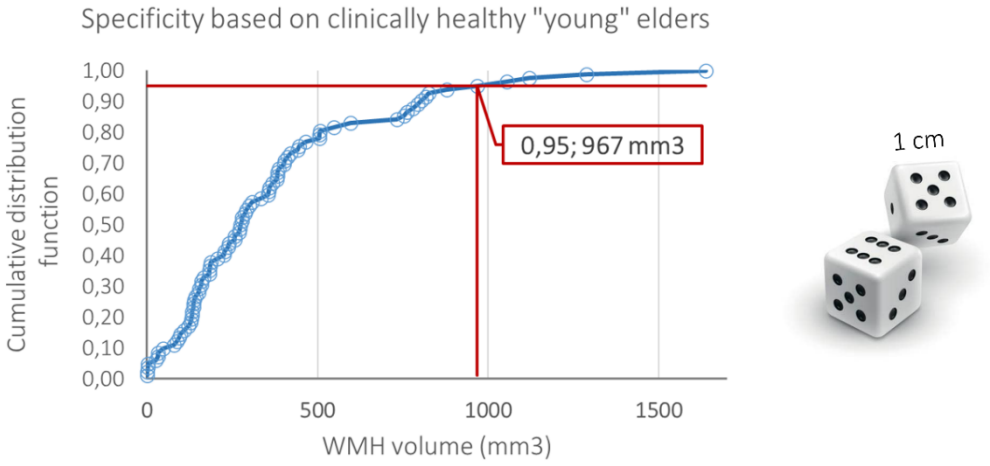

Figure 24 Left, graphical summary of the method used for determining WMH volume cut point. Cumulative distribution function indicates a WMH volume on the horizontal axis and the proportion of observations ≤ WMH volume on the vertical axis. On the right, representation of a dice with a side of 1 cm, whose volume corresponds to the cut-off point of the WMH.

Sample characterization according to the cerebrovascular damage (WMH)

This section describes the distribution pattern of the entire sample as a whole and divided by the cut-off point according to the central variable of this thesis (WMH volume). As described before, our final sample consists of 300 cognitively healthy older participants. After calculating the cerebrovascular damage for each person, we determined the cut-off, as explained above (see chapter 5 page.79), obtaining a volume cut point of 1000 mm^3. In Figure 25, it can be found the percentage of the population based on the amount of vascular damage detected in their MRI scans. According to this cut-off we constructed two subgroups: **low vascular impairment (Low-VI)**, for those below 1000 mm^3 of WMH and **mild vascular impairment (Mild-VI)**, for those above (see Figure 26). As it can be observed, 59% of the population fit the definition of having low-VI, while the remaining 41% presented WMH volumes above the 1000 mm^3 cut-point, showing an exponential increment reaching up to 23203 mm^3. From now on, all the analyses will be presented for the entire sample (whole), and for the two subgroups (low-VI and mild-VI) independently. This will be conducted to understand if the dissimilar patterns found in the amount of vascular damage could have different effects on brain function, structure, or cognition in our cognitively healthy older adults.

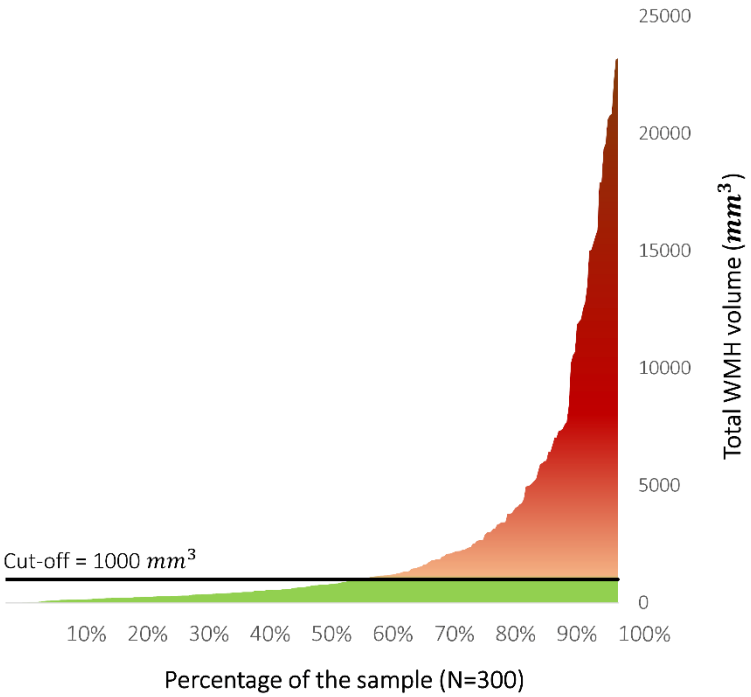

Figure 25 Total sample distribution according to cerebrovascular damage (WMH volume)

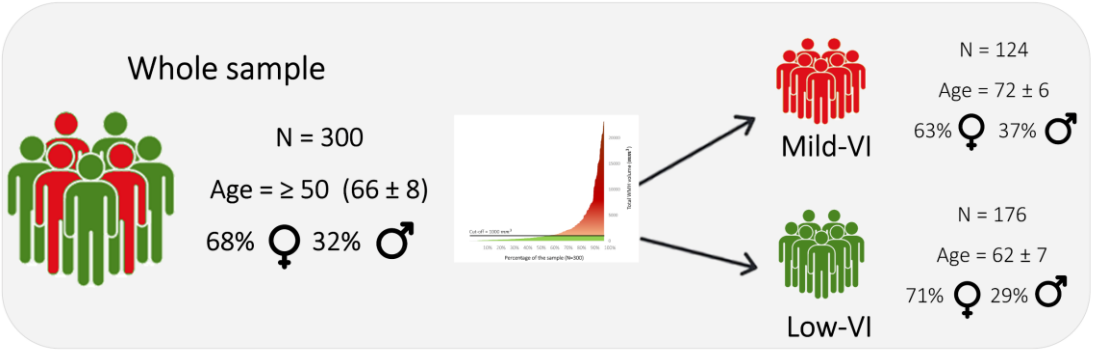

Figure 26 Subgroups description of the whole sample according to the WMH volume cut-off used for the experimental studies of this project.

C. Brain grey matter integrity (T1)

The resulting images from the T1 sequence were processed using the Freesurfer software (version 6.1.0) and its specialized tool for automated cortical parcellation and subcortical segmentation (Fischl et al., 2002). The measures that were included in further analyses were total volumes (mm^3) of gray matter, total white matter, lateral ventricles, and hippocampus; and the cortical thickness (mm). The volumes of bilateral structures were collapsed to obtain a single measure for each region.

D. Brain white matter integrity (DTI)

DWI images were processed using probabilistic fiber tractography run in the automated tool *AutoPtx* (https://fsl.fmrib.ox.ac.uk/fsl/fslwiki/AutoPtx). The methodology is detailed in (Verdejo-Román et al., 2018) but we will briefly summarize the procedure followed to obtain the fractional anisotropy (FA) markers.

The DTI images were processed using FMRIB-FSL (Jenkinson et al., 2012), including adjustment for minor head motion, eddy-current artifacts, rotation of the gradient direction table in the same way than the images in the previous step, and non-brain tissue removal using the Brain Extraction tool of FSL (S. M. Smith, 2002). The calculation of FA maps was done by fitting the diffusion tensor using dtifit function (PREOBE and NFBC 1986) or the RESTORE method implemented in Camino (Generation R). Quality of the data was checked with automatic tools (i.e., DTIPrep tool; https://www.nitrc.org/projects/dtiprep/) and visual assessment. AutoPtx automated pipeline was used to run a probabilistic tractography of brainstem, projection, association, callosal, thalamic, and limbic fibers in each individual. Tracts were defined using seed, target, termination, and exclusion masks that were warped to the original diffusion space. The connectivity distributions were normalized and thresholded (M. De Groot et al., 2015), and the mean FA parameter per each tract was extracted. Bilateral tracts were collapsed to obtain a single measure. The pipeline ended up providing mean FA values for the 15 tracts of interest described in Figure 27 and Table 8.

Table 8 WM Tracts included in the experimental studies.

General classification	FSL classification	WM main tracts	Abb.	Homologous
Projection fibers	Callosal fibers	Forceps Minor	fmi	
		Forceps Major	fma	
	Brainstem tracts	Middle cerebellar peduncle	mcp	
		Medial lemniscus	ml	l/r
	Projection Fibers	Corticospinal tract	cst	l/r
		Acoustic radiation	ar	l/r
Thalamic radiations		Anterior thalamic radiation	atr	l/r
		Superior thalamic radiation	str	l/r
		Posterior thalamic radiation	ptr	l/r
Association fibers	Association fibers	Superior longitudinal fasciculus	slf	l/r
		Inferior longitudinal fasciculus	ilf	l/r
		Inferior fronto-occipital fasciculus	ifo	l/r
		Uncinate fasciculus	unc	l/r
	Limbic System fibers	Cingulate gyrus part of cingulum	cgc	l/r
		Parahippocampal part of cingulum	cgh	l/r

Note: Classification, abbreviations, and information about bilateral WM Tracts whose FA scores were included in the studies of the present thesis.

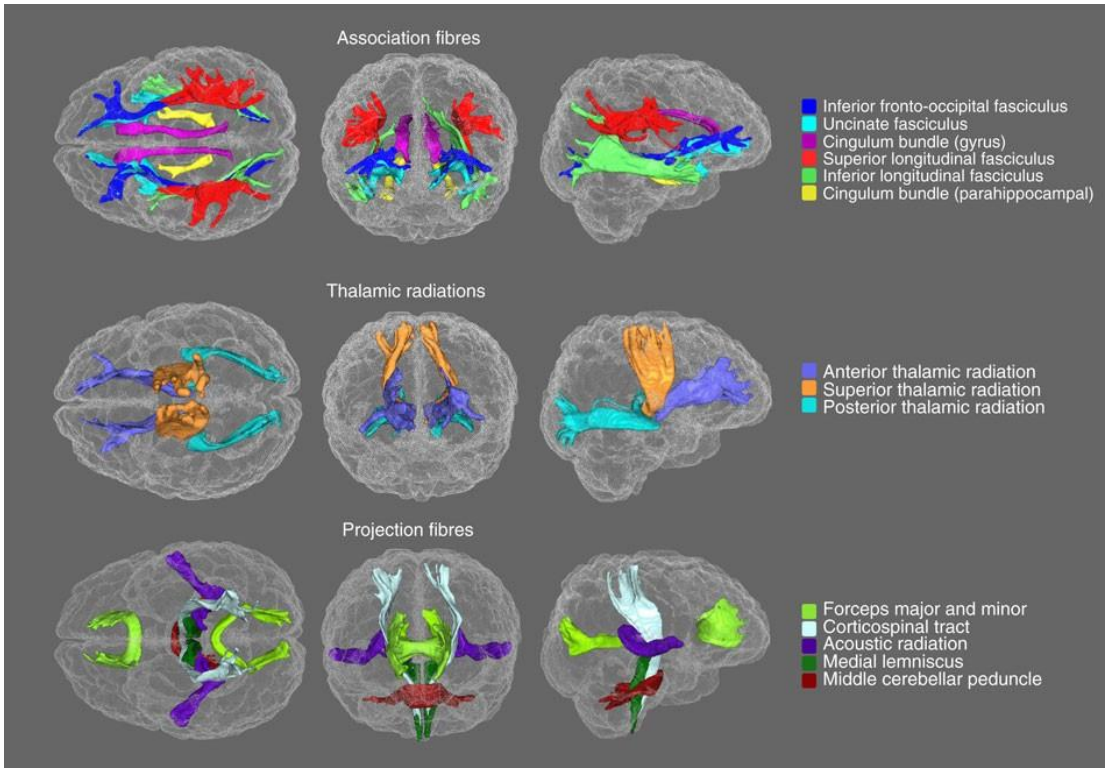

Figure 27 Tridimensional representation of the tracts assessed in the DTI processing. Image from: "Ageing and brain white matter structure in 3,513 UK Biobank participants". Cox, S. R., Ritchie, S. J., Tucker-Drob, E. M., Liewald, D. C., Hagenaars, S. P., Davies, G., Wardlaw, J. M., Gale, C. R., Bastin, M. E., & Deary, I. J., 2016. Nature Communications

Chapter 6: MEG recording and measures.

6.1. MEG data recordings

Five minutes of eyes-closed resting-state were recorded with a 306-channel whole-head MEG system (Vectorview, Elekta Neuromag) located in a magnetically shielded room (VacuumSchmelze, GmbH, Hanua, Germany) at the Center for Biomedical Technology (Madrid, Spain). All participants sat comfortably in a chair and each subject's level of arousal was monitored with a video camera and verified through conversation immediately after the measurement session. MEG data was collected at a sampling frequency of 1000Hz and online band-pass filtered between 0.1 and 330 Hz. Each subject's head shape was defined relative to three anatomical locations (nasion and bilateral preauricular points) using a 3D digitizer (Fastrak, Polhemus, VT, USA) and head movement was tracked via four head position indicator (HPI) coils attached to the scalp. These HPI coils continuously monitored the participants' head movements, while eye movements were monitored by a vertical electrooculogram assembly (EOG) comprised of a pair of bipolar electrodes. Raw recording data were first entered into Maxfilter software (v 2.2, correlation threshold = 0.9, time window = 10 seconds) to remove external noise using the temporal extension of the signal space separation method with movement compensation (Taulu & Simola, 2006). In the studies of the present thesis, we used only magnetometers data in order to avoid mixing MEG sensors with different sensitivities or resorting to scaling (Garcés et al., 2017). Consequently, the magnetometers data were automatically examined to detect ocular, muscle, and jump artifacts using Fieldtrip software (Oostenveld et al., 2011), which were visually confirmed by an MEG expert. The remaining artifact-free data was sectioned into four-second segments. Independent component analysis-based procedure (ICA) was applied to remove heart magnetic field artifacts and EOG components. Only those MEG recordings with at least 20 clean segments (80 seconds of brain activity) were used in further analysis. The entire MEG time series (2-second padding) was filtered in specific frequency bands (whose limits depended on the analysis to be performed) to avoid phase distortion and edge effects. The filtering consisted of applying a finite impulse response filter of order 1500 with a two-step procedure. For the spectral power analysis, the bandpass filter was applied with a frequency range of 2-45 Hz. For the functional connectivity analysis, the bandpass filtering was applied using the edges of the classical frequency bands: delta (2 to 4 Hz), theta (4 to 8 Hz), alpha (8 to 14 Hz), beta (14 to 30 Hz), and gamma (30-45 Hz).

6.2. MEG Source reconstruction

The calculation of source-level brain activity for each participant began with the creation of a source model consisting of a regular grid of 2455 nodes with a 1 cm gap defined in the Montreal Neurological Institute (MNI) brain template. These brain locations were labeled according to the automated anatomical labeling (AAL) atlas (Tzourio-Mazoyer et al., 2002), and only those nodes located within cortical or medial temporal lobe regions were included in the analysis (the ROIs of cerebellum, basal ganglia, thalamus, and olfactory cortices were dismissed). The final sources model consisted of 1202 grid nodes that were transformed to each participant´s space using a

linear transformation between the native T1-weighted MRI and the standard T1 in MNI template space. The T1-weighted MRI of each participant was also used to generate a single-shell head model defined by the inner skull surface. Then, we combined the head model, the source model, and the MEG sensors definition to create a lead field using a modified spherical solution (Nolte, 2003). Finally, using the leadfield and the corresponding band-filtered MEG signals, the sources time series were reconstructed using a Linearly Constrained Minimum Variance beamformer (Van Veen et al., 1997). For each individual, the covariance matrices of all trials were averaged to calculate the spatial filter coefficients, and these coefficients were applied to each individual trial, obtaining the time series by segment and source location.

6.3. MEG measurements (power and functional connectivity)

A. Power spectrum

The power spectrum of each of the 1202 source locations were computed similarly to previous studies (de Frutos-Lucas et al., 2020; Garcés et al., 2013; Nakamura et al., 2018) with the Fieldtrip toolbox (Oostenveld et al., 2011) using a multitaper method (mtmfft) with discrete prolate spheroidal sequences (dpss) as windowing function and 1 Hz smoothing. The spectral power was calculated for the 2-30 Hz range in 0.25 Hz steps. For the analysis, we employed relative power that was calculated by normalizing each frequency step by the total power in the whole frequency range, ending up with a source-reconstructed power matrix of 1202 nodes x 113 frequency steps x 300 participants. These matrices are the starting data analyzed with the statistical procedure described in Chapter 8, section 8.2. Material & methods, Statistical analysis.

Additionally, following previous studies of our group (D López-Sanz et al., 2016; María Eugenia López et al., 2020), we determined for each individual the individual alpha peak frequency (henceforth called Alpha peak) by visual inspection of the average power spectra of the occipital-parietal region of the brain. The bilateral AAL ROIs used for this purpose were: calcarine fissure and surrounding cortex; cuneus, lingual gyrus, right superior occipital lobe, middle occipital lobe, and inferior occipital lobe (María Eugenia López et al., 2020).

B. Functional Connectivity

The functional connectivity analysis was approached using a phase synchronization metric called Phase Lock Value (PLV) as defined in (Mormann et al., 2000). The concept of phase synchronization (Varela et al., 2001) refers to a situation in which the phases of the signals can be interdependent even though their amplitudes may not be not correlated. (Pereda et al., 2005). Briefly, the PLV is a straightforward evaluation of the distribution of the phase differences between each pair of time series (e.g., from two sources locations), which is a widely used method in the EEG/MEG literature (Chino et al., 2023; de Frutos-Lucas et al., 2020; María Eugenía López et al., 2014; Maestú, Peña, et al., 2015; Nakamura et al., 2017; Ramírez-Toraño et al., 2020), and offers high reliability across sessions (Colclough et al., 2016a; Garcés et al., 2016). The calculation of the PLV is carried out, for each frequency band and segment, on the time series reconstructed in the source space; matrices of 1202 brain locations by 4000 samples. The procedure consists of

the following steps: 1) for each source location j = 1,…,1202 and time sample t = 1,…,4000, the instantaneous phase of the signal $\varphi_j(t)$ is extracted by means of Hilbert transform: $Z_j(t) = x_j(t) + i \cdot Hilbert\big(x_j(t)\big) = A_j(t) \cdot e^{-i\varphi_j(t)}$; 2) the phase synchronization between each pair of signals l and k is computed by the following expression: $PLV = \frac{1}{M}\left|\sum_{m=1}^{M} e^{-i(\varphi_l(t_m)-\varphi_k(t_m))}\right|$, where M is the number of samples in each segment of the time series (4000 samples since the segments are 4 seconds long at 1000 Hz sampling rate); and 3) the resulting PLV matrices are averaged across segments to obtain a more robust estimator of resting-state FC, ending up with symmetrical connectivity matrices of 1202 nodes x 1202 nodes per frequency band and participant. Finally, we calculated the normalized weighted global connectivity of each node (also known as nodal strength), which is defined for each node as the sum of all its FC values with the rest of the network divided by the number of links connected to it. The FC computation resulted in a vector with the corresponding 1202 normalized node strengths per each participant and frequency band. These are the starting data that were submitted to the statistical procedure described in section Chapter 9, section 9.2. Material & methods, Statistical analysis.

Experimental studies

Chapter 7: WMH characterization

7.1. Objective

This first chapter, within the experimental studies section, has been designed to provide a detailed description of every aspect relevant to assess a deep understanding of the central variable of this thesis (WMH volume) and the sample utilized in the following studies (N = 300). In addition to the basic descriptive data for every variable collected, the possible differences found between the two groups are shown in Table 9. Subsequently, in order to achieve the fourth objective of the present thesis (*to characterize the behavior of sociodemographic features, brain integrity and cognitive performance according to the severity of the cerebrovascular damage (WMH volume) in aging*) correlations of any of the variables collected with the cerebrovascular damage are carefully described in this section (Table 10). The spearman correlations were executed across the whole sample and divided into the subgroups, to understand if exists different correlational patterns above and below the cut-off. To facilitate the comprehension, detailed description can be found for each group of variables. Given the exploratory nature of the objective, no preliminary hypothesis had been stablished.

7.2. Results

To facilitate the comprehension, we have synthesized the results in for blocks: sociodemographic, cognitive performance, brain structural integrity and white matter tracts integrity, following the same divisions that the variables in both tables.

WMH and sociodemographic features

According to the sociodemographic variables when we divided the sample into the two subgroups based on the WMH volume cut-off we do not have significant differences, except in age and WMH volumes. The difference found in WMH volume is absolutely expected as the groups were built on the basis of this variable. Regarding the age variable, additionally to the great differences between groups, it was the only sociodemographic variable that showed a significant correlation with the total amount of vascular damage, across all the sample aggrupation's (*whole*: p=6, E-35 rho=0,633; *mild-VI*: p=0,0003, rho= 0,319; and *low-VI*: p=0,0001, rho0,300). Given this strong association found between WMH volume and age, we covariate all the subsequent analysis with the age.

WMH and cognitive performance

Within the cognitive variables, we did not find an important difference in the cognitive ability between the two groups, only one significant difference (p= 0,041) emerged for delayed recall scores. That mean that independently of the amount of WMH volume our sample was still in early stages of the disease where vascular damage had not yet generated a significant cognitive impairment, and can therefore be considered as cognitively healthy people, probably at risk of future impairment. Focusing on the correlation analysis, only two associations with low significance

appeared. The first one, in the semantic fluency for the sample as a whole (p=0,0499; rho= -0,119), indicating that the higher amount of vascular damage is associated with lower fluency in the semantic trial. The other correlation emerged only for the mild-VI subsample with the TMT-A (time) (p=0,0495; rho=0,187). Keeping in mind that no significant differences were found in cognition between low and mild-VI subgroups, we can understand that even with no evidence of cognitive performance differences, slowness of speed of processing seems to be related higher amount of vascular damage.

WMH and brain structure

In line with to the brain structures integrity we were pleased to confirm that our sample did not show significant differences between groups in any of the typical dementia markers, such us brain grey matter or hippocampal atrophy. Nevertheless, we could observe interesting differences in brain neuroimaging markers broadly associated to SVD, and specially to WMH, like lateral ventricle dilatation (p=1E-08) and WM volume diminution (p=0,039)

When looking at the correlations we could appreciate that this mentioned lateral ventricles dilatation is extremely associated with the WMH volume for the whole population (p=6, E-09, rho= 0,329), but even stronger for those participants with greater amount of damage, mild-VI (p=5, E-06, rho=0,401). For these more damaged participants we had also found a relevant association with the total WM volume (p=0,0030, rho= -0,267). On the other side, when focusing on effects for the whole sample we could also observed significant correlations with the cortical thickness (p= 0,0049, rho=-0,163) and the total GM volume (p=0,0193, rho-0,136), being that last one also perceived for the vascular healthier group, low-VI (p=0,0413, rho=-0,155).

WMH and white matter microstructure

In consonance with the white matter integrity assessed as the fractional anisotropy of the main brain fibers, we could observe the critical effect of the WMH of presumed vascular origin have on most of them. Differences between subsamples emerged in 4 out of 5 projection fibers (i.e., fmi, fma, ml and cst) and 2 out of 3 thalamic radiations (i.e., atr and str), but also in 2 out of 6 association fibers (i.e., ilf and cgh) (for p-values see Table 9). Therefore, it seems that WMH volume makes a greater difference in those tracts connecting deep areas of the brain, such as brainstem or thalamus, with the cortex (i.e., projection fibers and thalamic radiations), than for those tracts that connect different areas of the cortex (i.e., association fibers).

With reference to the correlations, similarly, emerged negative associations between WMH volume and fractional anisotropy of most projection fiber and thalamus radiations and barely for the association fibers for both the whole sample, but specially for the mild-VI group (see Table 10).

Interestingly, for the low-VI, only three tracts significantly correlated with the WMH volume, all of them showed a positive correlation and additionally, two of them are association fibers (i.e., cgh and unc). That could mean that in the very early stages of the cerebrovascular degeneration more WMH could trigger higher fractional anisotropy in fibers that interconnect cortical areas.

Table 9 Sample characterization across all collected variables

		Mild VI (124)	Low VI (176)	p-value	F value	Partial η^2
Sample features	Sex (females)	63%	71%	0,168		
	Apoe-ε4	30%	27%	0,683		
	Age	72 ± 6	62 ± 7	9E-27	140,35	0,321
	Education (years)	14 ± 5	14 ± 5	0,533	0,39	0,002
	MMSE	29 ± 1	29 ± 1	0,330	0,95	0,003
	WMH volume (mm^3)	5643 ± 5782	380 ± 266	3E-15	69,40	0,190
	Alpha peak	10 ± 1	10 ± 1	0,549	0,36	0,001
Cognitive performance	Immediate Recall	35 ± 12	39 ± 11	0,106	2,63	0,009
	Delayed Recall	21 ± 10	25 ± 8	0,041	4,23	0,015
	Digit Spam Forward	9 ± 2	9 ± 2	0,286	1,14	0,004
	Digit Spam Backward	6 ± 2	6 ± 2	0,462	0,54	0,002
	Phonemic Fluency	14 ± 5	14 ± 4	0,852	0,03	1E-04
	Semantic Fluency	17 ± 3	19 ± 4	0,212	1,57	0,006
	TMT A (time)	52 ± 20	44 ± 18	0,892	0,02	7E-05
	TMT B (time)	133 ± 75	96 ± 56	0,132	2,28	0,008
Brain structure (Volume in mm^3)	Brain segmentation	1042299 ± 114543	1062790 ± 103158	0,069	3,32	0,011
	GM	0,53 ± 0,02	0,54 ± 0,03	0,214	1,55	0,005
	Cortical GM	0,39 ± 0,02	0,39 ± 0,02	0,386	0,75	0,003
	Subcortical GM	0,047 ± 0,003	0,047 ± 0,002	0,792	0,07	2E-04
	WM	0,40 ± 0,02	0,42 ± 0,03	0,039	4,29	0,014
	Cortical thickness (mm)	2,3 ± 0,1	2,3 ± 0,1	0,220	1,51	0,005
	Lateral ventricles	0,02 ± 0,01	0,01 ± 0,005	1E-08	34,25	0,104
	Hippocampus	0,007 ± 0,001	0,007 ± 0,001	0,146	2,12	0,007
WM microstructure (Fractional Anisotropy)	Forceps Minor (fmi)	0,39 ± 0,02	0,40 ± 0,02	0,003	9,08	0,032
	Forceps Major (fma)	0,39 ± 0,02	0,40 ± 0,02	0,003	8,89	0,032
	Middle cerebellar peduncle (mcp)	0,50 ± 0,04	0,50 ± 0,03	0,734	0,12	4E-04
	Medial lemniscus (ml)	0,44 ± 0,02	0,46 ± 0,02	7E-07	25,89	0,087
	Corticospinal tract (cst)	0,41 ± 0,02	0,42 ± 0,02	0,094	2,83	0,010
	Acoustic radiation (ar)	0,54 ± 0,02	0,54 ± 0,02	0,123	2,40	0,009
	Anterior thalamic radiation (atr)	0,47 ± 0,02	0,19 ± 0,02	6E-06	21,33	0,073
	Superior thalamic radiation (str)	0,43 ± 0,02	0,44 ± 0,02	0,002	10,17	0,04
	Posterior thalamic radiation (ptr)	0,40 ± 0,02	0,41 ± 0,02	0,179	1,82	0,007
	Superior longitudinal fasciculus (slf)	0,45 ± 0,03	0,45 ± 0,02	0,759	0,09	3E-04
	Inferior longitudinal fasciculus (ilf)	0,50 ± 0,02	0,47 ± 0,08	0,002	9,98	0,036
	Inferior fronto-occipital fasciculus (ifo)	0,44 ± 0,03	0,44 ± 0,03	0,255	1,30	0,005
	Uncinate fasciculus (unc)	0,47 ± 0,02	0,47 ± 0,02	0,884	0,02	8E-05
	Cingulate gyrus part of cingulum (cgc)	0,51 ± 0,03	0,53 ± 0,02	1E-08	34,21	0,112
	Parahippocampal part of cingulum (cgh)	0,41 ± 0,03	0,41 ± 0,02	0,911	0,01	5E-05

Note: Values are presented as mean ± SD. MMSE = Mini-Mental State Examination, TMT-A = Trail-Making Test part A, TMT-B = Trail-Making Test part B, GM = grey matter, WM = white matter. Each tract is the result of summing the values of that tract in both hemispheres (left and right), except Forceps major and minor and middle cerebellar peduncle because there are only one in the original atlas. p-values and F scores correspond with between-groups ANCOVA test with age and total brain volume segmentation as covariates. For age and brain segmentation volume we used between-groups ANCOVA test excluding the correspondent as covariate. For sex and ApoE-ε4 we used Fisher exact test. η2 account for partial-Eta squared for all comparisons but for the case of age and brain segmentation, where the values correspond to η2 values. Alpha peak responds for the individual alpha peak frequency obtained in the occipital-parietal region of the brain.

Table 10 Spearman correlation between WMH volume and every variable collected.

	Spearman correlation: WMH volume with…	pval whole	Rho whole	pval Mild VI	Rho Mild VI	pval Low VI	Rho Low VI
Sample features	Age	**6, E-35**	**0,633**	**0,0003**	**0,319**	**0,0001**	**0,300**
	Education (years)	0,1312	0,096	0,5322	0,059	**0,0385**	**0,178**
	MMSE	0,8873	-0,008	0,4470	0,070	0,7408	-0,026
	Alpha peak	0,1422	-0,086	0,1832	-0,122	0,6793	-0,032
Cognitive performance	Immediate Recall	0,5888	-0,032	0,5716	0,053	0,3450	0,074
	Delayed Recall	0,1367	-0,088	0,6371	0,044	0,7148	-0,029
	Digit Spam Forward	0,3947	-0,051	0,2476	-0,111	0,7325	-0,027
	Digit Spam Backward	0,8256	-0,013	0,6401	-0,045	0,5181	0,051
	Phonemic Fluency	0,3088	-0,061	0,4054	-0,080	0,1884	-0,103
	Semantic Fluency	**0,0499**	**-0,119**	0,9575	0,005	0,0672	-0,143
	TMT A (time)	0,5268	0,038	**0,0495**	**0,187**	0,7686	-0,023
	TMT B (time)	0,1660	0,083	0,5315	0,060	0,9303	-0,007
Brain structure (Volume in mm^3)	GM	**0,0193**	**-0,136**	0,9342	0,008	**0,0413**	**-0,155**
	Cortical GM	0,0623	-0,108	0,2839	-0,098	0,2360	-0,090
	Subcortical GM	0,9653	0,003	0,3122	0,092	0,8887	-0,011
	WM	0,1993	-0,075	**0,0030**	**-0,267**	0,0565	0,145
	Cortical thickness *(mm)	**0,0049**	**-0,163**	0,0727	-0,163	0,0927	-0,128
	Lateral ventricles	**6, E-09**	**0,329**	**5, E-06**	**0,401**	0,7037	0,029
	Hippocampus	0,0854	-0,100	0,5450	-0,055	0,2112	-0,095
WM microstructure (Fractional Anisotropy)	Forceps Minor (fmi)	**0,0006**	**-0,205**	**5, E-06**	**-0,415**	0,7148	0,029
	Forceps Major (fma)	**0,0001**	**-0,227**	**0,0001**	**-0,362**	0,8038	-0,020
	Middle cerebellar peduncle (mcp)	0,7970	0,016	0,0810	-0,165	0,1440	0,116
	Medial lemniscus (ml)	**2, E-07**	**-0,309**	**0,0016**	**-0,293**	0,5433	-0,049
	Corticospinal tract (cst)	0,0905	-0,102	**0,0357**	**-0,198**	0,5566	0,047
	Acoustic radiation (ar)	0,3092	-0,062	**0,0015**	**-0,295**	0,0876	0,136
	Anterior thalamic radiation (atr)	**4, E-05**	**-0,245**	**0,0001**	**-0,356**	0,3365	0,077
	Superior thalamic radiation (str)	**0,0365**	**-0,126**	**0,0001**	**-0,354**	**0,0011**	**0,256**
	Posterior thalamic radiation (ptr)	0,1721	-0,083	**0,0255**	**-0,210**	0,8837	0,012
	Superior longitudinal fasciculus (slf)	0,1949	0,079	0,9435	-0,007	0,1081	0,128
	Inferior longitudinal fasciculus (ilf)	**0,0003**	**0,219**	0,2438	0,111	0,1756	0,110
	Inferior fronto-occipital fasciculus (ifo)	0,4625	-0,045	0,1528	-0,135	0,2567	0,090
	Uncinate fasciculus (unc)	0,3789	0,053	0,4083	-0,079	**0,0344**	**0,168**
	Cingulate gyrus part of cingulum (cgc)	**1, E-07**	**-0,315**	**4, E-05**	**-0,375**	0,6596	0,035
	Parahippocampal part of cingulum (cgh)	0,6558	0,027	0,3191	-0,095	**0,0454**	**0,159**

Note: Results of the Spearman partial correlation analysis (age and brain segmentation volume as covariates) between total WMH volume and brain cognitive and structure integrity for each population analyzed in this thesis. MMSE = Mini-Mental State Examination, TMT-A = Trail-Making Test part A, TMT-B = Trail-Making Test part B, GM = grey matter, WM = white matter. Each tract is the result of summing the values of that tract in both hemispheres (left and right), except Forceps major and minor and middle cerebellar peduncle because there are only one in the original atlas.

7.3. Conclusion

In summary, we believe that this first chapter of the experimental studies section fulfills the objective of shedding some light on the understanding of the relationship of the load of cerebrovascular damage (WMH volume) with the sociodemographic characteristics, brain integrity, and cognitive performance, before moving on to electrophysiological experiments.

Here, we describe the highlights of this first exploratory study. We consider that this information is relevant to provide a richer context and a better understanding of the following chapters:

- WMH total volume is closely related to age.
- Although our subgroups did not show significant differences in their cognitive performance, lower processing speed (assessed with time in TMT-A) seems to be correlated with a higher volume WMH.
- Brain structural differences associated to SVD (i.e., ventricular dilatation, lower WM volume) are evidenced in our mild-VI group, although they are still cognitively healthy. The degree of deterioration of these brain structures appeared to be tightly associated to the WMH severity.

- It can be observed a critical effect of the WMH of presumed vascular origin on the integrity of the WM projection fibers and thalamic radiations that are tracts connecting deep areas of the brain with the cortex.

Chapter 8: Study I. Influence of cerebrovascular damage on electrophysiological power spectra of cognitively healthy old population.

8.1. Objective & Hypothesis

The first experimental study focused to electrophysiology included in the present thesis aimed to find power spectra patterns in resting-state electrophysiological signal, measured with MEG, associated to cerebrovascular damage (WMH), and their implication in cognitive performance and brain structure (i.e., grey, and white matter integrity) in aging.

As described in the systematic review, no paper has been published performing spectral analysis with MEG in older people diagnosed with mild or major VCI, and only few can be found with EEG (Torres-Simón et al., 2022). Fourteen articles were included in this section; 11 describing results of VCI compared to HC, 10 comparing VCI to AD, and most reporting comparisons between all three groups. Several methodologies were used to analyze the signal spectrum: evaluating the relative power of the signal in each frequency band, the ratios between the power found in different bands, the α peak's amplitude, frequency and dispersion, the symmetry of the power distribution across the brain, and the displacement of the general frequency of the spectrum. For all articles, the physiological signal was recorded using EEG during the resting-state, with the exception of three: Tsuno et al. (2004), Xu et al. (2011), and Al-Qazzaz et al. (2017b), that conducted the recordings during the transition from alertness to sleep, a visual task, and an auditory task respectively (Al-Qazzaz, Hamid Bin Mohd Ali, et al., 2017; Tsuno et al., 2004; Xu et al., 2011). From this pool of studies performed in resting-state signal, we could draw some general conclusions. On the one hand, the typical dementia profile known as "slowness" was found for VCI patients with increased power in slow bands: delta and theta; and decreased power in the beta band, related to cerebrovascular disease severity (either structural damage or cognitive impairment) compared to healthy controls (Al-Qazzaz, Ali, et al., 2017; Al-Qazzaz, Hamid Bin Mohd Ali, et al., 2017; Babiloni, Binetti, et al., 2004; Davide V. Moretti et al., 2004; Neto et al., 2015; Schreiter Gasser et al., 2008; van Straaten et al., 2012; Wu et al., 2014). This pattern seems to be stronger for VCI than AD with similar cognitive profiles (Babiloni, Binetti, et al., 2004; D. V. Moretti et al., 2007; Neto et al., 2015; Schreiter Gasser et al., 2008; Sheorajpanday et al., 2013a; C. Wang et al., 2014). On the other hand, according to alpha band results greater variability was found, likely due to differences in the band frequencies definition.

It is important to highlight that these studies with EEG were designed with mild or major VCI diagnosis groups, which implies certain degree of cognitive impairment and inclusion of more heterogenous participants in each group than our sample. Additionally, these studies performed group comparison analysis (i.e., VCI and HC or VCI and AD) while our main purpose was to find any robust correlation between cerebrovascular damage and power spectra patterns. In this concern, another paper out of the scope of the described review was published in 2020, including 35 cognitively healthy patients with and without WMH (Quandt et al., 2020). In this study, they performed correlation analysis between WMH volume and EEG resting-state signal, and again

they found higher theta power related to greater WMH volume. Keeping all these conditions in mind we built up some exploratory hypothesis looking at previous knowledge:

H1: We expect to find a broad “slowness” pattern, specially, higher power in the δ, θ, and lower in β band associated with the severity of the vascular damage.

H1.1: The cluster emerged will not correlate with cognitive performance, as our participants are still cognitively healthy.

H1.2.: The cluster emerged will negatively correlate with brain structure (i.e., grey, and white matter integrity), as it may be affected even before cognitive symptoms are evidenced.

8.2. Materials & Methods

The methodological pipeline designed to assess, in a data-driven manner, the existence of associations between MEG spectral power signatures and total WMH volume has been successfully employed before (Chino-Vilca et al., 2022; De Frutos-Lucas et al., 2020), and it is summarized in the Figure 28. Briefly, the methodology collects the spectral power matrices obtained as described in Chapter 6, section Power spectrum and applies a statistical procedure based on cluster-based permutation test (CBPT), with the aim of defining brain regions whose spectral signatures show a robust significant correlation with the WMH burden.

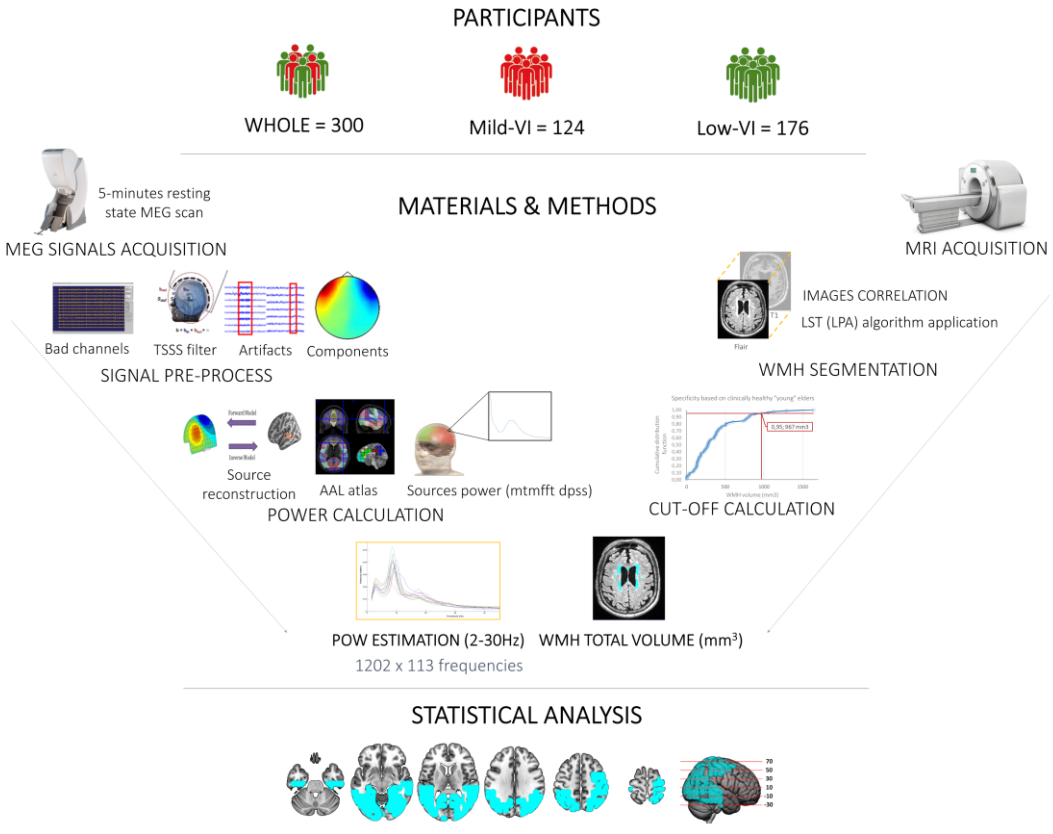

Figure 28 Graphical summary of the materials and methods utilized in the first experimental study (for detailed description see “Research methods section” and the corresponding “Material & methods section”).

Statistical analysis

The statistical pipeline was conceived to find brain regions (i.e., clusters) defined as a set of spatially adjacent nodes (sources locations) whose normalized power systematically (same sign and consecutive frequency steps) showed a significant correlation with the volume of WMH. The method relied on a cluster-based permutation test (CBPT) as implemented in Fieldtrip (Maris & Oostenveld, 2007; Oostenveld et al., 2011; Zalesky et al., 2010). The procedure was performed independently per three different samples: 1) the complete sample; 2) the Low VI subsample; and 3) the Mild VI subpopulation. The methodology involved the following steps:

1. We tested for each node and frequency step the partial correlation (age and brain segmentation volume as covariates) between the corresponding normalized power and the WMH burden. This procedure yielded one Spearman's rho statistic value and one p-value per node and frequency step.
2. The matrix with Spearman's rho values was thresholded using a critical p value < 0.01 (cluster-configuration threshold). The thresholded matrix was split into two matrices according to the sign of the Spearman's rho values.
3. For each sign-thresholded matrix, we used a clustering procedure (using the *bwlabel* function of Matlab) to identify clusters of adjacent nodes in the space and frequency dimensions.
4. For a cluster to be considered a "candidate", it had to have a volume greater than or equal to 1% of the total number of nodes (minimum spatial extension) and showed significant correlations in at least three consecutive frequency steps (minimum frequency extension). This minimum size criterion was included to suppress spurious findings. The clusters that did not meet any of the above conditions were automatically considered non-significant.
5. The Spearman's rho values were transformed to Fisher's Z values, and cluster mass statistics were calculated as the sum of the Z values of all nodes within the cluster and across all significant frequency steps.
6. To control for multiple comparisons, the entire analysis process (steps 1-5) was repeated 5,000 times, shuffling the correspondence between power values and WMH volume between subjects. At each repetition, the maximum cluster mass statistic of the surrogate clusters was kept, constructing a maximal null distribution to ensure the control of the family error rate at the cluster level.
7. This empirical distribution allowed us to calculate the p value (henceforth called CBPT p value) for each original candidate cluster. The CBPT p-value reflected the proportion of the null distribution with a cluster-mass statistic greater than or equal to the cluster-mass statistic of the corresponding candidate cluster. Only those clusters with a CBPT p value lower than 0.05 were considered for further analysis as potential MEG markers.

In this framework, significant clusters act as functional units, whose representative MEG value is calculated by averaging the power of all the nodes and frequencies that make up the corresponding cluster. These MEG signatures (1 value per significant cluster and participant) were used in the following subsequent analysis.

a) Regardless of the population with which the cluster was obtained, we tested the Spearman correlation between the markers of each cluster and the volume of WMH in the 3 populations (complete, Low VI and Mild VI).
b) We carried out additional Spearman partial correlation analysis between the clusters' signatures and indicators of brain structural and cognitive integrity.
c) Finally, we tested, for each cluster's marker, the possible existence of between-subgroups (i.e., Low VI & Mild VI) differences by means of ANCOVA test with age and brain segmentation volume as covariates.

Statistical analyses were carried out using Matlab R2022b (The MathWorks Inc., Natick, MA, USA) and SPSS v. 22 (IBM, Armonk, NY, USA) software. All tests were two tailed, and the significance level threshold was set at p = 0.05 unless explicitly stated otherwise.

8.3. Results

Power electrophysiological pattern associated with WMH volume.

When assessing the existence of significant associations between the total volume of WMH and the electrophysiological power, we only found significant results for the population with mild-VI.

The data-driven analysis found a significant cluster (CBPT, p value = 0.0120) in the frequency interval [17.50 – 38.00Hz] (see Figure 29, C) The cluster size oscillates between a minimum of 14 nodes at the beginning of the frequency range and 19 at the end of that frequency range (see Figure 29, D), reaching its maximum extension at 26.25 Hz (442 nodes). the intensity of the correlations (see Figure 29, E) varied between a minimum of -0.232 and a maximum of -0.333, values that were found at 29.00 Hz. As a representative marker of the cluster, we computed its average power across all nodes and significant frequency steps. We will refer to this marker henceforth as βpow. The βpow was found to be negatively correlated (rho = -0.326, p = 0.0003, see Figure 29, A) with the vascular damage load across the individuals with Mild-VI. When the correlation was carried out with the entire population and with the individuals with Low-VI we did not find any significant association (see Figure 29, A). The groups with Low and Mild VI did not show significant results in βpow (see Figure 29, A & B).

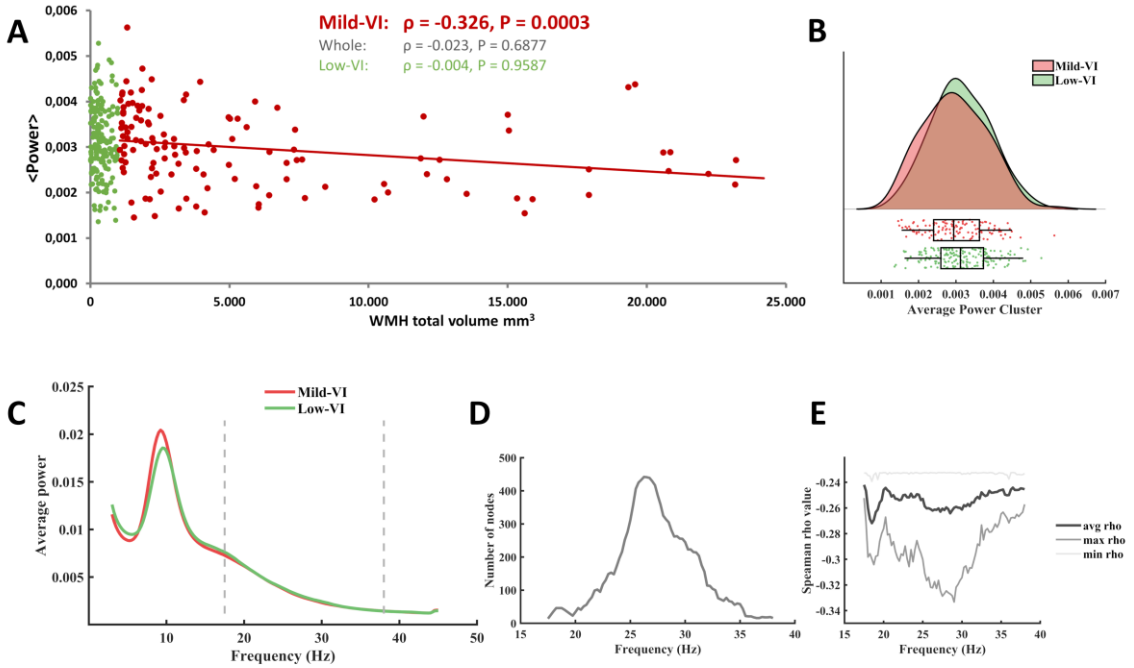

Figure 29 Quantitative description of the significant cluster. A, the scatter plot shows the correlations between the average power of the cluster (across all frequency steps and nodes) and the WMH total volume for the entire sample (grey), for the low VI population (green), and for the population with Mild-IV population (red). B, violin plots and boxplots graphics describing the individual values for the average power of the cluster in the significant frequency range. C, representation of the average spectral power across all significant nodes. The significant frequency interval is marked with dashes lines. D, number of grid nodes that are part of the cluster at each frequency step (maximum extension was found at 26.25 Hz). E: minimum, maximum, and average rho values across all nodes contained within the cluster at each frequency step (maximum correlation was found at 29 Hz)

This β cluster mainly comprises posterior regions of the brain (see Figure 30 and

Table 11). The result indicated that an increase in vascular lesion volume appeared to be associated with a decrease in power at each frequency step of the interval in the corresponding brain regions shown in the Figure 30.

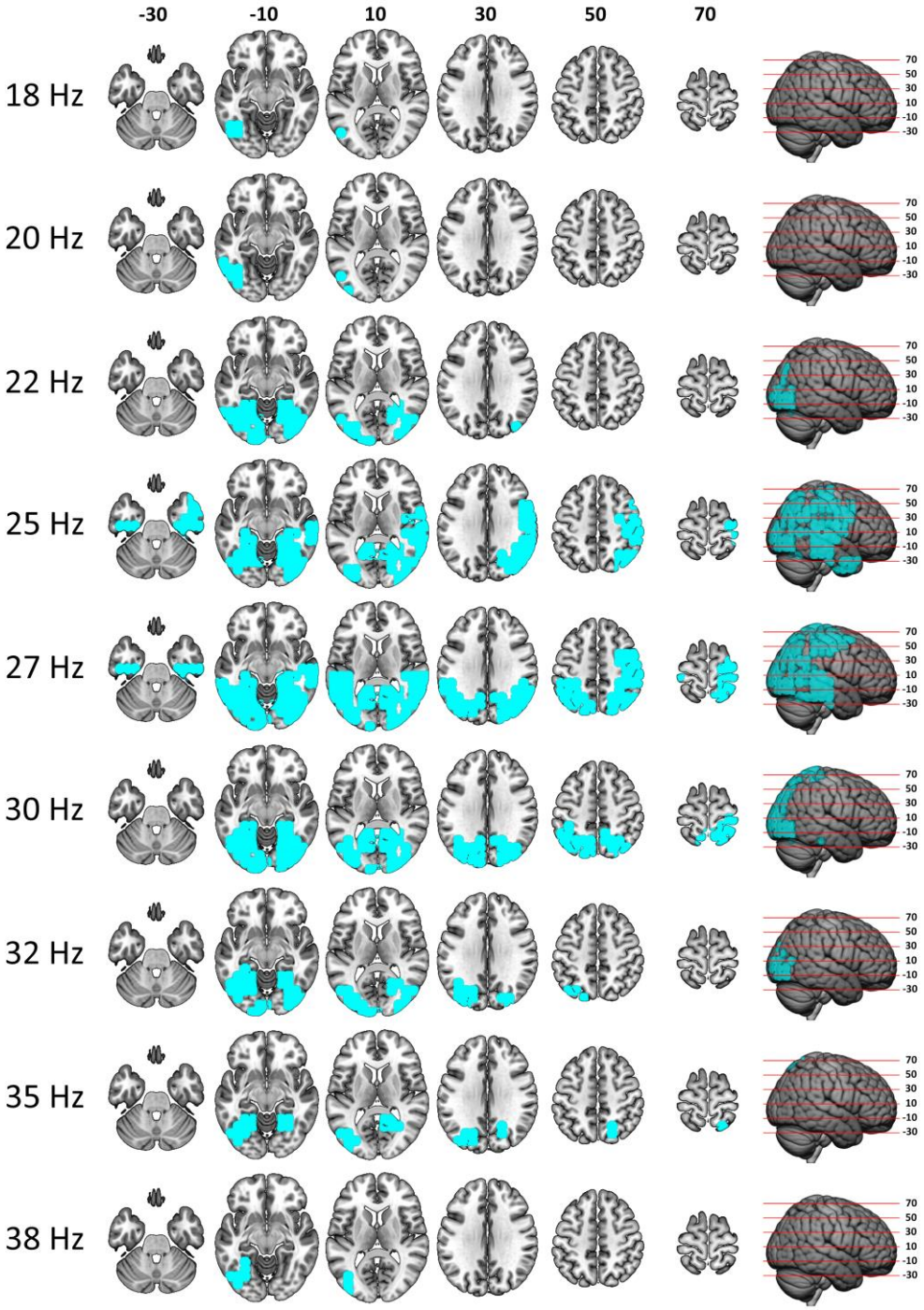

Figure 30 Correlation between beta spectral power and total WMH volume in the Mild-VI population. The figure shows the evolution of the cluster morphology (highlighted in cyan) through the different frequency steps. Axial slices of the brain are defined in MNI coordinates.

Table 11 Cluster θ description (ROIs)

ROI	% of cluster	% of ROI	Avg rho value
R Middle temporal gyrus (rMTG)	6,79	81,08	-0,259
R Postcentral gyrus (rPosCG)	6,11	81,82	-0,249
R Precentral gyrus (rPreCG)	4,75	77,78	-0,255
L Middle Occipital lobe (lMOccL)	4,75	72,41	-0,259
R Superior Temporal gyrus (rSTG)	4,30	70,37	-0,253
R Angular gyrus (rAng)	4,07	100,00	-0,265
R Middle Occipital lobe (rMOccL)	3,85	100,00	-0,280
R Fusiform gyrus (rFusiG)	3,85	89,47	-0,277
R Superior Parietal gyrus (rSPG)	3,85	94,44	-0,269
L Inferior Temporal gyrus (lITG)	3,62	66,67	-0,251
R Lingual gyrus (rLingual)	3,39	83,33	-0,267
L Inferior Parietal gyrus (lIPG)	3,39	83,33	-0,274
R Inferior Temporal gyrus (rITG)	3,39	57,69	-0,266
L Calcarine fissure and surrounding cortex (lCalc)	3,17	70,00	-0,256
L Precuneus (lPrecu)	2,71	42,86	-0,254
L Fusiform gyrus (lFusiG)	2,49	73,33	-0,289
L Superior Parietal gyrus (lSPG)	2,49	68,75	-0,260
L Middle temporal gyrus (lMTG)	2,49	25,00	-0,255
L Lingual gyrus (lLingual)	2,26	71,43	-0,265
R Superior Occipital lobe (rSOccL)	2,26	100,00	-0,265
R Inferior Parietal gyrus (rIPG)	2,26	90,91	-0,249
R Supramarginal gyrus (rSMG)	2,26	100,00	-0,261
L Angular gyrus (lAng)	2,04	100,00	-0,276
R Precuneus (rPrecu)	2,04	42,86	-0,270
R Middle Frontal gyrus (rMFG)	1,81	20,00	-0,252
R Calcarine fissure and surrounding cortex (rCalc)	1,81	66,67	-0,270
R Cuneus (rCu)	1,81	61,54	-0,263
R Hippocampus (rHip)	1,13	71,43	-0,265
L Superior Occipital lobe (lSOccL)	1,13	45,45	-0,251
L Inferior occipital lobe (lIOccL)	1,13	62,50	-0,280
R Inferior occipital lobe (rIOccl)	1,13	100,00	-0,282
L Precentral gyrus (lPreCG)	1,13	14,71	-0,245

***% ROI** = percentage of the ROI within the cluster. **% Clus** = percentage of the cluster within the ROI. **Avg rho value** = average rho value obtained for the Spearman correlation between WMH load and θ power across all nodes involved within the corresponding ROI. ROIs were ordered based on their cluster size percentage. Only ROIs that contained more than 1% of the cluster are listed. r/l=right/left.*

Brain structure and cognition linked to the electrophysiological βpow marker.

Finally, we used βpow to subsequent correlation analyses with cognitive performance and brain structure (see Table 12) in the entire population and for each sample based on the VI load. The results of these analyses showed a clear relationship between higher βpow and better structural brain integrity. In the entire population, βpow was found to be negatively correlated with age and positively correlated with the individual alpha central frequency. In the entire population and especially in the population with medium damage, a strong relationship was found between white matter structural integrity markers and βpow. The only conflicting results consisted of negative correlations between brain and gray matter volume with βpow, indicating that higher brain volume appeared to be associated with lower βpow.

Table 12 significant correlation between β power marker and brain health in the mild-VI group.

		rho	p val
Sample features	Age	-0,182	0.0430*
	WMH total	-0,348	2, E-04
	Alpha peak	0,305	0,0007
Brain structure (mm3)	WM	0,308	0,0006
	Lateral ventricles	-0,357	7, E-05
WM integrity (FA)	fmi	0,223	0,0187
	mcp	0,291	0,0018
	ml	0,212	0,0251
	atr	0,194	0.0412*
	cgc	0,235	0,0128

*Spearman correlation analyses between the average power of the β cluster and brain health markers in each sample of the study. All correlations were computed with age and brain segmentation volume as covariates. The normalization of the structural markers was computed using the brain segmentation volume. * Indicates that the result did not survive FDR (q = 0.1).*

8.4. Conclusion

As a conclusion of the first experimental study, we can partially confirm our initial hypothesis since our results showed a significant decrement of power in the β band associated with the severity of the vascular damage, but we did not find increment of power in the slower bands. It is important to notice, that we only found this effect for the subgroup with higher level of vascular damage. Additionally, as expected, we did not find any correlation between this βpow marker and cognitive performance in our sample. Finally, we can confirm the third hypothesis, because we found a correlation between different markers that signify lower brain integrity and the βpow marker. Specifically, we were able to observe the correlation of the βpow marker with bigger volume of lateral ventricles (i.e., ventricle dilatation), lower total WM volume and loss of fractional anisotropy in important brain WM tracts (i.e., fmi, mcp, ml, atr, and cgc). Interestingly, we also observed a negative correlation with alpha peak, a hallmark of electrophysiology in dementia.

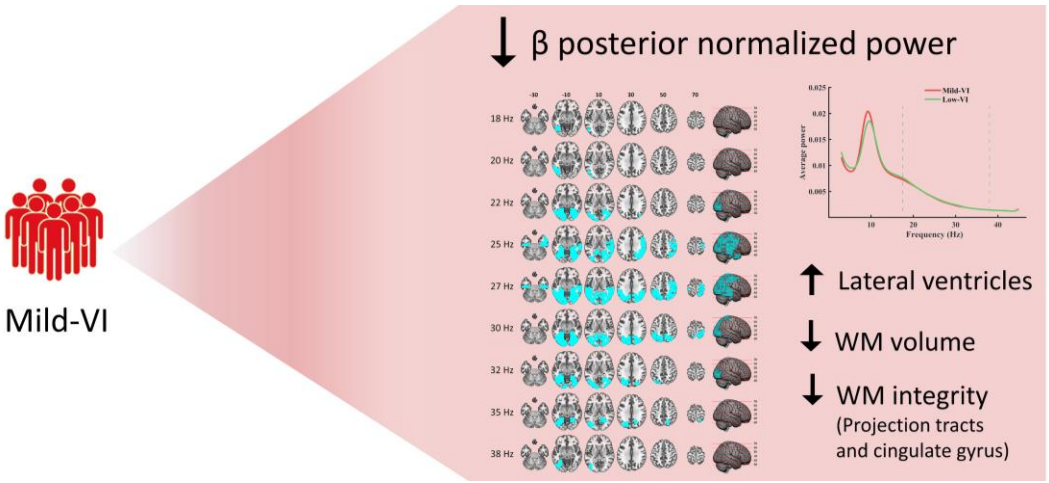

Figure 31 Graphical summary of power marker results

Hypothesis rejection or confirmation:

- ✓ H1: We expect to find a broad "slowness" pattern~~, specially, higher power in the δ, θ~~, and lower in β band associated with the severity of the vascular damage.

- ✓ H1.1: The cluster emerged will not correlate with cognitive performance, as our participants are still cognitively healthy.

- ✓ H1.2.: The cluster emerged will be associated with poorer brain structure (i.e., grey, and white matter integrity), as it may be affected even before cognitive symptoms are evidenced.

Chapter 9: Study II. Influence of cerebrovascular damage on brain electrophysiological functional connectivity of cognitively healthy old population.

9.1. Objective & Hypothesis

The second experimental study, centered in electrophysiological data, developed in the present thesis aimed to recognize the functional connectivity signatures during resting-state, measured with MEG, associated with cerebrovascular damage (WMH), and their relationship with cognitive performance and brain structure (i.e., grey, and white matter integrity) in aging.

As described in the systematic review, no paper has been published performing functional connectivity analysis with MEG in older people diagnosed with mild or major VCI, and only five can be found with EEG (Torres-Simón et al., 2022). Specifically, two recorded during resting-state (Babiloni, Ferri, et al., 2004; van Straaten et al., 2015) and three during visual tasks (C. Wang et al., 2014, 2016; Xu et al., 2015). All of the studies performing connectivity analyses were performed using EEG, and calculated directly between sensors, without performing source reconstruction. Connectivity analyses reported in these studies were heterogeneous in methodology, evaluating both functional connectivity (non-directional, statistical dependencies among neurophysiological signals), with techniques such as Synchronization Likelihood (SL) or Phase Lag Index (PLI); as well as effective connectivity (directional influence that a node exerts over another under a network model of causal dynamics), using directed Phase Lag Index (dPLI), Directed Transfer Function (DTF), or short Directed Transfer Function (sDTF). Additionally, some manuscripts used network analysis methods: clustering coefficient (Cp), characteristic path length (Lp), in-degree (number of incoming connections) and out-degree (number of outcoming connections), considering hubs those nodes with a higher (one SD in this specific paper) in-degree or out-degree than the average. While acknowledging that these metrics do not measure the same characteristics, we have tried to integrate the information in the most meaningful way; however, it is important to consider that this could easily lead to potential contradictions.

In a resting state study assessing FC, an all-band decrement of interhemispheric connectivity (using SL) was found in patients with subcortical ischemic damage compared to HC (Babiloni et al., 2004b). Additionally, a consistent front-to-back pattern of phase relations (using dPLI) in all bands except δ have been described for HC, but this pattern was not present in SiVaD patients and was even reversed in the β band (van Straaten et al., 2015). No significant relationships were found between cognitive performance and connectivity patterns (using either PLI or dPLI) (van Straaten et al., 2015). Again, it is important to highlight that these studies with EEG were designed with people with certain degree of cognitive impairment and they included more heterogenous participants. Additionally, these studies performed group comparison analysis. In this concern, the paper of Quandt and collaborators mentioned before, included 35 cognitively healthy patients with and without WMH and performed correlational analysis between the imaginary coherence at the source level in resting state EEG signal and WMH volume (Quandt et al., 2020). The found a disrupted network confined to the alpha band in participants with higher white

matter hyperintensities lesion load. The decrease of functional connectivity was evident in long-range connections, mostly originating or terminating in the frontal lobe.

The lack of literature in the field, made it impossible for us to generate coherent hypotheses with sufficient scientific support. In this concern, we proposed a completely exploratory analysis in order to understand the potential effect of the WMH on the brain functional connectivity of a big sample of old people cognitively healthy.

9.2. Materials & Methods

The methodology used for the FC analysis shared the main structure of the statistical procedure used in the analysis of the spectral power. In this case, the objective was the data-driven assessment of the existence of associations between MEG functional connectivity signatures and total WMH volume, and has been successfully applied in previous studies (Chino et al., 2023; de Frutos-Lucas et al., 2020). Briefly, the methodology collects the functional connectivity matrices described in Chapter 6, section Functional Connectivity and applies a statistical procedure based on CBPT, focused in defining brain regions whose weighted global connectivity show a robust significant correlation with the total WMH volume (see Figure 32 for a graphical description).

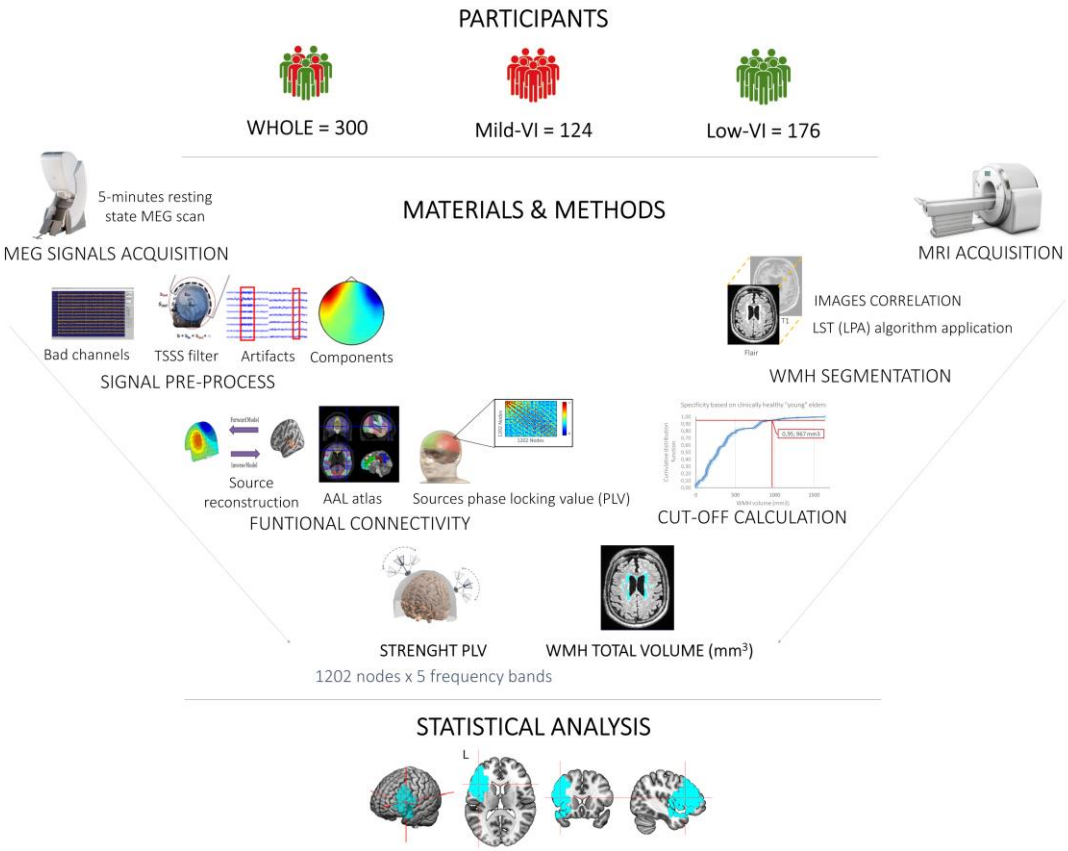

Figure 32 Graphical summary of the materials and methods utilized in the second experimental study (for detailed description see "Research methods section" and the corresponding "Material & methods section").

Statistical analysis

The statistical procedure was designed to find clusters defined as a set of spatially adjacent nodes (source locations) whose weighted global connectivity consistently showed a significant correlation (with the same sign) with WMH volume. The method relied on a cluster-based permutation test as implemented in Fieldtrip (Maris & Oostenveld, 2007; Oostenveld et al., 2011; Zalesky et al., 2010). The procedure was performed independently per each frequency band and for each different sample: 1) the complete sample; 2) the Low VI subsample; and 3) the Mild VI subpopulation. The methodology involved the following steps:

1. We tested for each node the partial correlation (age and brain segmentation volume as covariates) between the corresponding strength FC and the WMH burden. This procedure yielded one Spearman's rho statistic value and one p-value per node.
2. The matrix with Spearman's rho values was thresholded using a critical p value < 0.01 (cluster-configuration threshold). The thresholded matrix was split into two matrices according to the sign of the Spearman's rho values.
3. For each sign-thresholded matrix, we used a clustering procedure (using the *bwlabel* function of Matlab) to identify clusters of spatially adjacent nodes.
4. For a cluster to be considered a "candidate", it had to have a volume greater than or equal to 1% of the total number of nodes (minimum spatial extension). This minimum size criterion was included to suppress spurious findings. The clusters that did not reach the minimum size were automatically considered non-significant.
5. The Spearman's rho values were transformed to Fisher's Z values, and cluster mass statistics were calculated as the sum of the Z values of all nodes within the cluster.
6. To control for multiple comparisons, the entire analysis process (steps 1-5) was repeated 5,000 times, shuffling the correspondence between strength FC values and WMH volume between subjects. At each repetition, the maximum cluster mass statistic of the surrogate clusters was kept, constructing a maximal null distribution to ensure the control of the family error rate at the cluster level.
7. This empirical distribution allowed us to calculate the p value (henceforth called CBPT p value) for each original candidate cluster. The CBPT p-value reflected the proportion of the null distribution with a cluster-mass statistic greater than or equal to the cluster-mass statistic of the corresponding candidate cluster. Only those clusters with a CBPT p value lower than 0.05 were considered for further analysis as potential MEG markers.

In this framework, significant clusters act as functional units, whose representative MEG value is calculated by averaging the strength FC of all the nodes that make up the corresponding cluster. These MEG signatures (1 value per significant cluster and participant) were used in the following subsequent analysis.

a) Regardless of the population with which the cluster was obtained, we tested the Spearman correlation between the markers of each cluster and the volume of WMH in the 3 populations (complete, Low VI and Mild VI).
b) We carried out additional Spearman partial correlation analysis between the clusters' markers and indicators of brain structural and cognitive integrity.

c) Finally, we tested, for each cluster's marker, the possible existence of between-subgroups (i.e., Low VI & Mild VI) differences by means of ANCOVA test with age and brain segmentation volume as covariates.

Statistical analyses were carried out using Matlab R2022b (The MathWorks Inc., Natick, MA, USA) and SPSS v. 22 (IBM, Armonk, NY, USA) software. All tests were two tailed, and the significance level threshold was set at p = 0.05 unless explicitly stated otherwise.

9.3. Results

We calculated PLV-st as the average PLV between each specific node of the source grid and the rest of the network to obtain a marker of weighted global functional connectivity. The analysis consisted of searching for brain regions, hereinafter referred to as clusters, whose PLV-st values were significantly correlated with WMH burden, using age and brain volume as covariates. These clusters were considered as functional units, since all their components behave in the same way in terms of their relationship with WMH (i.e., their oscillatory activity (within these frequency bands) would be more/less synchronously paired with activity from all across the brain). For each significant cluster, we obtained a descriptive value, for each participant, averaging the PLV-st in all the nodes belonging to the cluster.

Whole population: WMH related to decreased anterior beta and central alpha bands PLV-st

We started by analyzing functional MEG networks to identify brain regions whose global connectivity appeared to be associated with WMH burden across the sample. The results showed three significant clusters (see Figure 33 and Table 13): two in the beta frequency band and one in the alpha frequency band. In all cases, the association was found to be inverse, indicating that the higher the total WMH volume, the lower the corresponding PLV-st.

The significant (CBPT, p value = 0.0060) cluster in the alpha frequency band (Figure 33, Bottom-left), henceforth called whole-α, involved 233 nodes that were located mainly in middle frontal regions (mass center [8 14 30] mm, MNI coordinates). A detailed description of the AAL atlas ROIs within the cluster is showed in Table 13-A. When evaluating the descriptive markers of the cluster, we found that its average PLV-st appeared to be negatively associated with the WMH burden (rho = -0.186; p = 0.0013). In addition, the correlation remained significant when looking at the population with Low-VI (rho = -0.162; p = 0.0323) and with Mild-VI (rho = -0.235; p = 0.0090) groups separately (Figure 33, Bottom-center). There were no significant differences between groups in the PLV-st scores (Figure 33, Bottom-right).

The first significant (CBPT, p value = 0.0100) cluster in the beta frequency band (Figure 33, Center-left), henceforth called whole-β1, involved 105 nodes that were located mainly in right middle frontal regions (mass center [35 8 39] mm, MNI coordinates, see Table 13-B). The significant correlation between the average PLV-st and WMH load (Figure 33, Center-center) in the whole sample (rho = -0.182; p = 0.0016) was preserved when assessing the population with Low-VI (rho = -0.216; p = 0.0042), but not when evaluating the population with Mild-VI (rho = -0.076; p = 0.4081). There were no significant differences between groups in the PLV-st scores (Figure 33, Center-right).

Finally, the second significant (CBPT, p value = 0.0200) cluster in the beta frequency band (Figure 33, Top-left), henceforth called whole-β2, involved 68 nodes that were located mainly in left inferior frontal regions (mass center [-44 18 10] mm, MNI coordinates, see Table 13-C). The behavior of the correlations between the average PLV-st and the WMH total volume (Figure 33, Top-center) replicated the results found for the cluster whole-β1, reaching a clear significance for the entire sample (rho = -0.175; p = 0.0024), remaining significant for the population with Low-VI (rho = -0.232; p = 0.0021) and being clearly non-significant for individuals with Mild-VI (rho = -0.081; p = 0.3775). There were no significant differences between groups in the PLV-st scores (Figure 33, Top-right).

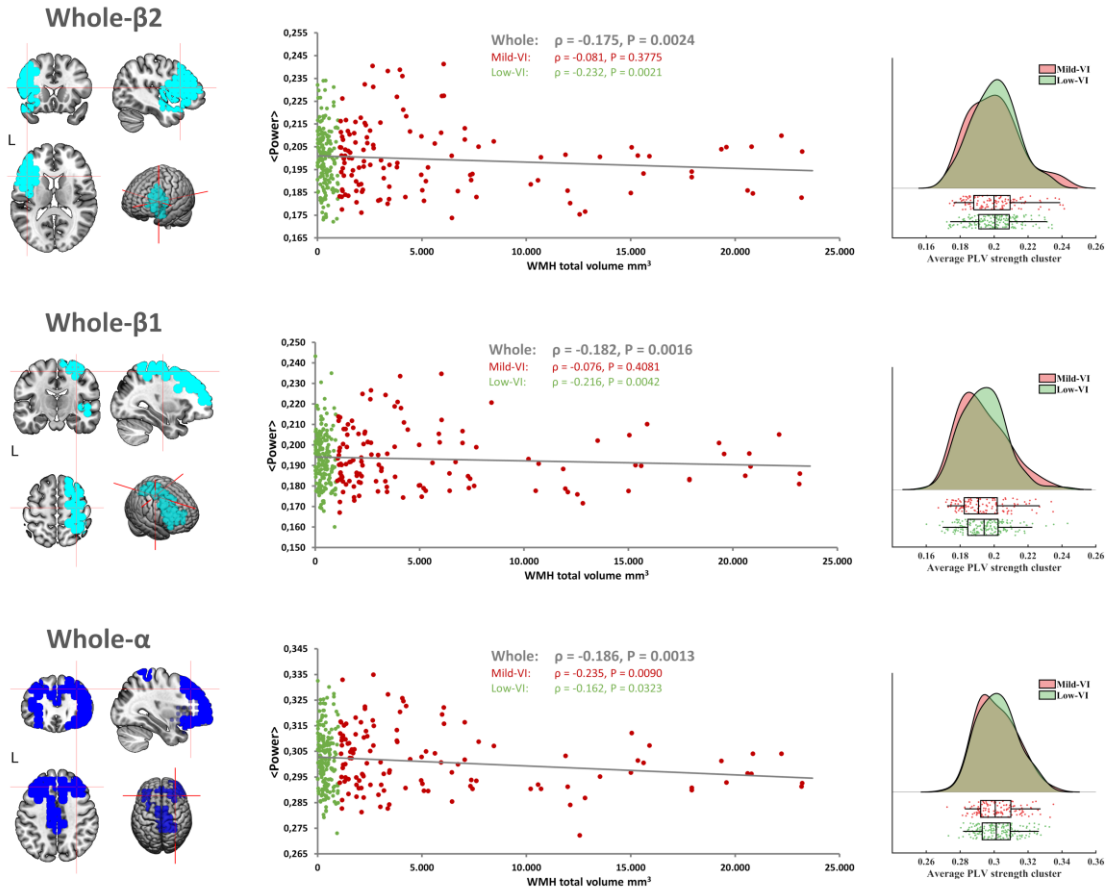

Figure 33 Association between PLV-st and WMH burden in the entire population. On the left we show the brain regions whose PLV-st appeared to be negatively associated with total WMH volume. Center, scatter plots displaying the correlation between PLV-st and WMH burden for the whole sample (grey), and the results obtained when evaluating the correlation between PLV-st of the cluster and WMH burden for the participants with Mild-VI (red), and for the individuals with Low-VI (green). On the right, violin plots and box plots representing the individual values for the mean PLV-st of the corresponding groups.

In order to better understand the role of these FC markers, we carried out additional correlation analyses between the PLV-st markers of these three clusters and brain cognitive and structural integrity scores collected for the studies (the results are depicted in the Table 14). As previously described, all three PLV-st markers negatively correlated with the WMH load. Additionally, for the PLV-st of the whole-α cluster, we found positive correlations with four brain structure integrity markers: the mean cortical thickness and the FA of medial lemniscus, corticospinal and acoustic radiation tracts. The PLV-st of the whole-β1 cluster correlated positively with the mean cortical thickness, FA of medial lemniscus, and corticospinal tracts and negatively with Digit Spam Forward. Lastly, the PLV-st of the whole- β2 appeared to be positively associated with FA of medial lemniscus, and corticospinal tracts and negatively with Digit Spam Forward.

Table 13 The three clusters emerged for the whole sample description (ROIs)

A. Cluster whole-α description

Nick ROI	% of cluster	% of ROI	Avg rho value
rMFG	12,88	75,00	-0,165
lMFG	8,15	55,88	-0,159
lMCC	5,58	81,25	-0,160
rSFG	4,72	35,48	-0,162
rIFGt	4,72	57,89	-0,174
rIFGo	4,72	91,67	-0,192
lMotor	4,72	45,83	-0,152
lSFGm	3,86	26,47	-0,158
rPosCG	3,86	27,27	-0,150
lIFGt	3,43	38,10	-0,174
lInsula	3,43	57,14	-0,187
rParaL	3,43	100,00	-0,151
lSFG	3,00	25,93	-0,155
rMFGo	3,00	100,00	-0,189
rMotor	3,00	50,00	-0,152
rInsula	3,00	50,00	-0,191
lACC	2,58	31,58	-0,167
lParaL	2,58	66,67	-0,152
rIFGor	2,15	38,46	-0,175
rSFGm	2,15	33,33	-0,160
lPreCG	1,72	12,50	-0,160
rMCC	1,72	26,67	-0,159
rPreCG	1,29	11,11	-0,150
lMFGo	1,29	42,86	-0,187
lIFGo	1,29	25,00	-0,195
rSPG	1,29	16,67	-0,151
lPrecu	1,29	10,71	-0,153
rPrecu	1,29	14,29	-0,152
rTPsup	1,29	37,50	-0,206

B. Cluster whole-β1 description

Nick ROI	% of cluster	% of ROI	Avg rho value
rMFG	31,43	82,50	-0,168
rSFG	16,19	54,84	-0,161
rPosCG	12,38	39,39	-0,157
rIFGt	9,52	52,63	-0,184
rPreCG	8,57	33,33	-0,154
rInsula	7,62	57,14	-0,197
rIFGor	4,76	38,46	-0,176
rSPG	2,86	16,67	-0,159
rSTG	2,86	11,11	-0,202
rIPG	1,90	18,18	-0,165

C. Cluster whole-β2 description

Nick ROI	% of cluster	% of ROI	Avg rho value
lIFGt	29,41	95,24	-0,161
lMFG	17,65	35,29	-0,153
lInsula	17,65	85,71	-0,169
lIFGo	10,29	100,00	-0,163
lTPsup	7,35	50,00	-0,180
lIFGo	5,88	33,33	-0,175
lSTG	4,41	15,00	-0,176
lPreCG	2,94	6,25	-0,158
lMTG	2,94	4,55	-0,184
lRO	1,47	20,00	-0,166

***% ROI** = percentage of the ROI within the cluster. **% Clus** = percentage of the cluster within the ROI. **Avg rho value** = average rho value obtained for the Spearman correlation between WMH load and ϐ power across all nodes involved within the corresponding ROI. ROIs were ordered based on their cluster size percentage. Only ROIs that contained more than 1% of the cluster are listed. r/l=right/left. ACC = Anterior cingulate cortex; IFGo = Inferior Frontal gyrus, Orbital; IFGor = Inferior Frontal gyrus, Opercular; IFGt = Inferior Frontal gyrus, Triangular; IPG = Inferior Parietal gyrus; MCC = Cingulate gyrus, Middle part; MFG = Middle Frontal gyrus; MFGo = Middle Frontal gyrus, Orbital; Motor = Supplementary Motor area; ParaL = Paracentral lobule; PosCG = Postcentral gyrus; PreCG = Precentral gyrus; Precu = Precuneus; RO = Rolandic operculum; SFG = Superior Frontal gyrus; SFGm = Superior Frontal gyrus, Medial; SPG = Superior Parietal gyrus; STG = Superior Temporal gyrus; TPsup = Temporal pole, Superior Temporal gyrus;*

Table 14 Significant correlation between PLV-st and brain health scores in the entire sample

	Cluster whole-α		Cluster whole-β1		Cluster whole-β2	
	rho	p val	rho	p val	rho	p val
WMH volume (mm^3)	-0,159	0,0070	-0,173	0,0032*	-0,167	0,0044*
Digit Spam Forward			-0,122	0,0429*	-0,140	0,0209*
Cortical Thickness	0,146	0,0122*	0,114	0,0499*		
Medial lemniscus (FA)	0,169	0,0052	0,121	0,0461*	0,154	0,0110*
Corticospinal tract (FA)	0,166	0,0062	0,131	0,0308*	0,154	0,0108*
Acoustic radiation (FA)	0,125	0,0390				

*Spearman correlation analyses between the average PLV-st of each cluster and brain health markers in the entire population. All correlations were computed with age and brain segmentation volume as covariates (only age in the case of brain segmentation volume). The normalization of the structural markers was computed using the brain segmentation volume. * Indicates that the result did not survive FDR (q = 0.1).*

Low-VI: WMH associated with decreased anterior beta frequency band PLV-st

When we applied the CBPT statistical methodology using only the individuals with low-VI, we obtained one significant cluster (CBPT, p value = 0.0090) in the beta frequency band that mirrored the clusters found, for the entire sample, in the same frequency band (Figure 34, left). This cluster, henceforth called Low-VI-β, involved 213 nodes that were located mainly in middle-superior frontal regions (mass center [-16 26 21] mm, MNI coordinates, see Table 15). In the same way that it occurred with the results obtained with the whole sample, the correlation between PLV-st and WMH burden (see Figure 34, center) was significant for the patients with Low-VI (rho = -0.239; p = 0.0015) and for the whole sample (rho = -0.159; p = 0.0060), but not for the patients with Mild-VI (rho = -0.049; p = 0.5888). The comparison of the PLV-st scores between both groups, did not show significant differences (Figure 34, right). Finally, when we computed the correlations between the PLV-st marker values of this cluster and brain structure and cognition scores we found one negative association with Digit Spam Forward (rho = -0.165; p = 0.0362), and one positive correlation with age (rho = 0.172; p = 0.0224), although none of them survived FDR.

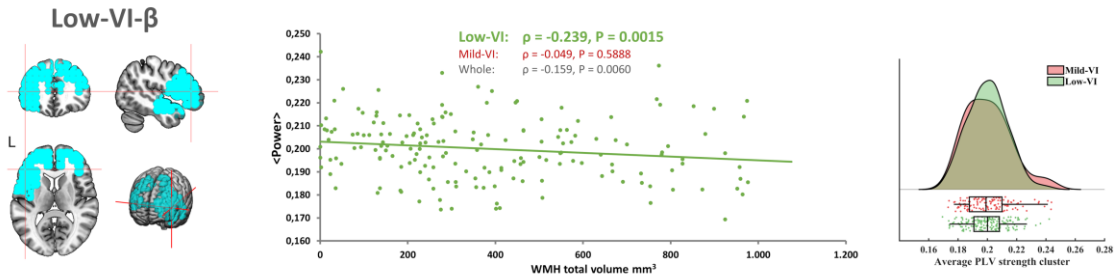

Figure 34 Association between PLV-st and WMH burden in the population with Low-VI. On the left we show the brain regions whose PLV-st appeared to be negatively associated with total WMH volume. Center, scatter plots displaying the correlation between PLV-st and WMH burden for the individuals with Low-VI (green), and the results obtained when evaluating the correlation between PLV-st of the cluster and WMH burden in the entire sample (grey) and for the participants with Mild-VI (red). On the right, violin plots and box plots representing the individual values for the mean PLV-st of the corresponding groups.

Table 15 Cluster Low-VI-β description

Nick ROI	% of cluster	% of ROI	Avg rho value
lMFG	14,08	88,24	-0,208
rMFG	12,68	67,50	-0,208
lIFGt	9,86	100,00	-0,220
rSFG	8,92	61,29	-0,205
lSFG	7,51	59,26	-0,207
lInsula	6,10	92,86	-0,229
lSFGm	5,63	35,29	-0,208
lSTG	4,23	45,00	-0,232
lIFGo	3,76	66,67	-0,233
lIFGo	3,29	100,00	-0,222
lMTG	2,82	13,64	-0,241
lPreCG	2,35	15,63	-0,213
rSFGm	2,35	33,33	-0,209
lTPsup	2,35	50,00	-0,241
lMotor	1,88	16,67	-0,196
rMotor	1,88	28,57	-0,197
lACC	1,88	21,05	-0,217
rACC	1,88	80,00	-0,218
rIFGt	1,41	15,79	-0,215

***. % ROI** = percentage of the ROI within the cluster. **% Clus** = percentage of the cluster within the ROI. **Avg rho value** = average rho value obtained for the Spearman correlation between WMH load and β power across all nodes involved within the corresponding ROI. ROIs were ordered based on their cluster size percentage. Only ROIs that contained more than 1% of the cluster are listed. r/l=right/left. ACC = Anterior cingulate cortex; IFGo = Inferior Frontal gyrus, Orbital; IFGt = Inferior Frontal gyrus, Triangular; MFG = Middle Frontal gyrus; Motor = Supplementary Motor area; MTG = Middle Temporal gyrus; PreCG = Precentral gyrus; SFG = Superior Frontal gyrus; SFGm = Superior Frontal gyrus, Medial; STG = Superior Temporal gyrus; TPsup = Temporal pole, Superior Temporal gyrus;*

Mild-VI: WMH associated with lower alpha band PLV-st in parietal regions.

The last analysis consisted of applying the data-driven CBPT analysis for the participants with Mild-VI. We found one significant cluster (CBPT, p value = 0.0200) in the alpha frequency band in parietal regions of the brain (see Figure 35, left). In this case, the result did not reflect the whole-α cluster found with the full sample because here the regions involved were located posterior rather than anterior. This cluster, henceforth called Mild-VI-α, involved 150 nodes whose mass center was located at [-9 -36 38] mm in MNI coordinates (see Table 16). The analysis of the correlations between the PLV-st marker of this cluster and the WMH load for each sample (see Figure 35, center) showed a significant result for the individuals with Mild-VI (rho = -0.293; p = 0.0011), and for the entire population (rho = -0.152; p = 0.0085). When we assessed this correlation with the participants with Low-VI we did find it non-significant (rho = -0.084; p = 0.2714). The comparison of the PLV-st between both groups did not show significant differences (see Figure 35, right).

Conclusively, when we calculated the associations between the PLV-st marker values of this cluster and brain cognitive and structural integrity scores we found one negative association with the volume of the lateral ventricles (rho = -0.219; p = 0.0169), and four positive correlations with fractional anisotropy markers: medial lemniscus (rho = 0.273; p = 0.0036), corticospinal tract (rho = 0.234; p = 0.0105), acoustic radiation (rho = 0.207; p = 0.0279), and cingulate gyrus part of cingulum (rho = 0.200; p = 0.0346). Importantly, none of them survived FDR, but considering the exploratory nature of this study and the consistency of the association between higher power and better structural integrity, we believe it pertinent to describe these results.

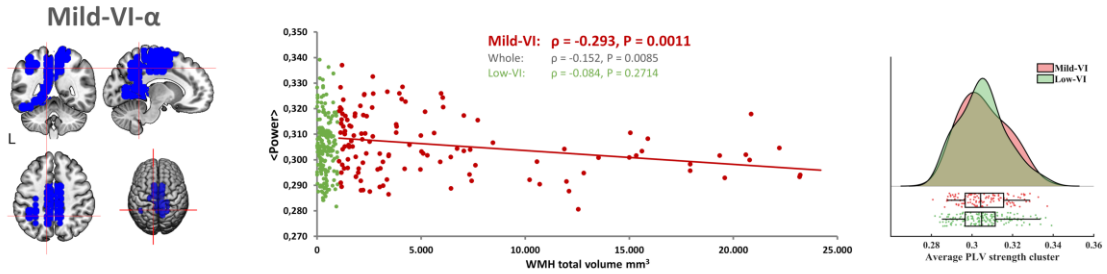

Figure 35 Association between PLV-st and WMH burden in the population with Low-VI. On the left we show the brain regions whose PLV-st appeared to be negatively associated with total WMH volume. Center, scatter plots displaying the correlation between PLV-st and WMH burden for the individuals with Mild-VI (red), and the results obtained when evaluating the correlation between PLV-st of the cluster and WMH burden in the entire sample (grey) and for the participants with Low-VI (green). On the right, violin plots and box plots representing the individual values for the mean PLV-st of the corresponding groups.

Table 16 Cluster α-Mild-VI description (ROIs)

Nick ROI	% of cluster	% of ROI	Avg rho value
lPrecu	10,67	57,14	-0,261
lMotor	10,00	62,50	-0,243
lMCC	8,00	75,00	-0,259
rMCC	6,67	66,67	-0,261
rMotor	6,00	64,29	-0,241
lLingual	6,00	64,29	-0,278
rPrecu	5,33	38,10	-0,250
lFusiG	4,67	46,67	-0,293
lIPG	4,67	38,89	-0,259
rParaL	4,67	87,50	-0,242
lParaL	4,00	66,67	-0,243
lPreCG	3,33	15,63	-0,246
lPCC	3,33	100,00	-0,268
rPosCG	3,33	15,15	-0,239
lParahip	2,67	50,00	-0,288
lCalc	2,67	20,00	-0,273
lIOccL	2,67	50,00	-0,291
lITG	2,67	16,67	-0,306
lPreG	2,00	8,82	-0,253
lHip	1,33	40,00	-0,286
rSPG	1,33	11,11	-0,244

***% ROI** = percentage of the ROI within the cluster. **% Clus** = percentage of the cluster within the ROI. **Avg rho value** = average rho value obtained for the Spearman correlation between WMH load and β power across all nodes involved within the corresponding ROI. ROIs were ordered based on their cluster size percentage. Only ROIs that contained more than 1% of the cluster are listed. r/l=right/left. ACC = Anterior cingulate cortex; Calc = Calcarine fissure and surronding cortex; FusiG = Fusiform gyrus; Hip = Hippocampus; IFGo = Inferior Frontal gyrus, Orbital; IFGt = Inferior Frontal gyrus, Triangular; IOccL = Inferior Occipital Lobe; IPG = Inferior Parietal gyrus; ITG = Inferior Temporal gyrus; MCC = Cingulate gyrus, Middle part; MFG = Middle Frontal gyrus; Motor = Supplementary Motor area; MTG = Middle Temporal gyrus; Parahip = Parahippocampus; ParaL = Paracentral lobule; PCC = Cingulate gyrus, Posterior part; PosCG = Postcentral gyrus; PreCG = Precentral gyrus; Precu = Precuneus; SFG = Superior Frontal gyrus; SFGm = Superior Frontal gyrus, Medial; SPG = Superior Parietal gyrus; STG = Superior Temporal gyrus; TPsup = Temporal pole, Superior Temporal gyrus;*

9.4. Conclusion

In essence, in the second experimental study we obtained a comprehensive view of the functional connectivity patterns that emerged as a function of cerebrovascular damage (WMH volume). As we did not describe hypothesis given the lack of literature in the field, we cannot confirm or regret them, but we have obtained statistically significant information based on a well characterized sample using robust methodologies, which could be useful as a baseline for future research.

The most relevant finding was that different patterns of functional connectivity emerged depending on the experimental group. That means that functional connectivity (PLV-st) is affected by WMH, but the effect is differently modulated depending on the stage of the cerebrovascular deterioration. Specifically, in early stages with low vascular impairment we observed a reduction in beta strength mainly localized in frontal areas (Low-VI-β). On the other hand, when focusing on more advanced stage of vascular deterioration, in mild-VI, we could find a reduction in alpha strength of the parietal regions of the brain (Mild-VI- α). When including the whole sample in the correlations, three clusters emerged, two of them representing a decrease in the beta strength in frontal areas of the brain (whole-β1 and whole-β2), and the third representing reduced alpha FC in middle-frontal regions (whole-α). Additionally, in order to better understand the role of these FC markers, we carried out additional correlation analyses between the PLV-st markers of these clusters and all the brain structure and cognition variables collected (see summary in Figure 36).

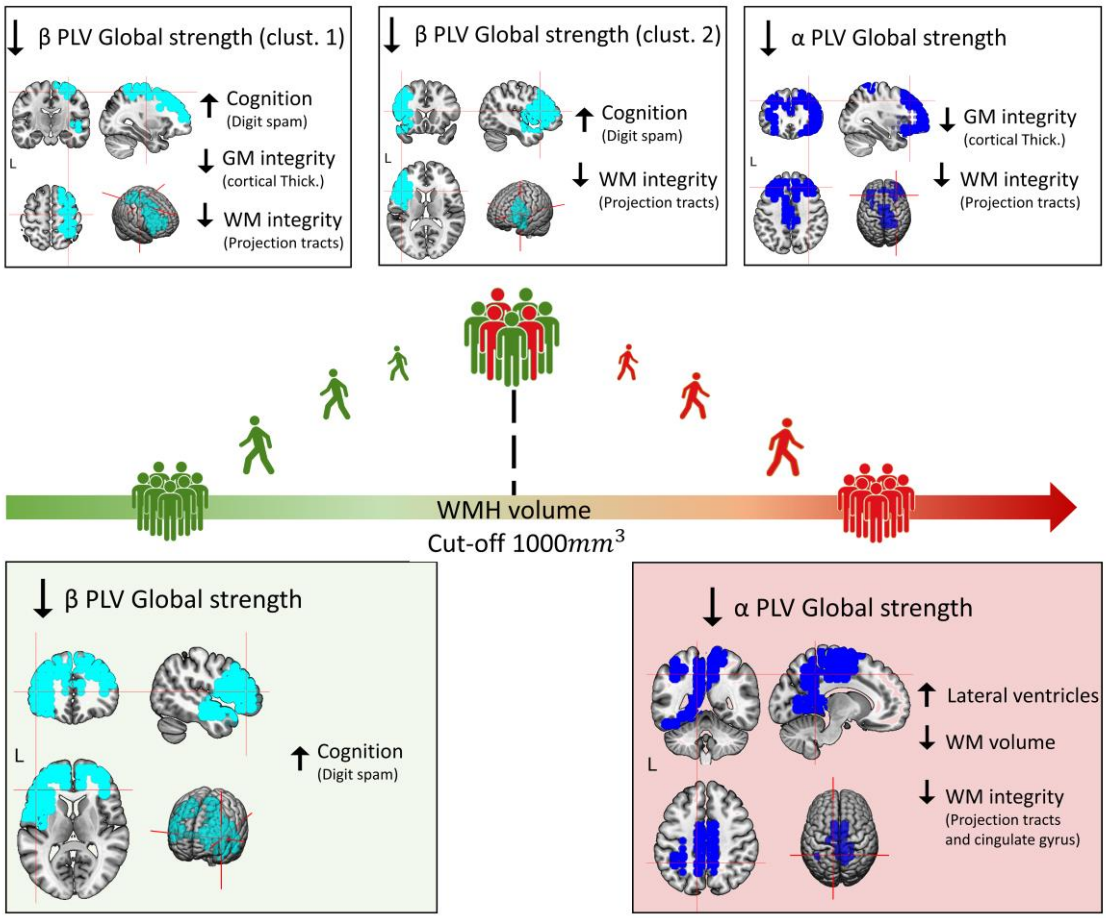

Figure 36 Graphical summary of FC markers associated to WMH volume.

General discussion

Chapter 10: Results integration and discussion

10.1. Pre-experimental results

The present thesis aimed to find specific electrophysiological markers, evaluated with MEG, for early detection of VCI. To address this ambitious goal, we begin by drawing a clear picture of the literature regarding electrophysiological patterns, with EEG and MEG, for mild and major VCI. We achieved this first objective through the development of a systematic review, already published in an international journal (Torres-Simón et al., 2022). In this work we concluded that in previous literature only general electrophysiological patterns can be found showing a low specificity for VCI diagnosis, for the differentiation of its subtypes, and for the understanding of the effect of CBVD on brain function. Additionally, we could get to know at close hand the methodological limitations that make the findings in the field inconsistent, and therefore, we could understand better why they are not currently being used in clinical practice. The characterization of the VCI samples might be highlighted as one of the most relevant limitations for results repeatability, consistency, and replicability, which hinders progress and collaboration in the field. In this concern, we proposed a reductionist approach that focuses our studies on specific MRI markers, which could help to understand particular symptoms common to different CBVD, instead of working with heterogenous diagnostic groups within VCI spectrum. Based on this idea, we chose the WMH load as the subject of study due to its high prevalence in older people and its important association with cognitive impairment, both in healthy and pathological aging. In addition to narrowing our research to a specific vascular damage, we set out to provide as objective and precise measures as possible to facilitate future replicability. With this purpose we developed two methodological studies.

The first one corresponds to the second specific objective proposed in this project, to identify the free software, for the automatic detection of WMH, that offers greater similarity with the results obtained by the clinicians' manual segmentations (gold standard) and the Fazekas clinical scale. With this study we pretended to get precise information about the vascular damage present on each of the participants included in our big sample in a time-efficient manner. Performing manual segmentation and reporting clinical scales for every participant would have required an enormous dedication of professional radiologists. Since we had not these resources available, we wanted to understand if we could have similar information using free automatic algorithms. We concluded that the LST package includes two promising and complementary methods that are widely available, easy to use, and have short execution times. Therefore. We could settle that calculating the WMH volume with LST-LPA (supervised) and controlling the possible errors in big samples with LST-LGA (unsupervised) is a feasible procedure with the ability to report accurate, objective, quantifiable and reproducible data.

The second methodological analysis pursued to establish a possible threshold from which the WMH volume in the brain of healthy people could potentially have clinical implications. Although every participant included in our sample were classified as cognitively healthy by clinicians and cognitive performance (we ensured that MMSE were at least 26), we could observe great differences in their WMH volumes. Specially, our sample showed an interesting pattern in the total WMH volumes where we could observe an exponential increment at some point. In this scenario, we wanted to better understand if there might be a tipping point at a given volume, with potential clinical impact. As previous literature has reported, WMH temporal evolution seems to follow a non-linear pattern and being a highly dynamic process (Van Leijsen et al., 2017).

In this process, the age seems to be a cornerstone, explaining slightly less than a one-third of the variance in WMH volume (Melazzini et al., 2021). Although we did not have longitudinal data, we had a broad representation of adults from 50 to 84 years old. In this way, the exponential increment of WMH volume depicted in our data is influenced, at least in part, by the age of the participants, as we were able to observe with the strong correlation that emerged (see Chapter 7. WMH Characterization). In this concern, we carry out two actions: 1) we calculated the WMH volume cut-off in our sample for the healthiest adults (50-60 years old) as Jack et al., 2017 recommended, obtaining a value of 1000 mm^3. It is important to notice that data on WMH volume in healthy adults have currently been reported to appear not to be comparable between studies, due to the characterization of the samples (i.e., cardiovascular risk factors, demographic features) and technical issues (i.e., different scanner fields, WMH segmentation methods) (Melazzini et al., 2021). Consequently, the cut-off described in the present thesis should be consider as a usable preliminary threshold for our sample, but further validation and replication analyses are required to potentially achieve a clinically practicable generalizable threshold; and 2) we decided to included age as a covariable in all the subsequent analyses.

Thank to these preliminary methodological studies we were able to accurately calculate the volume of WMH in the MR of each participant, which was used as the quantitative representation of vascular damage, overcoming the mentioned literature limitation, and promoting results repeatability, consistency, and replicability.

10.2. WMH clinical relevance

Once the bibliographic background was clarified and the main measure to characterize our sample was well analyzed, we moved on to the fourth specific objective included within this thesis project. We want to understand how sociodemographic features, brain structural integrity and cognitive performance might be affected by the amount of cerebrovascular damage in a population of cognitively healthy old people. What we found was of absolute clinical relevance, since in our sample, although they were cognitively healthy, and did not show significant differences in cognitive performance according to their vascular damage, they showed brain structural differences closely associated to the WMH presence (e.g., ventricular dilatation, lower WM volume or lower FA, especially in projection fibers). Furthermore, we found that having greater amount of WMH (in Mild-VI) was correlated with the speed processing of the participants. These results place particular importance on early detection and close follow-up of cognitively healthy people with evidence of WMH in their brain scans. Measuring this early cerebrovascular damage is an easy clinical protocol that could help delay neurodegeneration even before cognitive impairment begins, and in many cases just by controlling for vascular risk factors (e.g., healthy diet, exercise, or no smoking).

Given the evident brain structural implications that triggers the WMH presence, we want to understand what consequences it might have on brain function. As we described in the introduction, it is well known that electrophysiological techniques are capable of capturing brain functional changes induced by metabolic alteration that occur years before the onset of clinical symptoms. Finding robust electrophysiological markers associated to WMH in aging could be of great help for the clinical goal of early detection and better prognosis of cognitive impairment of vascular origin. With this purpose, we developed the two main experimental studies of the

present thesis to understand the association between cerebrovascular damage and brain electrophysiological function in older people.

10.3. MEG power spectra markers related to WMH load in cognitively healthy aging.

The first experimental study aimed to find patterns of power spectra in the resting-state electrophysiological signal, measured with MEG, associated to cerebrovascular damage (WMH), and their implication in cognitive performance and brain structure (i.e., grey, and white matter integrity) in cognitively healthy aging. In accordance with the previous literature described in the systematic review, our hypothesis was to find a broad "slowness" pattern, defined by a greater power in the δ, θ, and less power in β band associated with the severity of the vascular damage. Additionally, we expected that the cluster that emerged would not correlate with cognitive performance, as our participants were still cognitively healthy, but we anticipated negative correlations with brain integrity (i.e., grey, and white matter), as it may be affected even before the appearance of the cognitive symptoms.

Definitely, our main hypothesis was only partially accepted, as we found that lower β power was negatively associated WMH volume, implying that higher WMH volume was associated with lower β-power; but we did not find the δ and/or θ power increment. Although this result may appear to be a partial failure, we believe that it is in fact a very interesting finding itself. We must consider that given the lack of studies with MEG and WMH that carry out correlational analyzes for cognitively healthy old people, we built up the hypothesis based on studies performed with EEG data, with more heterogenous samples and doing between-groups comparisons. Most of these studies reported that patients with mild or/and major cognitive impairment and evidence of cerebrovascular damage experienced an augmentation of the power in slow bands, δ and θ, compared to healthy age-matched controls (Al-Qazzaz, Ali, et al., 2017; Al-Qazzaz, Hamid Bin Mohd Ali, et al., 2017; Babiloni, Binetti, et al., 2004; Davide V. Moretti et al., 2004; Neto et al., 2015; Schreiter Gasser et al., 2008; van Straaten et al., 2012; Wu et al., 2014). Interestingly, this increment was even greater for patients with VCI than for patients with AD even with the same degree of cognitive impairment (Babiloni, Binetti, et al., 2004; Gawel et al., 2009; D. V. Moretti et al., 2007; Davide V. Moretti et al., 2004; Quandt et al., 2020; Sheorajpanday et al., 2013b). These results appear to show the most reliable and reported outcome in resting state studies in aging, the typical dementia profile known as "slowness" (Rossini et al., 2007; Stam and van Straaten, 2012). As we described in the introduction, dementia has been defined primarily by the presence of cognitive impairment and its effects on people's daily life. Analyzing these results carefully, we can see that they show an association between the increase in power in the slow bands and cognitive impairment as it appears in those experimental groups, diagnosed with mild or major neurocognitive disorder (i.e., in VCI patients compared to HC and both in VCI and AD patients). Reinforcing this idea, theta band power increment has been previously linked to general cognitive impairment, assessed with MMSE (Moretti et al., 2007). Taking this premise, it is important to remember that the sample included in our studies is made up of cognitively healthy older people with MMSE ≥ 26, so this could be the explanation why we did not obtain this broad increment in the slow bands power in our results.

On the other hand, the β band power decrement in posterior brain regions depicted in our data have been also commonly described in patients with VCI compared to HC, negatively correlated with disease severity. Furthermore, this marker of βpow marker showed correlations with other well established structural and functional markers of brain degradation. Specifically, we could observe strong correlations with a lower alpha peak, greater volume of lateral ventricles, lower total WM volume and loss of FA in important brain WM tracts (i.e., fmi, mcp, ml, atr, and cgc). Nevertheless, the most interesting finding was that this βpow marker did not correlate with the cognitive performance in our sample. It is important to remember, that this electrophysiological marker (βpow) related to the WMH volume was only observed for the subgroup with higher level of vascular damage (Mild-VI). This means that the βpow marker appears in cognitively healthy older adults with substantial vascular damage even before the onset of the clinical symptoms, but it is already correlated with brain structural changes, which are predictors of this potential future cognitive deterioration. Finally, we did not find correlations between WMH volume and other power markers for the people with low vascular impairment. Therefore, this posterior βpow marker appears to have important clinical information, playing a crucial role in the early identification of those still cognitively healthy older adults at risk of future cognitive impairment of vascular origin.

10.4. MEG FC markers associated with WMH load in cognitively healthy aging.

The second experimental study included in this thesis aimed to recognize the functional connectivity signatures (resting-state MEG) associated with cerebrovascular damage (WMH), and their relationship with cognitive performance and brain structure (i.e., grey, and white matter integrity) in cognitively healthy aging. In this experiment, we did not suggest any hypothesis due to the lack of background literature to build any premise based on prior knowledge. Therefore, we proposed a fully exploratory analysis to understand the potential effect of WMH on brain functional connectivity (strength in PLV) of a large sample of old people cognitively healthy that covered a broad spectrum of WMH loads. Additionally, we tried to come up with potential underlying physiological explanations for these results.

From this perspective, as concluded in chapter 9, the most relevant finding was that different patterns of functional connectivity emerged depending on the experimental group. That means that functional connectivity (PLV-st) is indeed affected by WMH, but the effect is modulated differently depending on the stage of the cerebrovascular deterioration. Specifically, in early stages with low vascular impairment, we observed a reduction in beta strength located mainly in frontal areas (Low-VI-β). On the other hand, when focusing on more advanced stage of vascular deterioration; in mild-VI, we could find a reduction in the alpha strength of the parietal regions of the brain (Mild-VI- α). When including the whole sample in the correlations, three clusters emerged, two of them representing a decrease in the beta strength in frontal areas of the brain (whole-β1 and whole-β2), and the third representing reduced alpha connectivity in middle-frontal regions (whole-α).

As explained in the introduction, the pathophysiology underlying VCI involves a cascade of neurovascular dysfunction (see Figure 8), which among many consequences we can observed the dysregulation of neurotransmitter systems. In this sense, it is important to highlight the previously

stablished association between the functioning of the brain oscillatory activity and the cholinergic system (Giustiniani et al., 2023; Holschneider et al., 1998; Weiss et al., 2023). Specifically, it has been previously described that abnormal functioning of the cholinergic system could explain the reduction in alpha and beta oscillations (Giustiniani et al., 2023). This type of deficit is a typical characteristic of AD, where it has been related to degenerative neuronal loss in the basal forebrain (M. Sarter & Bruno, 1999; Martin Sarter & Bruno, 1997, 2002, 2004). However, a cholinergic deficit could also be caused by subcortical cerebrovascular damage to the cholinergic corticospinal pathways (Lim et al., 2020; J. Wang et al., 2009). Cholinergic basal system can be divided into two different pathways: cholinergic brainstem and cholinergic basal forebrain (see Figure 37).

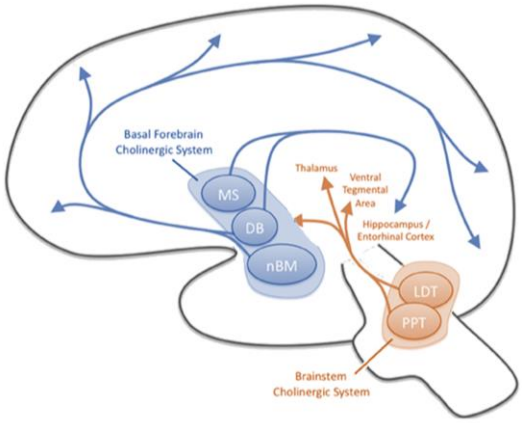

Figure 37 Schematic representation of the brain cholinergic pathways. Abb: the medial septal nucleus (MS), the diagonal band of Broca (DB), and the nucleus basalis magnocellularis (nBM), the pedunculopontine tegmental nucleus (PPT) and the laterodorsal pontine tegmentum (LDT). Modified from: "Cholinergic modulation of cognitive processing: insights drawn from computational models". Newman, E. L., Gupta, K., Climer, J. R., Monaghan, C. K., & Hasselmo, M. E., 2012. Frontiers in behavioral neuroscience, 24.

Brainstem projections are directed to thalamus, cerebellum, and ventral tegmental brain areas, while forebrain pathways drive thalamo–cortical and cortico–cortical loops. Consistent with the relationship of this neurotransmitter system and the oscillatory rhythms of the brain, cholinergic neurons in the brainstem have been shown to suppress specific low-frequency oscillations including delta, theta, and alpha, while high-frequency bands such as beta and gamma are accompanied by increased release of acetylcholine in the thalamus and cortex, more related to the basal forebrain pathway. Interestingly, in our results it can be observed that the decrease in β PLV-st, both for the whole sample and for the low-VI, occurred predominantly in the frontal areas, more related to the influence of the basal forebrain cholinergic system. In the same line, the α PLV-st decrement, again for the whole sample and for the Mild-VI, seems to appear more in middle and parietal brain regions, this time coinciding with the cholinergic branch of the brainstem. Additionally, some studies have specifically shown that white matter hyperintensities could be related to the anatomical tracks of the cholinergic pathways (Behl et al., 2007; Shin et al., 2012). In this concern, our result not only supports this finding, but also adds an important correlation between arisen functional connectivity clusters and FA reduction in projection and cingulate gyrus white matter tracts.

Finally, in an attempt to understand why we only found results in α and β frequency bands, we examine the hypothesis that transient brain rhythms are a signature of metastable synchronization, occurring at reduced collective frequencies due to delays between brain areas (Cabral et al., 2022). We already know that cerebrovascular damage not only triggers the alteration of neurotransmitters' functioning, but also influences the neurons spike timing, which is vital for proper communication between neurons. The loss of myelin found in CBVD is known to cause reduction in the speed conduction that can disrupt connectivity on a microscopic scale (i.e., the cell-to-cell communication)(Hase et al., 2018; Jang et al., 2017; Venkat et al., 2017). When this microscopic interaction is disrupted, the macroscopic synchronization is definitely altered. Up to this point this idea had already been reported (van Straaten et al., 2015). Nevertheless, in an effort to go a bit further in understanding why we only find these connectivity disturbances in high frequency bands (i.e., α and β), we hypothesize that the WMH load drives the extent of changes that can be observed in the macroscopic connectivity. Since our sample showed very low levels of vascular damage (WMH volumes), the number of neurons with their spiking time affected is not that great, so synchronization at the macroscopic level is only disturbed, indeed reduced, at higher frequencies. The groups of neurons of different brain areas are unable to synchronize their rhythms at these faster frequencies, but they still have no problem synchronizing at slower rates. Thus, following this idea, the alteration of the connectivity in the lower frequency bands will emerge later in the progression of the cerebrovascular deterioration.

Chapter 11: Limitations & Future research directions

After the comprehensive analysis described about the influence of a specific cerebrovascular damage (i.e., WMH) on brain functioning, structure and cognition is important to consider and analyze the possible impact of several limitations identified in the protocol, and to provide some suggestions to future research in the field.

11.1. WMH location and size

As it has been extensively described throughout the present thesis, WMH total volume has been strong associated with many clinical implications. However, the location of WMH, the number and size of the lesions, or the distribution on MRI may show unique signatures for each pathology, providing crucial information on the etiology, prognosis, and progression of diseases (Balakrishnan et al., 2021).

In this context, the location and pattern of distribution of WMH in the brain have been widely associated to different underlying pathological processes (i.e., SVD, multiple sclerosis, etc.) (Sarbu et al., 2016), with divergent clinical outcomes (i.e., different cognitive domains impairment) (Jokinen et al., 2020), and also with the presence of other neuroimaging markers (i.e., brain gray or white matter integrity disruption, Aβ deposition and ApoE) (Gaubert et al., 2021; C. Groot et al., 2018; Seiler et al., 2019). One of the most reported classifications in the clinical and scientific context is subcortical or deep (DWMH), periventricular (PWMH) and juxtacortical WMH (Alber et al., 2019; Griffanti et al., 2018). Higher PWMH load has been reported to be associated with reduced cognitive function, especially processing speed (Jan Cees De Groot et al., 2002), higher mean arterial pressure, and age (Griffanti et al., 2018), while higher DWMH burden has been associated with psychiatric symptoms, impaired of ADLs, increased risk of developing vascular dementia (J. C. De Groot et al., 2000; Parks et al., 2011; C. D. Smith et al., 2016) and higher body mass index (Griffanti et al., 2018). Furthermore, PWMH has a lower fractional anisotropy than DWMH, which also has a more heterogeneous microstructure (Griffanti et al., 2018). These findings support the hypothesis that PWMH and DWMH are different entities and that their distinction may provide useful information about healthy and pathological aging processes (Griffanti et al., 2018). In addition to this classification, one can also find literature that divides WMH by cerebral lobes (Dadar et al., 2021), or white matter tracts (Seiler et al., 2019)

In the present thesis we have only reported the total WMH volume regardless of the location, number, or size of the lesions. Given the lack of literature evaluating the association of WMH with electrophysiological patterns of MEG, we decided to start the work at the bases, trying to search for electrophysiological markers correlated with the general presence of WMH. However, we have already begun work, for future studies, evaluating WMH at the individual lesion level. This has been addressed using spatial clustering procedures that cluster voxels based on their location, neighbors, and intensity. This new approach will allow us to obtain information on the specific location and size of each lesion. Specifically, we are now working from tree different approaches: 1) we labeled the brain images of the entire sample according to custom atlases from the Automated Atlas Labeling (AAL); 2) we analyzed WMH at the lobes level (i.e., frontal, temporal,

parietal and occipital); and 3) we have mapped the distance to the ventricles of each individual WMH lesion. In summary, we can now assess the presence of WMH based on its location (raw anatomy, AAL atlas and lobes, distance to the ventricles), number of lesions, and their size, hopping that we will be able to enlighten the deleterious effect of cerebrovascular damage.

11.2. What about cognition impairment?

With the aim of finding robust electrophysiological markers related to WMH and its effect on cognition and brain structure in the old population, only cognitively healthy older participants were included in the experimental studies of the present research project. Although this is a suitable research scenario, it is unrealistic in clinical settings. Most older people who visit their doctor's office do so for problems that interfere with their normal activities of daily living, whether they are physical or cognitive problems. In this framework, it would be interesting to study the influence of the cerebrovascular damage in more advanced stages of the vascular disease (i.e., mild, or major VCI), or in patients presenting mixed neuropathology, like AD or MCI with presence of WMH. With the results found in the present thesis, we hope to contribute our bit to build a solid foundation for the development of research on the effects of cerebrovascular damage on brain function, structure, and cognition. Nevertheless, aware of this limitation, simultaneously to the work developed in the thesis, we have recently published a study that compares the power spectra in resting-state assessed with MEG of two groups with MCI with low and mild presence of WMH (Torres-Simon et al., 2023). We considered this study interesting in helping us to understand the commonly held idea that vascular lesions aggravate the deleterious effects of AD pathology by reducing the threshold for cognitive impairment and accelerating the pace of the dementia (Iadecola, 2013). Furthermore, in the absence of mechanism-based approaches to counteract cognitive dysfunction, addressing vascular risk factors and improving cerebrovascular health offers the opportunity to reduce its impact.

11.3. Reductionist approach vs. complex models

Exactly like the last point, we believe that the reductionist approach used in our studies represent a strength in this specific research field in accordance with the idea of establishing a robust and replicable baseline. Our purpose was focused on finding electrophysiological markers associated with a specific cerebrovascular damage (WMH volume). Nevertheless, as described in the introduction, not only CBVD, but even SVD, involves a number of imaging markers that we have not controlled in these studies (i.e. small subcortical infarcts, cerebral microbleeds, perivascular spaces or lacunes (Wardlaw et al., 2013)). In this regard, it was previously reported that the combined measure of different imaging features of cerebral SVD and brain atrophy was a more powerful predictor of cognitive decline than the individual measures alone (Jokinen et al., 2020). Despite this, when considered in isolation, total WMH and GM volumes had the strongest relationships with both global and domain-specific cognitive performance (Jokinen et al., 2020). Global quantification of SVD-related brain changes will provide a comprehensive neuroimaging metric associated with vascular damage and its possible cognitive impairment, being more desirable as a more valid surrogate than single MRI findings. In this concern, we have begun to search for available automatic detection tools for other markers of SVD such as perivascular

spaces (Boespflug et al., 2018; Schwartz et al., 2019; Valdes-Hernandez et al., 2013) or silent infarcts (Zhu et al., 2011), in order to mimic the work developed with the WMH and combine them to understand their role in the disease progression.

Additionally, previous literature has stated that different demographic characteristics, such as black race, female sex, and apolipoprotein E ε4 allele, could be associated with higher cross-sectional WMH burden or WMH progression, (Alber et al., 2019). In the same way, risk factors such as vascular, cardiometabolic, and nutritional information have been identified as crucial for the severity and progression of WMH (Fuhrmann et al., 2019; Jorgensen et al., 2018). In this sense, our experimental studies included a large sample, but relatively homogenous in terms of sociodemographic variables (i.e., race or educational level) and we could not control for these mentioned risk factors, which could be really informative and significant to include in future research. In spite of this, we tried to manage, in the most appropriate way, some of those variables that we identified as relevant in the literature. Given the importance of age for SVD progression, and specially for WMH (Van Leijsen et al., 2017), our analyses were always covariate by the age variable. Other variables that the scientific literature relates to the volume and severity of WMH are ApoE (C. Groot et al., 2018; Rojas et al., 2018), and sex (Alqarni et al., 2021). In this concern, it is true that we have not developed our electrophysiological experiments focused on these variables, but we tried to control them by making sure that there were no differences between the two groups.

As most studies we have used univariate statistical techniques to explain the associations between the cerebrovascular damage and the brain functioning, which historically has produced fragmentary and sometimes inconsistent results. Therefore, we are trying to develop a structural equation model (SEM) that encompasses most of these variables, as it could provide a framework to examine the complex relationship between the cerebrovascular damage (extended to other SVD markers) and brain function, structure, and cognition, while considering other sociodemographic (i.e., age and sex), genetic (i.e., ApoE), lifestyle (i.e. smoking, diet, exercise) or cardiovascular (i.e., blood pressure, heart rate) variables, or even including different diagnosis groups (i.e. cognitively healthy old population, MCI). With these models we could try to understand the weight of each variable in the cerebrovascular disease progression, providing important information on specific therapeutic targets in the event that the scientific community work to curb the deleterious effects in people's cognitive function and daily activities.

Conclusions & Contribution to the field

To clarify and bring closure to all the information that has been carefully described throughout this manuscript, we will return to the objectives that have guided the development of the whole project. The general objective pursued was to characterize the effect of cerebrovascular damage on brain function, structure, and cognition in the cognitively healthy aging, searching for new possible electrophysiological biomarkers in the preclinical stages. The best way to evaluate the data provided throughout the chapters is by relating each of the results to the achievement of a specific objective:

- ✓ Objective 1: *To obtain a clear picture of the literature regarding neurophysiological patterns (EEG and MEG) for mild and major VCI.* This first specific goal was fully achieved through the Systematic review described in chapter 3 and published in an international journal (Torres-Simón et al., 2022).

- ✓ Objective 2: *To identify the most accurate software for the automatic detection of white matter hyperintensities according to clinicians' manual segmentations (gold standard) and Fazekas scale.* This objective was also largely met thanks to the development of the first methodological study I, described in chapter 5, section 5.2.A. This study is under review in an international journal, but it is available in MedRxiv (*https://doi.org/10.1101/2023.03.30.23287946*).

- ✓ Objective 3: *To establish a possible threshold from which WMH volume in the brain could have clinical implications*. We could say that this specific objective was achieved, pending validation in future studies, since we were able to identify a valid cut-off for our sample in the methodological study II (described in chapter 5, section 5.2.B). As mentioned, however, further replication studies with other samples and including more variables need to be performed to potentially achieve a clinically practicable generalizable threshold. This study has not been published because we are still working on this general validation study.

- ✓ Objective 4: *To characterize the behavior of sociodemographic features, brain structural integrity and cognitive performance according to the cerebrovascular damage (WMH volume) in aging*. Although only general analysis has been performed for this purpose, we have obtained a truly comprehensive picture of the effect of WMH on cognition and brain structural integrity, as well as its relationship with different sociodemographic variables for a large sample of cognitively healthy old people (Characterization of WMH exploratory results, in chapter 7). Our group is already performing additional analyses, including complex models (i.e., structural equation model) prior to the dissemination of the results.

- ✓ Objective 5: *To find spectral power signatures in resting-state electrophysiological signal (MEG) associated with cerebrovascular damage (WMH), and their association with cognitive performance and brain structure (i.e., grey, and white matter integrity) in aging*. We are very satisfied with the consecution of this specific objective since it is one of the main pillars from which the initial idea of this thesis arose. We believe that the results obtained in the experimental study I (chapter 8) are based on a well-defined sample and a carefully selected methodological framework. Consequently, we found that in addition

to achieving the objective of this thesis, we could bring to the scientific field robust results on the electrophysiological power markers associated with WMH in the brain.

- ✓ Objective 6: *To recognize the functional connectivity signatures (resting-state MEG) associated with cerebrovascular damage (WMH), and their relationship with cognitive performance and brain structure (i.e., grey, and white matter integrity) in aging*. Unlike the previous experimental study, previous knowledge about functional connectivity was quite limited and heterogeneous, so we did not generate hypothesis, but we did perform an exploratory analysis. With this premise, we consider that the objective was achieved with the results described in experimental study (II) (chapter 9).

Therefore, after this step-by-step review of the objective, we could say that the findings described in this manuscript are an excellent initial baseline to characterize the effect of cerebrovascular damage on brain function, structure, and cognition in the cognitively healthy aging (see main findings in

Figure 38).

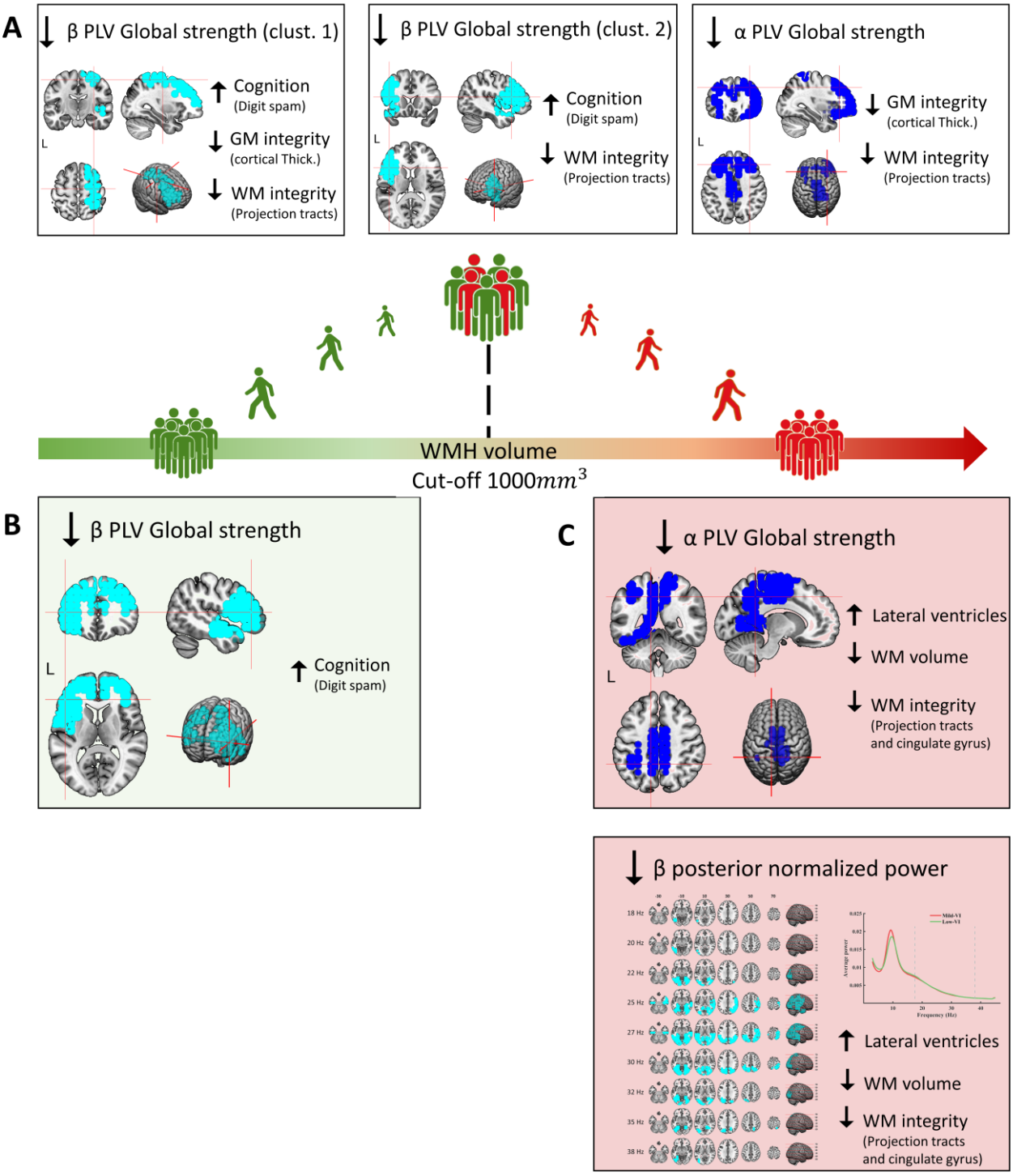

Figure 38 Graphical summary of the power and FC electrophysiological markers in resting state signal (MEG) associated with cerebrovascular damage in cognitively healthy aging. A) Main findings for the whole sample; B) Main results for the low-VI subgroup; and C) Main outcomes for the mild-VI subgroup.

After completing this research project, our main conclusion is the crucial importance of vascular system for healthy aging. As we began writing this thesis, the population pyramids around the world are inverting, and the percentage of older people is increasing significantly. In this context, the healthy progress of aging is probably one of the most important goals of the 21st century (United Nations, 2023). Additionally, within the pathologies related to aging, vascular diseases have the great advantage of being mostly treatable or at least controlled, with medical treatments or even attending to risk factors such as high blood pressure or cholesterol, leading a healthy lifestyle. Despite this, little is known about the consequences of vascular system degradation within the aging process for the brain function, structure, and the cognitive performance. As described in the introduction, around 20% of the dementias worldwide correspond to pure major VCI (Kalaria, 2018), about 50% of the dementias worldwide present concomitant vascular pathologies with other neurodegenerative diseases (Schneider et al., 2007; Wardlaw et al., 2019), and some degree of cerebrovascular damage is present on neuroimaging in practically every individual over 60 years old (Drebette & Markus, 2010; Kloppenborg et al., 2014). Given the high prevalence of cerebrovascular damage, both in healthy and pathological aging, its clinical consequences, and the opportunity to slow down the impact of degradation of the vascular system, early detection becomes a crucial scientific and social objective and the ultimate purpose of this work.

The results described in the present thesis give special importance to the task of early detection of old people at risk of suffering cognitive impairment of vascular origin. First, we analyzed the available free automatic methods to identify the WMH of vascular origin in an easy, and cost-effective manner, ensuring their accuracy compared with clinical scales and radiologists' manual segmentations. We hope that this methodological study may facilitate clinicians the early detection, accurate measure and the close monitoring or follow-up of cognitively healthy people with evidence of WMH in their brain scans. With this methodology, clinicians can have an objective quantification of the volume of the lesion and its progression for each MRI scan performed in the hospital in just a few minutes. Obviously, these algorithms are not intended to replace medical control and opinion, but they could be used as a massive screening tool with an incredible preventive power. In addition to this MRI study, the present thesis aimed to understand whether low loads of WMH in the brain could entail some brain functional alterations even before evidence of cognitive impairment. We tried to search for robust electrophysiological markers with MEG, which might have additional information about the pathological implications of subclinical cerebrovascular damage detected in the MRI images of the old population. Nowadays, the study of VCI with MEG is an unexplored field, so it is expected that the findings described in this thesis can provide valuable information to the field of electrophysiology, establishing a solid starting point for the development of a line of interesting and necessary research. The possible transfer of the results obtained with MEG to EEG would facilitate an inexpensive and non-invasive test to provide electrophysiological markers that can act as surrogate signatures for the progression of vascular damage within healthy and pathological aging, providing information associated with downstream changes in brain structure and cognition.

Bibliography

Aguirre, G. K. (2014). Functional Neuroimaging: Technical, Logical, and Social Perspectives. *Hastings Center Report*, *44*(SUPPL2). https://doi.org/10.1002/hast.294

Al-Qazzaz, N. K., Ali, S. H. B. M., Ahmad, S. A., Islam, M. S., & Escudero, J. (2017). Discrimination of stroke-related mild cognitive impairment and vascular dementia using EEG signal analysis. *Medical and Biological Engineering and Computing*, *56*(1), 137–157. https://doi.org/10.1007/s11517-017-1734-7

Al-Qazzaz, N. K., Hamid Bin Mohd Ali, S., Anom Ahmad, S., Shabiul Islam, M., & Escudero, J. (2017). Automatic artifact removal in EEG of normal and demented individuals using ICA-WT during working memory tasks. *Sensors (Switzerland)*, *17*(6). https://doi.org/10.3390/s17061326

Alber, J., Alladi, S., Bae, H. J., Barton, D. A., Beckett, L. A., Bell, J. M., Berman, S. E., Biessels, G. J., Black, S. E., Bos, I., Bowman, G. L., Brai, E., Brickman, A. M., Callahan, B. L., Corriveau, R. A., Fossati, S., Gottesman, R. F., Gustafson, D. R., Hachinski, V., … Hainsworth, A. H. (2019). White matter hyperintensities in vascular contributions to cognitive impairment and dementia (VCID): Knowledge gaps and opportunities. *Alzheimer's and Dementia: Translational Research and Clinical Interventions*, *5*, 107–117. https://doi.org/10.1016/j.trci.2019.02.001

Albert, M. S., DeKosky, S. T., Dickson, D., Dubois, B., Feldman, H. H., Fox, N. C., Gamst, A., Holtzman, D. M., Jagust, W. J., Petersen, R. C., Snyder, P. J., Carrillo, M. C., Thies, B., & Phelps, C. H. (2011). The diagnosis of mild cognitive impairment due to Alzheimer's disease: Recommendations from the National Institute on Aging-Alzheimer's Association workgroups on diagnostic guidelines for Alzheimer's disease. *Alzheimer's & Dementia*, *7*(3), 270–279. https://doi.org/10.1016/j.jalz.2011.03.008

Allan, L. M., Rowan, E. N., Firbank, M. J., Thomas, A. J., Parry, S. W., Polvikoski, T. M., O'Brien, J. T., & Kalaria, R. N. (2011). Long term incidence of dementia, predictors of mortality and pathological diagnosis in older stroke survivors. *Brain*, *134*(12), 3713–3724. https://doi.org/10.1093/brain/awr273

Alqarni, A., Jiang, J., Crawford, J. D., Koch, F., Brodaty, H., Sachdev, P., & Wen, W. (2021). Sex differences in risk factors for white matter hyperintensities in non-demented older individuals. *Neurobiology of Aging*, *98*, 197–204. https://doi.org/10.1016/j.neurobiolaging.2020.11.001

Alzheimer´s Association. (2020). 2020 Alzheimer' s disease facts and figures. *Alzheimer's & Dementia*. https://doi.org/10.1002/alz.12068

American Psychiatric Association. (2000). *Diagnostic and Statistical manual of mental disorders. Fourth edition, text revision (DSM-IV-TR)*. https://doi.org/https://doi.org/10.1176/appi.books.9780890420249.dsm-iv-tr

American Psychiatric Association. (2013). *Diagnostic and statistical manual of mental disorders. Fifth edition (DSM-5)* (Fifth). Panamericana. https://doi.org/https://doi.org/10.1176/appi.books.9780890425596

Arnold, A. M., Longstreth, T., Elster, D., Jungreis, A., Leary, H. O., Poirier, C., Bryan, R. N., & Chs, H. S. (1997). *Neuroradiology and White Changes at MR Imaging in the Data from the Cardiovascular Aging Health Brain : Study '*. 41–46.

Arvanitakis, Z., Capuano, A. W., Leurgans, S. E., Bennett, D. A., & Schneider, J. A. (2016). Relation of cerebral vessel disease to Alzheimer's disease dementia and cognitive function in elderly

people: a cross-sectional study. *The Lancet Neurology*, *15*(9), 934–943. https://doi.org/10.1016/S1474-4422(16)30029-1

Arvanitakis, Z., Fleischman, D. A., Arfanakis, K., Leurgans, S. E., Barnes, L. L., & Bennett, D. A. (2016). Association of white matter hyperintensities and gray matter volume with cognition in older individuals without cognitive impairment. *Brain Structure and Function*, *221*(4), 2135–2146. https://doi.org/10.1007/s00429-015-1034-7

Azarpazhooh, M. R., Avan, A., Cipriano, L. E., Munoz, D. G., Sposato, L. A., & Hachinski, V. (2017). Concomitant vascular and neurodegenerative pathologies double the risk of dementia. *Alzheimer's and Dementia*. https://doi.org/10.1016/j.jalz.2017.07.755

Babiloni, C., Arakaki, X., Bonanni, L., Bujan, A., Carrillo, M. C., Del Percio, C., Edelmayer, R. M., Egan, G., Elahh, F. M., Evans, A., Ferri, R., Frisoni, G. B., Güntekin, B., Hainsworth, A., Hampel, H., Jelic, V., Jeong, J., Kim, D. K., Kramberger, M., … Yener, G. (2021). EEG measures for clinical research in major vascular cognitive impairment: recommendations by an expert panel. *Neurobiology of Aging*, *103*, 78–97. https://doi.org/10.1016/j.neurobiolaging.2021.03.003

Babiloni, C., Binetti, G., Cassetta, E., Cerboneschi, D., Dal Forno, G., Del Percio, C., Ferreri, F., Ferri, R., Lanuzza, B., Miniussi, C., Moretti, D. V., Nobili, F., Pascual-Marqui, R. D., Rodriguez, G., Romani, G. L., Salinari, S., Tecchio, F., Vitali, P., Zanetti, O., … Rossini, P. M. (2004). Mapping distributed sources of cortical rhythms in mild Alzheimer's disease. A multicentric EEG study. *NeuroImage*, *22*(1), 57–67. https://doi.org/10.1016/j.neuroimage.2003.09.028

Babiloni, C., Ferri, R., Moretti, D. V., Strambi, A., Binetti, G., Dal Forno, G., Ferreri, F., Lanuzza, B., Bonato, C., Nobili, F., Rodriguez, G., Salinari, S., Passero, S., Rocchi, R., Stam, C. J., & Rossini, P. M. (2004). Abnormal fronto-parietal coupling of brain rhythms in mild Alzheimer's disease: a multicentric EEG study. *European Journal of Neuroscience*, *19*(1), 2583–2590. https://doi.org/10.1111/j.1460-9568.2004.03333.x

Baillet, S., Mosher, J. C., & Leahy, R. M. (2001). Electromagnetic brain mapping. *IEEE Signal Processing Magazine*, *18*(6), 14–30. https://doi.org/10.1109/79.962275

Balakrishnan, R., Valdés Hernández, M. del C., & Farrall, A. J. (2021). Automatic segmentation of white matter hyperintensities from brain magnetic resonance images in the era of deep learning and big data – A systematic review. *Computerized Medical Imaging and Graphics*, *88*(December 2020). https://doi.org/10.1016/j.compmedimag.2021.101867

Banerjee, D., Muralidharan, A., Hakim Mohammed, A. R., & Malik, B. H. (2020). Neuroimaging in Dementia: A Brief Review. *Cureus*, *12*(Mci), 6–13. https://doi.org/10.7759/cureus.8682

Behl, P., Bocti, C., Swartz, R. H., Gao, F. Q., Sahlas, D. J., Lanctot, K. L., Streiner, D. L., & Black, S. E. (2007). Strategic subcortical hyperintensities in cholinergic pathways and executive function decline in treated Alzheimer patients. *Archives of Neurology*, *64*(2), 266–272. https://doi.org/10.1001/archneur.64.2.266

Benton, A., & Hamsher, K. (1989). *Multilingual aphasia examination manual*. University of Iowa.

Bjerke, M., Jonsson, M., Nordlund, A., Eckerström, C., Blennow, K., Zetterberg, H., Pantoni, L., Inzitari, D., Schmidt, R., & Wallin, A. (2014). Cerebrovascular Biomarker Profile Is Related to White Matter Disease and Ventricular Dilation in a LADIS Substudy. *Dementia and Geriatric Cognitive Disorders Extra*, *4*(3), 385–394. https://doi.org/10.1159/000366119

Blennow, K., Dubois, B., Fagan, A. M., Lewczuk, P., de Leon, M. J., & Hampel, H. (2015). Clinical

utility of cerebrospinal fluid biomarkers in the diagnosis of early Alzheimer's disease. *Alzheimer's & Dementia*, *11*(1), 58–69. https://doi.org/10.1016/j.jalz.2014.02.004

Boespflug, E. L., Schwartz, D. L., Lahna, D., Pollock, J., Iliff, J. J., Kaye, J. A., Rooney, W., & Silbert, L. C. (2018). MR imaging-based multimodal autoidentification of perivascular spaces (mMAPS): Automated morphologic segmentation of enlarged perivascular spaces at clinical field strength. *Radiology*, *286*(2), 632–642. https://doi.org/10.1148/radiol.2017170205

Bos, D., Wolters, F. J., Darweesh, S. K. L., Vernooij, M. W., de Wolf, F., Ikram, M. A., & Hofman, A. (2018). Cerebral small vessel disease and the risk of dementia: A systematic review and meta-analysis of population-based evidence. *Alzheimer's and Dementia*, *14*(11), 1482–1492. https://doi.org/10.1016/j.jalz.2018.04.007

Brady, B., & Bardouille, T. (2022). Periodic/Aperiodic parameterization of transient oscillations (PAPTO)–Implications for healthy ageing. *NeuroImage*, *251*(September 2021), 118974. https://doi.org/10.1016/j.neuroimage.2022.118974

Buzsáki, G. (2006). *Rhythms of the Brain*. Oxford University Press. https://doi.org/10.1093/acprof:oso/9780195301069.001.0001

Buzsáki, G., Anastassiou, C. A., & Koch, C. (2012). The origin of extracellular fields and currents-EEG, ECoG, LFP and spikes. *Nature Reviews Neuroscience*, *13*(6), 407–420. https://doi.org/10.1038/nrn3241

Cabral, J., Castaldo, F., Vohryzek, J., Litvak, V., Bick, C., Lambiotte, R., Friston, K., Kringelbach, M. L., & Deco, G. (2022). Metastable oscillatory modes emerge from synchronization in the brain spacetime connectome. *Communications Physics*, *5*(1). https://doi.org/10.1038/s42005-022-00950-y

Cai, W., Zhang, K., Li, P., Zhu, L., Xu, J., Yang, B., Hu, X., Lu, Z., & Chen, J. (2017). Dysfunction of the neurovascular unit in ischemic stroke and neurodegenerative diseases: An aging effect. *Ageing Research Reviews*, *34*, 77–87. https://doi.org/10.1016/j.arr.2016.09.006

Campbell, M., McKenzie, J. E., Sowden, A., Katikireddi, S. V., Brennan, S. E., Ellis, S., Hartmann-Boyce, J., Ryan, R., Shepperd, S., Thomas, J., Welch, V., & Thomson, H. (2020). Synthesis without meta-analysis (SWiM) in systematic reviews: Reporting guideline. *The BMJ*, *368*, 1–6. https://doi.org/10.1136/bmj.l6890

Cancino, M., & Rehbein, L. (2016). Factores de riesgo y precursores del Deterioro Cognitivo Leve (DCL): Una mirada sinóptica Anticipatory signs and risk factors for Mild Cognitive Impairment (MCI): A synoptic view. *Sociedad Chilena de Psicología Clínica*, *34*, 183–189. https://scielo.conicyt.cl/pdf/terpsicol/v34n3/art02.pdf

Cao, Q., Tan, C. C., Xu, W., Hu, H., Cao, X. P., Dong, Q., Tan, L., & Yu, J. T. (2020). The Prevalence of Dementia: A Systematic Review and Meta-Analysis. *Journal of Alzheimer's Disease : JAD*, *73*(3), 1157–1166. https://doi.org/10.3233/JAD-191092

Caruso, P., Signori, R., & Moretti, R. (2019). Small vessel disease to subcortical dementia: A dynamic model, which interfaces aging, cholinergic dysregulation and the neurovascular unit. *Vascular Health and Risk Management*, *15*, 259–281. https://doi.org/10.2147/VHRM.S190470

Catindig, J. A. S., Venketasubramanian, N., Ikram, M. K., & Chen, C. (2012). Epidemiology of dementia in Asia: Insights on prevalence, trends and novel risk factors. *Journal of the Neurological Sciences*, *321*(1–2), 11–16. https://doi.org/10.1016/j.jns.2012.07.023

Cerri, S., Puonti, O., Meier, D. S., Wuerfel, J., Mühlau, M., Siebner, H. R., & Van Leemput, K. (2021). A contrast-adaptive method for simultaneous whole-brain and lesion segmentation in multiple sclerosis. *NeuroImage*, *225*, 117471. https://doi.org/10.1016/j.neuroimage.2020.117471

Chino-Vilca, B., Rodríguez-Rojo, I. C., Torres-Simón, L., Cuesta, P., Vendrell, A. C., Piñol-Ripoll, G., Huerto, R., Tahan, N., & Maestú, F. (2022). Sex specific EEG signatures associated with cerebrospinal fluid biomarkers in mild cognitive impairment. *Clinical Neurophysiology*, *142*, 190–198. https://doi.org/10.1016/j.clinph.2022.08.007

Chino, B., Cuesta, P., Pacios, J., de Frutos-Lucas, J., Torres-Simón, L., Doval, S., Marcos, A., Bruña, R., & Maestú, F. (2023). Episodic memory dysfunction and hypersynchrony in brain functional networks in cognitively intact subjects and MCI: a study of 379 individuals. *GeroScience*, *45*(1), 477–489. https://doi.org/10.1007/s11357-022-00656-7

Chui, H. C., Victoroff, J. I., Margolin, D., Jagust, W., Shankle, R., & Katzman, R. (1992). Criteria for the diagnosis of ischemic vascular dementia proposed by the State of California Alzheimer's Disease Diagnostic and Treatment Centers. *Neurology*, *42*(3). https://doi.org/10.1212/WNL.42.3.473

Chutinet, A., & Rost, N. S. (2014). White matter disease as a biomarker for long-term cerebrovascular disease and dementia topical collection on cerebrovascular disease and stroke. *Current Treatment Options in Cardiovascular Medicine*, *16*(3). https://doi.org/10.1007/s11936-013-0292-z

Cohen, M. X. (2014). *Analyzing Neural Time Series Data*. MIT Press 238 Main St., Suite 500, Cambridge, MA 02142-1046 USA journals-info@mit.edu.

Colclough, G. L., Woolrich, M. W., Tewarie, P. K., Brookes, M. J., Quinn, A. J., & Smith, S. M. (2016a). How reliable are {MEG} resting-state connectivity metrics? *Neuroimage*, *138*, 284–293.

Colclough, G. L., Woolrich, M. W., Tewarie, P. K., Brookes, M. J., Quinn, A. J., & Smith, S. M. (2016b). How reliable are MEG resting-state connectivity metrics? *NeuroImage*, *138*, 284–293. https://doi.org/10.1016/j.neuroimage.2016.05.070

Cox, S. R., Ritchie, S. J., Tucker-Drob, E. M., Liewald, D. C., Hagenaars, S. P., Davies, G., Wardlaw, J. M., Gale, C. R., Bastin, M. E., & Deary, I. J. (2016). Ageing and brain white matter structure in 3,513 UK Biobank participants. *Nature Communications*, *7*, 1–13. https://doi.org/10.1038/ncomms13629

Dadar, M., Mahmoud, S., Zhernovaia, M., Camicioli, R., Maranzano, J., & Duchesne, S. (2021). *White Matter Hyperintensity Distribution Differences in Aging and Neurodegenerative Disease Cohorts Corresponding Author Information*. https://doi.org/10.1101/2021.11.23.469690

de Frutos-Lucas, J., Cuesta, P., López-Sanz, D., Peral-Suárez, Á., Cuadrado-Soto, E., Ramírez-Toraño, F., Brown, B. M., Serrano, J. M., Laws, S. M., Rodríguez-Rojo, I. C., Verdejo-Román, J., Bruña, R., Delgado-Losada, M. L., Barabash, A., López-Sobaler, A. M., López-Higes, R., Marcos, A., & Maestú, F. (2020). The relationship between physical activity, apolipoprotein E ε4 carriage, and brain health. *Alzheimer's Research & Therapy*, *12*(1), 48. https://doi.org/10.1186/s13195-020-00608-3

De Frutos-Lucas, J., Cuesta, P., Ramírez-Toraño, F., Nebreda, A., Cuadrado-Soto, E., Peral-Suárez,

Á., Lopez-Sanz, D., Bruña, R., Marcos-De Pedro, S., Delgado-Losada, M. L., López-Sobaler, A. M., Concepción Rodríguez-Rojo, I., Barabash, A., Serrano Rodriguez, J. M., Laws, S. M., Dolado, A. M., López-Higes, R., Brown, B. M., & Maestú, F. (2020). Age and APOE genotype affect the relationship between objectively measured physical activity and power in the alpha band, a marker of brain disease. *Alzheimer's Research and Therapy*, *12*(1), 1–12. https://doi.org/10.1186/s13195-020-00681-8

De Groot, J. C., De Leeuw, F. E., Oudkerk, M., Hofman, A., Jolles, J., & Breteler, M. M. B. (2000). Cerebral white matter lesions and depressive symptoms in elderly adults. *Archives of General Psychiatry*, *57*(11), 1071–1076. https://doi.org/10.1001/archpsyc.57.11.1071

De Groot, Jan Cees, De Leeuw, F. E., Oudkerk, M., Van Gijn, J., Hofman, A., Jolles, J., & Breteler, M. M. B. (2002). Periventricular cerebral white matter lesions predict rate of cognitive decline. *Annals of Neurology*, *52*(3), 335–341. https://doi.org/10.1002/ana.10294

De Groot, M., Ikram, M. A., Akoudad, S., Krestin, G. P., Hofman, A., Van Der Lugt, A., Niessen, W. J., & Vernooij, M. W. (2015). Tract-specific white matter degeneration in aging: The Rotterdam Study. *Alzheimer's and Dementia*, *11*(3), 321–330. https://doi.org/10.1016/j.jalz.2014.06.011

Dey, A. K., Stamenova, V., Turner, G., Black, S. E., & Levine, B. (2016). Pathoconnectomics of cognitive impairment in small vessel disease: A systematic review. *Alzheimer's and Dementia*, *12*(7), 831–845. https://doi.org/10.1016/j.jalz.2016.01.007

Donato, A. J., Machin, D. R., & Lesniewski, L. A. (2018). Mechanisms of Dysfunction in the Aging Vasculature and Role in Age-Related Disease. *Circulation Research*, *123*(7), 825–848. https://doi.org/https://doi.org/10.1161/CIRCRESAHA.118.312563

Donoghue, T., Haller, M., Peterson, E. J., Varma, P., Sebastian, P., Gao, R., Noto, T., Lara, A. H., Wallis, J. D., Knight, R. T., Shestyuk, A., & Voytek, B. (2020). Parameterizing neural power spectra into periodic and aperiodic components. *Nature Neuroscience*, *23*(12), 1655–1665. https://doi.org/10.1038/s41593-020-00744-x

Drebette, S., & Markus, H. S. (2010). The clinical importance or WMH on brain MR systematic review and meta-analysis. *BMJ Open*, *314*. https://doi.org/https://doi.org/10.1136/bmj.c3666

Dubois, B., Hampel, H., Feldman, H. H., Scheltens, P., Aisen, P., Andrieu, S., Bakardjian, H., Benali, H., Bertram, L., Blennow, K., Broich, K., Cavedo, E., Crutch, S., Dartigues, J. F., Duyckaerts, C., Epelbaum, S., Frisoni, G. B., Gauthier, S., Genthon, R., … Jack, C. R. (2016). Preclinical Alzheimer's disease: Definition, natural history, and diagnostic criteria. In *Alzheimer's and Dementia* (Vol. 12, Issue 3). https://doi.org/10.1016/j.jalz.2016.02.002

Duering, M., Righart, R., Csanadi, E., Jouvent, E., Herve, D., Chabriat, H., & Dichgans, M. (2012). Incident subcortical infarcts induce focal thinning in connected cortical regions. *Neurology*, *79*(20), 2025–2028. https://doi.org/10.1212/WNL.0b013e3182749f39

Engel, A. K., & Fries, P. (2010). Beta-band oscillations--signalling the status quo? *Current Opinion in Neurobiology*, *20*(2), 156–165. https://doi.org/10.1016/j.conb.2010.02.015

Erkinjuntti, T., Román, G., Gauthier, S., Feldman, H., & Rockwood, K. (2004). Emerging Therapies for Vascular Dementia and Vascular. *Stroke*, 1010–1017. https://doi.org/10.1161/01.STR.0000120731.88236.33

Farrall, A. J., & Wardlaw, J. M. (2009). *Blood – brain barrier : Ageing and microvascular disease –*

systematic review and meta-analysis. *30*, 337–352. https://doi.org/10.1016/j.neurobiolaging.2007.07.015

Fischl, B., Salat, D. H., Busa, E., Albert, M., Dieterich, M., Haselgrove, C., Kouwe, A. Van Der, Killiany, R., Kennedy, D., Klaveness, S., Montillo, A., Makris, N., Rosen, B., & Dale, A. M. (2002). Whole Brain Segmentation : Neurotechnique Automated Labeling of Neuroanatomical Structures in the Human Brain. *Neuron*, *33*, 341–355.

Fornito, A., Zalesky, A., & Bullmore, E. T. (2016). *Fundamentals of Brain Network Analysis*. Elsevier.

Frisoni, G. B., Geroldi, C., Beltramello, A., Bianchetti, A., Binetti, G., Bordiga, G., DeCarli, C., Laakso, M. P., Soininen, H., Testa, C., Zanetti, O., & Trabucchi, M. (2002). Radial Width of the Temporal Horn: A Sensitive Measure in Alzheimer Disease. *American Journal of Neuroradiology*, *23*(1), 35–47.

Fuhrmann, D., Nesbitt, D., Shafto, M., Rowe, J. B., Price, D., Gadie, A., Tyler, L. K., Brayne, C., Bullmore, E. T., Calder, A. C., Cusack, R., Dalgleish, T., Duncan, J., Henson, R. N., Matthews, F. E., Marslen-Wilson, W. D., Shafto, M. A., Campbell, K., Cheung, T., … Kievit, R. A. (2019). Strong and specific associations between cardiovascular risk factors and white matter micro- and macrostructure in healthy aging. *Neurobiology of Aging*, *74*, 46–55. https://doi.org/10.1016/j.neurobiolaging.2018.10.005

Fulham, M. J., Prince, R., & Hospital, A. (2004). *Neuroimaging*. 459–469.

Garcés, P., López-Sanz, D., Maestú, F., & Pereda, E. (2017). Choice of Magnetometers and Gradiometers after Signal Space Separation. *Sensors (Basel, Switzerland)*, *17*(12). https://doi.org/10.3390/s17122926

Garces, P., Martin-Buro, M. C., & Maestu, F. (2016). Quantifying the test-retest reliability of MEG resting state functional connectivity. *Brain Connectivity*, *6*(6), 448–460. https://doi.org/https://doi.org/10.1089/brain.2015.0416

Garcés, P., Martín-Buro, M. C., & Maestú, F. (2016). Quantifying the Test-Retest Reliability of Magnetoencephalography Resting-State Functional Connectivity. *Brain Connectivity*, *6*(6), 448–460. https://doi.org/10.1089/brain.2015.0416

Garcés, P., Vicente, R., Wibral, M., Pineda-Pardo, J. Á., López, M. E., Aurtenetxe, S., Marcos, A., de Andrés, M. E., Yus, M., Sancho, M., Maestú, F., & Fernández, A. (2013). Brain-wide slowing of spontaneous alpha rhythms in mild cognitive impairment. *Frontiers in Aging Neuroscience*, *5*, 100. https://doi.org/10.3389/fnagi.2013.00100

Gaubert, M., Lange, C., Garnier-Crussard, A., Köbe, T., Bougacha, S., Gonneaud, J., de Flores, R., Tomadesso, C., Mézenge, F., Landeau, B., de la Sayette, V., Chételat, G., & Wirth, M. (2021). Topographic patterns of white matter hyperintensities are associated with multimodal neuroimaging biomarkers of Alzheimer's disease. *Alzheimer's Research and Therapy*, *13*(1), 1–11. https://doi.org/10.1186/s13195-020-00759-3

Gawel, M., Zalewska, E., Szmidt-Sałkowska, E., & Kowalski, J. (2009). The value of quantitative EEG in differential diagnosis of Alzheimer's disease and subcortical vascular dementia. *Journal of the Neurological Sciences*, *283*, 127–133. https://doi.org/10.1016/j.jns.2009.02.332

Giustiniani, A., Danesin, L., Bozzetto, B., Macina, A., Benavides-Varela, S., & Burgio, F. (2023). Functional changes in brain oscillations in dementia: A review. *Reviews in the Neurosciences*, *34*(1), 25–47. https://doi.org/10.1515/revneuro-2022-0010

Gorelick, P. B., Scuteri, A., Black, S. E., DeCarli, C., Greenberg, S. M., Iadecola, C., Launer, L. J., Laurent, S., Lopez, O. L., Nyenhuis, D., Petersen, R. C., Schneider, J. A., Tzourio, C., Arnett, D. K., Bennett, D. A., Chui, H. C., Higashida, R. T., Lindquist, R., Nilsson, P. M., … Seshadri, S. (2011). Vascular Contributions to Cognitive Impairment and Dementia. *Stroke*, *42*(9), 2672–2713. https://doi.org/10.1161/str.0b013e3182299496

Griffanti, L., Jenkinson, M., Suri, S., Zsoldos, E., Mahmood, A., Filippini, N., Sexton, C. E., Topiwala, A., Allan, C., Kivimäki, M., Singh-Manoux, A., Ebmeier, K. P., Mackay, C. E., & Zamboni, G. (2018). Classification and characterization of periventricular and deep white matter hyperintensities on MRI: A study in older adults. *NeuroImage*, *170*(March 2017), 174–181. https://doi.org/10.1016/j.neuroimage.2017.03.024

Griffanti, L., Zamboni, G., Khan, A., Li, L., Bonifacio, G., Sundaresan, V., Schulz, U. G., Kuker, W., Battaglini, M., Rothwell, P. M., & Jenkinson, M. (2016). BIANCA (Brain Intensity AbNormality Classification Algorithm): A new tool for automated segmentation of white matter hyperintensities. *NeuroImage*, *141*, 191–205. https://doi.org/10.1016/j.neuroimage.2016.07.018

Groot, C., Sudre, C. H., Barkhof, F., Teunissen, C. E., Van Berckel, B. N. M., Seo, S. W., Ourselin, S., Scheltens, P., Cardoso, M. J., Van Der Flier, W. M., & Ossenkoppele, R. (2018). Clinical phenotype, atrophy, and small vessel disease in APOE2 carriers with Alzheimer disease. *Neurology*, *91*(20), E1851–E1859. https://doi.org/10.1212/WNL.0000000000006503

Hachinski, V., Iadecola, C., Petersen, R. C., Breteler, M. M., Nyenhuis, D. L., Black, S. E., Powers, W. J., DeCarli, C., Merino, J. G., Kalaria, R. N., Vinters, H. V., Holtzman, D. M., Rosenberg, G. A., Dichgans, M., Marler, J. R., & Leblanc, G. G. (2006). National Institute of Neurological Disorders and Stroke-Canadian Stroke Network vascular cognitive impairment harmonization standards. *Stroke*, *37*(9), 2220–2241. https://doi.org/10.1161/01.STR.0000237236.88823.47

Hachinski, V., Lassen, N. A., & Marshall, J. (1974). Multi-infarct dementia. A cause of mental deterioration in elderly. *Lancet*, *2*, 207–210. https://doi.org/10.1016/s0733-8619(18)31169-1

Hämäläinen, M., Hari, R., Ilmoniemi, R. J., Knuutila, J., & Lounasmaa, O. V. (1993). Magnetoencephalography—theory, instrumentation, and applications to noninvasive studies of the working human brain. *Reviews of Modern Physics*, *65*(2), 413–497. https://doi.org/10.1103/RevModPhys.65.413

Hämäläinen, M. S., & Ilmoniemi, R. J. (1994). Interpreting magnetic fields of the brain: minimum norm estimates. *Medical & Biological Engineering & Computing*, *32*(1), 35–42. https://doi.org/10.1007/BF02512476

Hampel, H., Blennow, K., Shaw, L. M., Hoessler, Y. C., Zetterberg, H., & Trojanowski, J. Q. (2010). Total and phosphorylated tau protein as biological markers of Alzheimer's disease. *Experimental Gerontology*, *45*(1), 30–40. https://doi.org/10.1016/j.exger.2009.10.010

Hampel, H., Schneider, L. S., Giacobini, E., Kivipelto, M., Sindi, S., Dubois, B., Broich, K., Nisticò, R., Aisen, P. S., & Lista, S. (2014). Advances in the therapy of Alzheimer's disease: Targeting amyloid beta and tau and perspectives for the future. *Expert Review of Neurotherapeutics*, *15*(1), 83–105. https://doi.org/10.1586/14737175.2015.995637

Hans Berger. (1929). Über das Elektrenkephalogramm des Menschen. *Archiv Für Psychiatrie Und Nervenkrankheiten*, *87*(1), 527–570. https://doi.org/10.1007/BF01797193

Hase, Y., Horsburgh, K., Ihara, M., & Kalaria, R. N. (2018). White matter degeneration in vascular and other ageing-related dementias. *Journal of Neurochemistry*, *144*(5), 617–633. https://doi.org/10.1111/jnc.14271

Hedrich, T., Pellegrino, G., Kobayashi, E., Lina, J. M., & Grova, C. (2017). Comparison of the spatial resolution of source imaging techniques in high-density EEG and MEG. *NeuroImage*, *157*(June), 531–544. https://doi.org/10.1016/j.neuroimage.2017.06.022

Holschneider, D. P., Leuchter, A. F., Scremin, O. U., Treiman, D. M., & Walton, N. Y. (1998). Effects of cholinergic deafferentation and NGF on brain electrical coherence. *Brain Research Bulletin*, *45*(5), 531–541. https://doi.org/10.1016/S0361-9230(97)00446-2

Hotz, I., Deschwanden, P. F., Liem, F., Mérillat, S., Malagurski, B., Kollias, S., & Jäncke, L. (2021). Performance of three freely available methods for extracting white matter hyperintensities: FreeSurfer , UBO Detector, and BIANCA . *Human Brain Mapping*, *January*, 1–20. https://doi.org/10.1002/hbm.25739

Iadecola, C. (2013). The Pathobiology of Vascular Dementia. *Neuron*, *80*(4), 844–866. https://doi.org/10.1016/j.neuron.2013.10.008

Jack, C. R., Wiste, H. J., Weigand, S. D., Therneau, T. M., Lowe, V. J., Knopman, D. S., Gunter, J. L., Senjem, M. L., Jones, D. T., Kantarci, K., Machulda, M. M., Mielke, M. M., Roberts, R. O., Vemuri, P., Reyes, D. A., Petersen, R. C., Jack Jr, C. R., Wiste, H. J., Weigand, S. D., … Petersen, R. C. (2017). Defining imaging biomarker cut points for brain aging and Alzheimer's disease. *Alzheimers. Dement.*, *13*(3), 205–216. https://doi.org/10.1016/j.jalz.2016.08.005

Jang, H., Kwon, H., Yang, J. J., Hong, J., Kim, Y., Kim, K. W., Lee, J. S., Jang, Y. K., Kim, S. T., Lee, K. H., Lee, J. H., Na, D. L., Seo, S. W., Kim, H. J., & Lee, J. M. (2017). Correlations between Gray Matter and White Matter Degeneration in Pure Alzheimer's Disease, Pure Subcortical Vascular Dementia, and Mixed Dementia. *Scientific Reports*, *7*(1), 1–9. https://doi.org/10.1038/s41598-017-10074-x

Jellinger, K. A. (2013). Pathology and pathogenesis of vascular cognitive impairment-a critical update. *Frontiers in Aging Neuroscience*, *5*(APR), 1–19. https://doi.org/10.3389/fnagi.2013.00017

Jenkinson, M., Beckmann, C. F., Behrens, T. E. J., Woolrich, M. W., & Smith, S. M. (2012). FSL. *Neuroimage*, *62*, 782–790. https://doi.org/10.1016/j.neuroimage.2011.09.015

Jiang, S., Yan, C., Qiao, Z., Yao, H., Jiang, S., Qiu, X., Yang, X., Fang, D., Yang, Y., Zhang, L., Wang, L., & Zhang, L. (2017). Mismatch negativity as a potential neurobiological marker of early-stage Alzheimer disease and vascular dementia. *Neuroscience Letters*, *647*, 26–31. https://doi.org/10.1016/j.neulet.2017.03.032

Jokinen, H., Koikkalainen, J., Laakso, H. M., Melkas, S., Nieminen, T., Brander, A., Korvenoja, A., Rueckert, D., Barkhof, F., Scheltens, P., Schmidt, R., Fazekas, F., Madureira, S., Verdelho, A., Wallin, A., Wahlund, L. O., Waldemar, G., Chabriat, H., Hennerici, M., … Erkinjuntti, T. (2020). Global Burden of Small Vessel Disease-Related Brain Changes on MRI Predicts Cognitive and Functional Decline. *Stroke*, *51*(1), 170–178. https://doi.org/10.1161/STROKEAHA.119.026170

Jorgensen, D. R., Shaaban, C. E., Wiley, C. A., Gianaros, P. J., Mettenburg, J., & Rosano, C. (2018). A population neuroscience approach to the study of cerebral small vessel disease in midlife and late life: An invited review. *American Journal of Physiology - Heart and Circulatory*

Physiology, *314*(6), H1117–H1136. https://doi.org/10.1152/ajpheart.00535.2017

Kalaria, R. N. (2018). The pathology and pathophysiology of vascular dementia. *Neuropharmacology*, *134*, 226–239. https://doi.org/10.1016/j.neuropharm.2017.12.030

Klem, G. H., Lüders, H. O., Jasper, H. H., & Elger, C. (1999). The ten-twenty electrode system of the International Federation. The International Federation of Clinical Neurophysiology. *Electroencephalography and Clinical Neurophysiology. Supplement*, *52*, 3–6.

Kloppenborg, R. P., Nederkoorn, P. J., Geerlings, M. I., & Van Den Berg, E. (2014). Presence and progression of white matter hyperintensities and cognition: A meta-analysis. *Neurology*, *82*(23), 2127–2138. https://doi.org/10.1212/WNL.0000000000000505

Kukull, W. A., Larson, E. B., Teri, L., Bowen, J., McCormick, W., & Pfanschmidt, M. L. (1994). The mini-mental state examination score and the clinical diagnosis of dementia. *Journal of Clinical Epidemiology*, *47*(9), 1061–1067. https://doi.org/10.1016/0895-4356(94)90122-8

Lam, S., Lipton, R. B., Harvey, D. J., Zammit, A. R., & Ezzati, A. (2021). White matter hyperintensities and cognition across different Alzheimer's biomarker profiles. *Journal of the American Geriatrics Society*, *69*(7), 1906–1915. https://doi.org/10.1111/jgs.17173

Lawton, M. P., & Brody, E. M. (1969). Assessment of older people: self-maintaining and instrumental activities of daily living. *The Gerontologist*, *9*(3), 179–186.

Leovsky, C., Fabian, C., Naaldijk, Y., Jäger, C., Jang, H. W. A. J. I. N., Böhme, J., Rudolph, L., & Stolzing, A. (2015). Biodistribution of in vitro e derived microglia applied intranasally and intravenously to mice : effects of aging. *Journal of Cytotherapy*, *17*(11), 1617–1626. https://doi.org/10.1016/j.jcyt.2015.07.019

Lim, J. S., Kwon, H. M., & Lee, Y. S. (2020). Effect of cholinergic pathway disruption on cortical and subcortical volumes in subcortical vascular cognitive impairment. *European Journal of Neurology*, *27*(1), 210–212. https://doi.org/10.1111/ene.14073

Lobo, A., Ezquerra, J., Gómez Burgada, F., Sala, J. M., & Seva Díaz, A. (1979). El miniexamen, cognoscitivo (un "test" sencillo, práctico, para detectar alteraciones intelectuales en pacientes médicos). *Actas Luso-Espanolas de Neurologia Psiquiatria y Ciencias Afines*, *7*(3), 189–202. http://www.ncbi.nlm.nih.gov/pubmed/474231

Lopes da Silva, F. (2013). EEG and MEG: Relevance to neuroscience. *Neuron*, *80*(5), 1112–1128. https://doi.org/10.1016/j.neuron.2013.10.017

López-Sanz, D, Bruña, R., Garcés, P., Camara, C., Serrano, N., Rodríguez-Rojo, I. C., Delgado, M. L., Montenegro, M., López-Higes, R., Yus, M., & Maestú, F. (2016). Alpha band disruption in the AD-continuum starts in the Subjective Cognitive Decline stage: a MEG study. *Scientific Reports*, *6*, 37685. https://doi.org/10.1038/srep37685

López-Sanz, David, Bruña, R., de Frutos-Lucas, J., & Maestú, F. (2019). Magnetoencephalography applied to the study of Alzheimer's disease. *Progress in Molecular Biology and Translational Science*, *165*, 25–61. https://doi.org/10.1016/bs.pmbts.2019.04.007

López-Sanz, David, Bruña, R., Garcés, P., Martín-Buro, M. C., Walter, S., Delgado, M. L., Montenegro, M., López Higes, R., Marcos, A., & Maestú, F. (2017). Functional Connectivity Disruption in Subjective Cognitive Decline and Mild Cognitive Impairment: A Common Pattern of Alterations. *Frontiers in Aging Neuroscience*, *9*, 109. https://doi.org/10.3389/fnagi.2017.00109

López-Sanz, David, Serrano, N., & Maestú, F. (2018). The Role of Magnetoencephalography in the Early Stages of Alzheimer's Disease. *Frontiers in Neuroscience*, *12*, 572. https://doi.org/10.3389/fnins.2018.00572

López, María Eugenía, Bruña, R., Aurtenetxe, S., Pineda-Pardo, J. A. Á. A., Marcos, A., Arrazola, J., Reinoso, A. I., Montejo, P., Bajo, R., Maestú, F., Lopez, M. E., Bruna, R., Aurtenetxe, S., Pineda-Pardo, J. A. Á. A., Marcos, A., Arrazola, J., Reinoso, A. I., Montejo, P., Bajo, R., … Maestú, F. (2014). Alpha-Band Hypersynchronization in Progressive Mild Cognitive Impairment: A Magnetoencephalography Study. *Journal of Neuroscience*, *34*(44), 14551–14559. https://doi.org/10.1523/JNEUROSCI.0964-14.2014

López, María Eugenia, Turrero, A., Cuesta, P., Rodríguez-Rojo, I. C., Barabash, A., Marcos, A., Maestú, F., & Fernández, A. (2020). A multivariate model of time to conversion from mild cognitive impairment to Alzheimer's disease. *Geroscience*, *42*(6), 1715–1732. https://doi.org/10.1007/s11357-020-00260-7

Lourbopoulos, A., Ertürk, A., & Hellal, F. (2015). *Microglia in action : how aging and injury can change the brain ' s guardians*. *9*(February), 1–8. https://doi.org/10.3389/fncel.2015.00054

Lundgaard, I., Li, B., Xie, L., Kang, H., Sanggaard, S., Haswell, J. D. R., Sun, W., Goldman, S., Blekot, S., Nielsen, M., Takano, T., Deane, R., & Nedergaard, M. (2015). Direct neuronal glucose uptake heralds activity-dependent increases in cerebral metabolism. *Nature Communications*, *6*. https://doi.org/10.1038/ncomms7807

Maestú, F., Peña, J.-M., Garcés, P., González, S., Bajo, R., Bagic, A., Cuesta, P., Funke, M., Mäkelä, J. P., Menasalvas, E., Nakamura, A., Parkkonen, L., López, M. E., Del Pozo, F., Sudre, G., Zamrini, E., Pekkonen, E., Henson, R. N., & Becker, J. T. (2015). A multicenter study of the early detection of synaptic dysfunction in Mild Cognitive Impairment using Magnetoencephalography-derived functional connectivity. *NeuroImage. Clinical*, *9*, 103–109. https://doi.org/10.1016/j.nicl.2015.07.011

Maestú, F., Pereda, E., & Del-Pozo, F. (2015). *Conectividad funcional y anatómica en el cerebro humano*. Elsevier.

Mandal, P. K., Banerjee, A., Tripathi, M., & Sharma, A. (2018). A comprehensive review of magnetoencephalography (MEG) studies for brain functionality in healthy aging and Alzheimer's disease (AD). *Frontiers in Computational Neuroscience*, *12*(August). https://doi.org/10.3389/fncom.2018.00060

Maris, E., & Oostenveld, R. (2007). Nonparametric statistical testing of EEG- and MEG-data. *J. Neurosci. Methods*, *164*(1), 177–190. https://doi.org/10.1016/j.jneumeth.2007.03.024

Matar, E., Shine, J. M., Halliday, G. M., & Lewis, S. J. G. (2019). Cognitive fluctuations in Lewy body dementia: towards a pathophysiological framework. *Brain*, *1992*. https://doi.org/10.1093/brain/awz311

Mattson, M. P., & Magnus, T. (2006). *Ageing and neuronal vulnerability*. *7*(April). https://doi.org/10.1038/nrn1886

McKhann, G. M., Knopman, D. S., Chertkow, H., Hyman, B. T., Jack, C. R., Kawas, C. H., Klunk, W. E., Koroshetz, W. J., Manly, J. J., Mayeux, R., Mohs, R. C., Morris, J. C., Rossor, M. N., Scheltens, P., Carrillo, M. C., Thies, B., Weintraub, S., & Phelps, C. H. (2011). The diagnosis of dementia due to Alzheimer's disease: Recommendations from the National Institute on Aging-Alzheimer's Association workgroups on diagnostic guidelines for Alzheimer's disease.

Alzheimer's and Dementia, *7*(3), 263–269. https://doi.org/10.1016/j.jalz.2011.03.005

Melazzini, L., Vitali, P., Olivieri, E., Bolchini, M., Zanardo, M., Savoldi, F., Di Leo, G., Griffanti, L., Baselli, G., Sardanelli, F., & Codari, M. (2021). White Matter Hyperintensities Quantification in Healthy Adults: A Systematic Review and Meta-Analysis. *Journal of Magnetic Resonance Imaging*, *53*(6), 1732–1743. https://doi.org/10.1002/jmri.27479

Miller, S. A., & Forrest, J. L. (2001). Enhancing your practice through evidence-based decision making: PICO, learning how to ask good questions. *The Journal of Evidenced-Based Dental Practice*, *1*(2), 136–141. https://doi.org/10.1067/med.2001.118720

Millet, D. (2022). The origins of EEG. *In 7th Annual Meeting of the International Society for the History of the Neurosciences (ISHN).*

Moher, D., Booth, A., & Stewart, L. (2014). How to reduce unnecessary duplication: Use PROSPERO. *BJOG: An International Journal of Obstetrics and Gynaecology*, *121*(7), 784–786. https://doi.org/10.1111/1471-0528.12657

Moher, D., Liberati, A., Tetzlaff, J., Altman, D. ., & Group, T. P. (2010). Preferred reporting items for systematic reviews and meta-analyses: the PRISMA statement. *International Journal of Surgery*, *8*, 336–341. https://doi.org/10.1016/j.ijsu.2010.02.007

Moretti, D. V., Miniussi, C., Frisoni, G., Zanetti, O., Binetti, G., Geroldi, C., Galluzzi, S., & Rossini, P. M. (2007). Vascular damage and EEG markers in subjects with mild cognitive impairment. *Clinical Neurophysiology*, *118*(8), 1866–1876. https://doi.org/10.1016/j.clinph.2007.05.009

Moretti, Davide V., Babiloni, C., Binetti, G., Cassetta, E., Dal Forno, G., Ferreric, F., Ferri, R., Lanuzza, B., Miniussi, C., Nobili, F., Rodriguez, G., Salinari, S., & Rossini, P. M. (2004). Individual analysis of EEG frequency and band power in mild Alzheimer's disease. *Clinical Neurophysiology*, *115*(2), 299–308. https://doi.org/10.1016/S1388-2457(03)00345-6

Mormann, F., Lehnertz, K., David, P., & E. Elger, C. (2000). Mean phase coherence as a measure for phase synchronization and its application to the EEG of epilepsy patients. *Physica D: Nonlinear Phenomena*, *144*(3), 358–369. https://doi.org/10.1016/S0167-2789(00)00087-7

Mortamais, M., Artero, S., & Ritchie, K. (2014). White Matter Hyperintensities as Early and Independent Predictors of Alzheimer's Disease Risk. *Journal of Alzheimer's Disease*, *42*, S393–S400. https://doi.org/10.3233/JAD-141473

Nakamura, A., Cuesta, P., Fernández, A., Arahata, Y., Iwata, K., Kuratsubo, I., Bundo, M., Hattori, H., Sakurai, T., Fukuda, K., Washimi, Y., Endo, H., Takeda, A., DIers, K., Bajo, R., Maestú, F., Ito, K., & Kato, T. (2018). Electromagnetic signatures of the preclinical and prodromal stages of Alzheimer's disease. *Brain*, *141*(5), 1470–1485. https://doi.org/10.1093/brain/awy044

Nakamura, A., Cuesta, P., Kato, T., Arahata, Y., Iwata, K., Yamagishi, M., Kuratsubo, I., Kato, K., Bundo, M., Diers, K., Fernández, A., Maestú, F., & Ito, K. (2017). Early functional network alterations in asymptomatic elders at risk for Alzheimer's disease. *Scientific Reports*, *7*(1), 6517. https://doi.org/10.1038/s41598-017-06876-8

Nations, U. (2023). *World Social Report 2023: Leaving no one behind in aging world*. https://doi.org/https://doi.org/10.18356/9789210019682

Neto, E., Allen, E. A., Aurlien, H., Nordby, H., & Eichele, T. (2015). EEG spectral features discriminate between Alzheimer's and vascular dementia. *Frontiers in Neurology*, *6*(FEB), 1–9. https://doi.org/10.3389/fneur.2015.00025

Nicholson, W. T., Vaa, B., Hesse, C., Eisenach, J. H., & Joyner, M. J. (2009). *Aging Is Associated With Reduced Prostacyclin-Mediated Dilation in the Human Forearm*. https://doi.org/10.1161/HYPERTENSIONAHA.108.121483

Nolte, G. (2003). The magnetic lead field theorem in the quasi-static approximation and its use for magnetoencephalography forward calculation in realistic volume conductors. *Phys. Med. Biol.*, *48*(22), 3637–3652. https://doi.org/10.1088/0031-9155/48/22/002

Norrving, B. (2008). Lacunar infarcts: No black holes in the brain are benign. *Practical Neurology*, *8*(4), 222–228. https://doi.org/10.1136/jnnp.2008.153601

O'Brien, J. T., Erkinjuntti, T., Reisberg, B., Roman, G., Sawada, T., Pantoni, L., Bowler, J. V., Ballard, C., DeCarli, C., Gorelick, P. B., Rockwood, K., Burns, A., Gauthier, S., & DeKosky, S. T. (2003). Vascular cognitive impairment. *Lancet Neurology*, *2*(2), 89–98. https://doi.org/10.1016/S1474-4422(03)00305-3

O'Brien, J. T., & Thomas, A. (2015). Vascular dementia. *The Lancet*, *386*(10004), 1698–1706. https://doi.org/10.1016/S0140-6736(15)00463-8

Olde Dubbelink, K. T. E., Hillebrand, A., Stoffers, D., Deijen, J. B., Twisk, J. W. R., Stam, C. J., & Berendse, H. W. (2014). Disrupted brain network topology in Parkinson's disease: A longitudinal magnetoencephalography study. *Brain*, *137*(1), 197–207. https://doi.org/10.1093/brain/awt316

Oostenveld, R., Fries, P., Maris, E., & Schoffelen, J.-M. (2011). FieldTrip: Open source software for advanced analysis of MEG, EEG, and invasive electrophysiological data. *Computational Intelligence and Neuroscience*, *2011*, 156869. https://doi.org/10.1155/2011/156869

Oschwald, J., Guye, S., Liem, F., Rast, P., Willis, S., Röcke, C., Jäncke, L., Martin, M., & Mérillat, S. (2019). Brain structure and cognitive ability in healthy aging: A review on longitudinal correlated change. *Reviews in the Neurosciences*, *31*(1), 1–57. https://doi.org/10.1515/revneuro-2018-0096

Pantoni, L. (2010). Cerebral small vessel disease: from pathogenesis and clinical characteristics to therapeutic challenges. *The Lancet Neurology*, *9*(7), 689–701. https://doi.org/10.1016/S1474-4422(10)70104-6

Parks, C. M., Losif, A.-M., Farias, S., Reed, B., Mungas, D., & Decarli, C. (2011). Executive function mediates effects of white matter hyperintensities on Episodic Memory. *Neuropsychologia*, *49*(10), 2817–2824. https://doi.org/10.1016/j.neuropsychologia.2011.06.003. Executive

Pendlebury, S. T., & Rothwell, P. M. (2009). Prevalence, incidence, and factors associated with pre-stroke and post-stroke dementia: a systematic review and meta-analysis. *The Lancet Neurology*, *8*(11), 1006–1018. https://doi.org/10.1016/S1474-4422(09)70236-4

Pereda, E., Quiroga, R. Q., & Bhattacharya, J. (2005). Nonlinear multivariate analysis of neurophysiological signals. *Progress in Neurobiology*, *77*(1–2), 1–37. https://doi.org/10.1016/j.pneurobio.2005.10.003

Peters, A. (2009). *The effects of normal aging on myelinated nerve fi bers in monkey central nervous system*. *3*(July), 1–10. https://doi.org/10.3389/neuro.05.011.2009

Petersen, R. C. (2004). Mild cognitive impairment as a diagnostic entity. *Journal of Internal Medicine*, *256*(3), 183–194. https://doi.org/10.1111/j.1365-2796.2004.01388.x

Pfeffer, R. I., Kurosaki, T. T., Harrah C. H., J., Chance, J. M., & Filos, S. (1982). Measurement of Functional Activities in Older Adults in the Community1. *Journal of Gerontology*, *37*(3), 323–329. https://doi.org/10.1093/geronj/37.3.323

Porcu, M., Operamolla, A., Scapin, E., Garofalo, P., Destro, F., Caneglias, A., Suri, J. S., Falini, A., Defazio, G., Marrosu, F., & Saba, L. (2020). Effects of White Matter Hyperintensities on Brain Connectivity and Hippocampal Volume in Healthy Subjects According to Their Localization. *Brain Connectivity*, *10*(8), 436–447. https://doi.org/10.1089/brain.2020.0774

Prins, N. D., & Scheltens, P. (2015). White matter hyperintensities, cognitive impairment and dementia: An update. *Nature Reviews Neurology*, *11*(3), 157–165. https://doi.org/10.1038/nrneurol.2015.10

Prisby, R. D., Wilkerson, M. K., Sokoya, E. M., Bryan, R. M., Wilson, E., Delp, M. D., Rhonda, D., Wilkerson, M. K., Sokoya, E. M., Bryan, R. M., Wilson, E., & Delp, M. D. (2006). *Regulation of the Cerebral Circulation Endothelium-dependent vasodilation of cerebral arteries is altered with simulated microgravity through nitric oxide synthase and EDHF mechanisms*. *26506*, 348–353. https://doi.org/10.1152/japplphysiol.00941.2005.

Pusil, S., López, M. E., Cuesta, P., Bruña, R., Pereda, E., & Maestú, F. (2019). Hypersynchronization in mild cognitive impairment: the "X" model. *Brain*, *142*(12), 3936–3950.

Quandt, F., Fischer, F., Schröder, J., Heinze, M., Lettow, I., Frey, B. M., Kessner, S. S., Schulz, M., Higgen, F. L., Cheng, B., Gerloff, C., & Thomalla, G. (2020). Higher white matter hyperintensity lesion load is associated with reduced long-range functional connectivity. *Brain Communications*, *2*(2), 1–12. https://doi.org/10.1093/braincomms/fcaa111

Ramírez-Toraño, F., Bruña, R., de Frutos-Lucas, J., Rodríguez-Rojo, I. C., Marcos de Pedro, S., Delgado-Losada, M. L., Gómez-Ruiz, N., Barabash, A., Marcos, A., López Higes, R., & Maestú, F. (2020). Functional Connectivity Hypersynchronization in Relatives of Alzheimer's Disease Patients: An Early E/I Balance Dysfunction? *Cerebral Cortex*, *31*(2), 1–10. https://doi.org/10.1093/cercor/bhaa286

Regenhardt, R. W., Das, A. S., Lo, E. H., & Caplan, L. R. (2018). Advances in Lacunar Stroke Pathophysiology: A Review. *JAMA Neurology*, *75*(10), 1273–1281. https://doi.org/10.1001/jamaneurol.2018.1073

Regier, D. A., Kuhl, E. A., & Kupfer, D. J. (2013). The DSM-5: Classification and criteria changes. *World Psychiatry*, *12*(2), 92–98. https://doi.org/10.1002/wps.20050

Reisberg, B., Ferris, S. H., de Leon, M. J., & Crook, T. (1982). The Global Deterioration Scale for assessment of primary degenerative dementia. *The American Journal of Psychiatry*, *139*(9), 1136–1139. https://doi.org/10.1176/ajp.139.9.1136

Reitan, R. M. (1958). Validity of the Trail Making Test as an Indicator of Organic Brain Damage. *Perceptual and Motor Skills*, *8*(3), 271–276. https://doi.org/10.2466/pms.1958.8.3.271

Rizzi, L., Rosset, I., & Roriz-Cruz, M. (2014). Global epidemiology of dementia: Alzheimer's and vascular types. *BioMed Research International*, *2014*(Figure 1). https://doi.org/10.1155/2014/908915

Rockwood, K. (2002). Vascular cognitive impairment and vascular dementia. *Journal of the Neurological Sciences*, *203–204*, 23–27. https://doi.org/10.1016/S0022-510X(02)00255-1

Rojas, S., Brugulat-Serrat, A., Bargalló, N., Minguillón, C., Tucholka, A., Falcon, C., Carvalho, A.,

Morán, S., Esteller, M., Gramunt, N., Fauria, K., Camí, J., Molinuevo, J. L., & Gispert, J. D. (2018). Higher prevalence of cerebral white matter hyperintensities in homozygous APOE-ε4 allele carriers aged 45–75: Results from the ALFA study. *Journal of Cerebral Blood Flow and Metabolism*, *38*(2), 250–261. https://doi.org/10.1177/0271678X17707397

Román, G. C., Tatemichi, T. K., Erkinjuntti, T., Cummings, J. L., Masdeu, J. C., Garcia, J. H., Amaducci, L., Orgogozo, J. M., Brun, A., Hofman, A., Moody, D. M., O'Brien, M. D., Yamaguchi, T., Grafman, J., Drayer, B. P., Bennett, D. A., Fisher, M., Ogata, J., Kokmen, E., … Scheinberg, P. (1993). Vascular dementia: Diagnostic criteria for research studies: Report of the ninds-airen international workshop*. *Neurology*, *43*(2), 250–260. https://doi.org/10.1212/wnl.43.2.250

Roth, G. A., Mensah, G. A., Johnson, C. O., Addolorato, G., Ammirati, E., Baddour, L. M., Barengo, N. C., Beaton, A., Benjamin, E. J., Benziger, C. P., Bonny, A., Brauer, M., Brodmann, M., Cahill, T. J., Carapetis, J. R., Catapano, A. L., Chugh, S., Cooper, L. T., Coresh, J., … Fuster, V. (2020). Global Burden of Cardiovascular Diseases and Risk Factors, 1990-2019: Update From the GBD 2019 Study. *Journal of the American College of Cardiology*, *76*(25), 2982–3021. https://doi.org/10.1016/j.jacc.2020.11.010

Sachdev, P., Kalaria, R., O'Brien, J., Skoog, I., Alladi, S., Black, S. E., Blacker, D., Blazer, D. G., Chen, C., Chui, H., Ganguli, M., Jellinger, K., Jeste, D. V., Pasquier, F., Paulsen, J., Prins, N., Rockwood, K., Roman, G., & Scheltens, P. (2014). Diagnostic criteria for vascular cognitive disorders: A VASCOG statement. *Alzheimer Disease and Associated Disorders*, *28*(3), 206–218. https://doi.org/10.1097/WAD.0000000000000034

Santos, C. Y., Snyder, P. J., Wu, W. C., Zhang, M., Echeverria, A., & Alber, J. (2017). Pathophysiologic relationship between Alzheimer's disease, cerebrovascular disease, and cardiovascular risk: A review and synthesis. *Alzheimer's and Dementia: Diagnosis, Assessment and Disease Monitoring*, *7*, 69–87. https://doi.org/10.1016/j.dadm.2017.01.005

Sarbu, N., Shih, R. Y., Jones, R. V., Horkayne-Szakaly, I., Oleaga, L., & Smirniotopoulos, J. G. (2016). White matter diseases with radiologic-pathologic correlation. *Radiographics*, *36*(5), 1426–1447. https://doi.org/10.1148/rg.2016160031

Sarter, M., & Bruno, J. P. (1999). Cortical cholinergic inputs mediating arousal, attentional processing and dreaming: Differential afferent regulation of the basal forebrain by telencephalic and brainstem afferents. *Neuroscience*, *95*(4), 933–952. https://doi.org/10.1016/S0306-4522(99)00487-X

Sarter, Martin, & Bruno, J. P. (1997). Cognitive functions of cortical acetylcholine: Toward a unifying hypothesis. *Brain Research Reviews*, *23*(1–2), 28–46. https://doi.org/10.1016/S0165-0173(96)00009-4

Sarter, Martin, & Bruno, J. P. (2002). The neglected constituent of the basal forebrain corticopetal projection system: GABAergic projections. *European Journal of Neuroscience*, *15*(12), 1867–1873. https://doi.org/10.1046/j.1460-9568.2002.02004.x

Sarter, Martin, & Bruno, J. P. (2004). Developmental origins of the age-related decline in cortical cholinergic function and associated cognitive abilities. *Neurobiology of Aging*, *25*(9), 1127–1139. https://doi.org/10.1016/j.neurobiolaging.2003.11.011

Schacter, D. L. (1977). EEG theta waves and psychological phenomena: a review and analysis. *Biological Psychology*, *5*(1), 47–82.

Scheltens, P., Leys, D., Barkhof, F., Huglo, D., Weinstein, H. C., Vermersch, P., Kuiper, M., Steinling, M., Wolters, E. C., & Valk, J. (1992). Atrophy of medial temporal lobes on MRI in "probable" Alzheimer's disease and normal ageing: diagnostic value and neuropsychological correlates. *Journal of Neurology, Neurosurgery, and Psychiatry*, *55*, 967–972. https://doi.org/10.1136/jnnp.55.10.967

Schmidt, P. (2016). *Bayesian inference for structured additive regression models for large-scale problems with applications to medical imaging. Dissertation, LMU München: Faculty of Mathematics, Computer Science and Statistics*. *November*, Chapter 6.1.

Schmidt, P., Gaser, C., Arsic, M., Buck, D., Förschler, A., Berthele, A., Hoshi, M., Ilg, R., Schmid, V. J., Zimmer, C., Hemmer, B., & Mühlau, M. (2012). An automated tool for detection of FLAIR-hyperintense white-matter lesions in Multiple Sclerosis. *NeuroImage*, *59*(4), 3774–3783. https://doi.org/10.1016/j.neuroimage.2011.11.032

Schneider, J. A., Arvanitakis, Z., Bang, W., & Bennett, D. A. (2007). Mixed brain pathologies account for most dementia cases in community-dwelling older persons. *Neurology*, *69*(24), 2197–2204. https://doi.org/10.1212/01.wnl.0000271090.28148.24

Schreiber, S., Bueche, C. Z., Garz, C., & Braun, H. (2013). Blood brain barrier breakdown as the starting point of cerebral small vessel disease? - New insights from a rat model. *Experimental and Translational Stroke Medicine*, *5*(1), 1–8. https://doi.org/10.1186/2040-7378-5-4

Schreiter Gasser, U., Rousson, V., Hentschel, F., Sattel, H., & Gasser, T. (2008). Alzheimer disease versus mixed dementias: An EEG perspective. *Clinical Neurophysiology*, *119*(10), 2255–2259. https://doi.org/10.1016/j.clinph.2008.07.216

Schwartz, D. L., Boespflug, E. L., Lahna, D., Pollock, J., Roese, N. E., & Silbert, L. C. (2019). Autoidentification of Perivascular Spaces In White Matter Using Clinical Field Strength T1 and FLAIR MR Imaging. *NeuroImage*, *15*(202). https://doi.org/10.1016/j.neuroimage.2019.116126.

Seals, D. R., Jablonski, K. L., & Donato, A. J. (2011). *Aging and vascular endothelial function in humans*. *375*, 357–375. https://doi.org/10.1042/CS20100476

Seiler, S., Fletcher, E., Hassan-Ali, K., Weinstein, M., Beiser, A., Himali, J., Satizabal, C. L., Seshardi, S., DeCarli, C., & Maillard, P. (2019). Cerebral tract integrity relates to white matter hyperintensities, cortex volume, and cognition. *Neurobiology of Aging*, *17*, 14–22. https://doi.org/10.1016/j.neurobiolaging.2018.08.005. Cerebral tract integrity relates to white matter hyperintensities, cortex volume, and cognition Stephan Seilera,b,c, Evan Fletchera,b, Kinsy Hassan-Alia,b, Michelle Weinsteina,b, Alexa Beiserd,e,f, Jayandra J. Himalid,e,f, Claudia L. Satizabald,e, Sudha Seshadrid,e, Charles DeCarlia,b, and Pauline Maillarda,b aDepartment of Neurology and Center for Neurosciences, University of California at Davis, 1544 Newton Court, Davis, CA 95616, USA bImaging of Dementia

Sgarbieri, V. C., & Pacheco, M. T. B. (2017). Healthy human aging: intrinsic and environmental factors. *Brazilian Journal of Food Technology*, *20*(0). https://doi.org/10.1590/1981-6723.00717

Sheorajpanday, R. V. A., Marien, P., Weeren, A. J. T. M., Nagels, G., Saerens, J., Van Putten, M. J. A. M., & De Deyn, P. P. (2013a). EEG in silent small vessel disease: sLORETA mapping reveals cortical sources of vascular cognitive impairment no dementia in the default mode network. *Journal of Clinical Neurophysiology*, *30*(2), 178–187. https://doi.org/10.1097/WNP.0b013e3182767d15

Sheorajpanday, R. V. A., Marien, P., Weeren, A. J. T. M., Nagels, G., Saerens, J., Van Putten, M. J. A. M., & De Deyn, P. P. (2013b). EEG in silent small vessel disease: sLORETA mapping reveals cortical sources of vascular cognitive impairment no dementia in the default mode network. *Journal of Clinical Neurophysiology*, *30*(2), 178–187. https://doi.org/10.1097/WNP.0b013e3182767d15

Shin, J., Choi, S., Lee, J. E., Lee, H. S., Sohn, Y. H., & Lee, P. H. (2012). Subcortical white matter hyperintensities within the cholinergic pathways of Parkinson's disease patients according to cognitive status. *Journal of Neurology, Neurosurgery and Psychiatry*, *83*(3), 315–321. https://doi.org/10.1136/jnnp-2011-300872

Skrobot, O. A., Black, S. E., Chen, C., DeCarli, C., Erkinjuntti, T., Ford, G. A., Kalaria, R. N., O'Brien, J., Pantoni, L., Pasquier, F., Roman, G. C., Wallin, A., Sachdev, P., Skoog, I., Taragano, F. E., Kril, J., Cavalieri, M., Jellinger, K. A., Kovacs, G. G., … Kehoe, P. G. (2018). Progress toward standardized diagnosis of vascular cognitive impairment: Guidelines from the Vascular Impairment of Cognition Classification Consensus Study. *Alzheimer's and Dementia*, *14*(3), 280–292. https://doi.org/10.1016/j.jalz.2017.09.007

Skrobot, O. A., Love, S., Kehoe, P. G., O'Brien, J., Black, S., Chen, C., DeCarli, C., Erkinjuntti, T., Ford, G. A., Kalaria, R. N., Pantoni, L., Pasquier, F., Roman, G. C., Wallin, A., Taragano, F. E., Kril, J., Cavalieri, M., Jellinger, K. A., Kovacs, G. G., … Zarow, C. (2017). The Vascular Impairment of Cognition Classification Consensus Study. *Alzheimer's and Dementia*, *13*(6), 624–633. https://doi.org/10.1016/j.jalz.2016.10.007

Smith, C. D., Johnson, E. S., Van Eldik, L. J., Jicha, G. A., Schmitt, F. A., Nelson, P. T., Kryscio, R. J., Murphy, R. R., & Wellnitz, C. V. (2016). Peripheral (deep) but not periventricular MRI white matter hyperintensities are increased in clinical vascular dementia compared to Alzheimer's disease. *Brain and Behavior*, *6*(3), 1–11. https://doi.org/10.1002/brb3.438

Smith, S. M. (2002). Fast robust automated brain extraction. *Human Brain Mapping*, *17*(3), 143–155. https://doi.org/10.1002/hbm.10062

Sperling, R. A., Aisen, P. S., Beckett, L. A., Bennett, D. A., Craft, S., Fagan, A. M., Iwatsubo, T., Jack, C. R., Kaye, J., Montine, T. J., Park, D. C., Reiman, E. M., Rowe, C. C., Siemers, E., Stern, Y., Yaffe, K., Carrillo, M. C., Thies, B., Morrison-Bogorad, M., … Phelps, C. H. (2011). Toward defining the preclinical stages of Alzheimer's disease: Recommendations from the National Institute on Aging-Alzheimer's Association workgroups on diagnostic guidelines for Alzheimer's disease. *Alzheimer's and Dementia*, *7*(3), 280–292. https://doi.org/10.1016/j.jalz.2011.03.003

Sperling, R. a, Rentz, D. M., Johnson, K. a, Karlawish, J., Donohue, M., Salmon, D. P., & Aisen, P. (2014). The A4 study: stopping AD before symptoms begin? *Science Translational Medicine*, *6*(228), 228fs13. https://doi.org/10.1126/scitranslmed.3007941

Stam, C. J. (2010). Use of magnetoencephalography (MEG) to study functional brain networks in neurodegenerative disorders. *Journal of the Neurological Sciences*, *289*(1–2), 128–134. https://doi.org/10.1016/j.jns.2009.08.028

Stewart, L., Moher, D., & Shekelle, P. (2012). Why prospective registration of systematic reviews makes sense. *Systematic Reviews*, *1*(1), 7–10. https://doi.org/10.1186/2046-4053-1-7

Stoffers, D., Bosboom, J. L. W., Deijen, J. B., Wolters, E. C., Stam, C. J., & Berendse, H. W. (2008). Increased cortico-cortical functional connectivity in early-stage Parkinson's disease: An MEG study. *NeuroImage*, *41*(2), 212–222. https://doi.org/10.1016/j.neuroimage.2008.02.027

Sungura, R., Onyambu, C., Mpolya, E., Sauli, E., & Vianney, J. M. (2021). The extended scope of neuroimaging and prospects in brain atrophy mitigation: A systematic review. *Interdisciplinary Neurosurgery: Advanced Techniques and Case Management*, *23*(August 2020), 100875. https://doi.org/10.1016/j.inat.2020.100875

Tak, S., Yoon, S. J., Jang, J., Yoo, K., Jeong, Y., & Ye, J. C. (2011). Quantitative analysis of hemodynamic and metabolic changes in subcortical vascular dementia using simultaneous near-infrared spectroscopy and fMRI measurements. *NeuroImage*, *55*(1), 176–184. https://doi.org/10.1016/j.neuroimage.2010.11.046

Talairach, J., & Tournoux, P. (1988). *Co-planar stereotaxic atlas of the human brain: 3-Dimensional proportional system: An approach to cerebral imaging.* Thieme Medical Publishers.

Taulu, S., & Simola, J. (2006). Spatiotemporal signal space separation method for rejecting nearby interference in MEG measurements. *Physics in Medicine and Biology*, *51*(7), 1759–1768. https://doi.org/10.1088/0031-9155/51/7/008

Thal, D. R., Grinberg, L. T., & Attems, J. (2012). Vascular dementia: Different forms of vessel disorders contribute to the development of dementia in the elderly brain. *Experimental Gerontology*, *47*(11), 816–824. https://doi.org/10.1016/j.exger.2012.05.023

Thuwal, K., Banerjee, A., & Roy, D. (2021). Aperiodic and Periodic Components of Ongoing Oscillatory Brain Dynamics Link Distinct Functional Aspects of Cognition across Adult Lifespan. *ENeuro*, *8*(5). https://doi.org/10.1523/ENEURO.0224-21.2021

Torres-Simon, L., Cuesta, P., del Cerro-Leon, A., Chino, B., Orozco, L. H., Marsh, E. B., Gil, P., & Maestu, F. (2023). The effects of white matter hyperintensities on MEG power spectra in population with mild cognitive impairment. *Frontiers in Human Neuroscience*, *17*(February), 1–11. https://doi.org/10.3389/fnhum.2023.1068216

Torres-Simón, L., Doval, S., Nebreda, A., Llinas, S. J., Marsh, E. B., & Maestú, F. (2022). Understanding brain function in vascular cognitive impairment and dementia with EEG and MEG: A systematic review. *NeuroImage: Clinical*, *35*(January), 103040. https://doi.org/10.1016/j.nicl.2022.103040

Tsuno, N., Shigeta, M., Hyokid, K., Faber, P. L., & Lehmann, D. (2004). Fluctuations of source locations of EEG activity during transition from alertness to sleep in Alzheimer's disease and vascular dementia. *Neuropsychobiology*, *50*(3), 267–272. https://doi.org/10.1159/000079982

Tzourio-Mazoyer, N., Landeau, B., Papathanassiou, D., Crivello, F., Etard, O., Delcroix, N., Mazoyer, B., & Joliot, M. (2002). Automated anatomical labeling of activations in SPM using a macroscopic anatomical parcellation of the MNI MRI single-subject brain. *NeuroImage*, *15*(1), 273–289. https://doi.org/10.1006/nimg.2001.0978

United Nations. (2019). *Revision of world population prospects*. United Nations. https://population.un.org/wpp/

Valdes-Hernandez, M. del C., Piper, R. J., Wang, X., Deary, I. J., & Wardlaw, J. M. (2013). Towards the automatic computational assessment of enlarged perivascular spaces on brain magnetic resonance images: A systematic review. *Journal of Magnetic Resonance Imaging*, *38*(4), 774–785. https://doi.org/10.1002/jmri.24047

Van Den Berg, E., Geerlings, M. I., Biessels, G. J., Nederkoorn, P. J., & Kloppenborg, R. P. (2018). White Matter Hyperintensities and Cognition in Mild Cognitive Impairment and Alzheimer's

Disease: A Domain-Specific Meta-Analysis. *Journal of Alzheimer's Disease*, *63*(2), 515–527. https://doi.org/10.3233/JAD-170573

van Drimmelen-Krabbe, J. J. (1995). The neurological adaptation of ICD-10 (ICD-10 NA). *Arquivos de Neuro-Psiquiatria*, *53*(2), 342–343. https://doi.org/10.1590/s0004-282x1995000200029

Van Leijsen, E. M. C., Van Uden, I. W. M., Ghafoorian, M., Bergkamp, M. I., Lohner, V., Kooijmans, E. C. M., Van Der Holst, H. M., Tuladhar, A. M., Norris, D. G., Van DIjk, E. J., Rutten-Jacobs, L. C. A., Platel, B., Klijn, C. J. M., & De Leeuw, F. E. (2017). Nonlinear temporal dynamics of cerebral small vessel disease. *Neurology*, *89*(15), 1569–1577. https://doi.org/10.1212/WNL.0000000000004490

van Straaten, E. C. W., de Haan, W., de Waal, H., Scheltens, P., van der Flier, W. M., Barkhof, F., Koene, T., & Stam, C. J. (2012). Disturbed oscillatory brain dynamics in subcortical ischemic vascular dementia. *BMC Neuroscience*, *13*(1). https://doi.org/10.1186/1471-2202-13-85

van Straaten, E. C. W., den Haan, J., de Waal, H., van der Flier, W. M., Barkhof, F., Prins, N. D., & Stam, C. J. (2015). Disturbed phase relations in white matter hyperintensity based vascular dementia: An EEG directed connectivity study. *Clinical Neurophysiology*, *126*(3), 497–504. https://doi.org/10.1016/j.clinph.2014.05.018

Van Veen, B. D., van Drongelen, W., Yuchtman, M., Suzuki, A., Veen, B. D. Van, Drongelen, W. Van, Yuchtman, M., & Suzuki, A. (1997). Localization of brain electrical activity via linearly constrained minimum variance spatial filtering. *IEEE Trans. Biomed. Eng.*, *44*(9), 867–880. https://doi.org/10.1109/10.623056

Varela, F., Lachaux, J. P., Rodriguez, E., & Martinerie, J. (2001). The brainweb: phase synchronization and large-scale integration. *Nature Reviews. Neuroscience*, *2*(4), 229–239. https://doi.org/10.1038/35067550

Veldsman, M., Tai, X. Y., Nichols, T., Smith, S., Peixoto, J., Manohar, S., & Husain, M. (2020). Cerebrovascular risk factors impact frontoparietal network integrity and executive function in healthy ageing. *Nature Communications*, *11*(1), 1–10. https://doi.org/10.1038/s41467-020-18201-5

Venkat, P., Chopp, M., Zacharek, A., Cui, C., Zhang, L., Li, Q., Lu, M., Zhang, T., Liu, A., & Chen, J. (2017). White matter damage and glymphatic dysfunction in a model of vascular dementia in rats with no prior vascular pathologies. *Neurobiology of Aging*, *50*, 96–106. https://doi.org/10.1016/j.neurobiolaging.2016.11.002

Verdejo-Román, J., Björnholm, L., Muetzel, R. L., Torres-Espínola, F. J., Lieslehto, J., Jaddoe, V., Campos, D., Veijola, J., White, T., Catena, A., Nikkinen, J., Kiviniemi, V., Järvelin, M.-R., Tiemeier, H., Campoy, C., Sebert, S., & El Marroun, H. (2018). Maternal prepregnancy body mass index and offspring white matter microstructure : results from three birth cohorts. *International Journal of Obesity*. https://doi.org/10.1038/s41366-018-0268-x

Veritas Health Innovation. (n.d.). *Covidence systematic review software*. www.covidence.org

Vlassenko, A. G., Benzinger, T. L., & Morris, J. C. (2012). PET Amyloid-Beta Imaging in Preclinical Alzheimer's Disease Andrei. *Biochimica et Biophysica Acta*, *1822*(3), 370–379. https://doi.org/10.1016/j.bbadis.2011.11.005.

Wahlund, L. O., Barkhof, F., Fazekas, F., Bronge, L., Augustin, M., Sjögren, M., Wallin, A., Ader, H., Leys, D., Pantoni, L., Pasquier, F., Erkinjuntti, T., & Scheltens, P. (2001). A new rating scale for age-related white matter changes applicable to MRI and CT. *Stroke*, *32*(6), 1318–1322.

https://doi.org/10.1161/01.STR.32.6.1318

Wallin, A., Sjögren, M., Blennow, K., & Davidsson, P. (2003). Decreased cerebrospinal fluid acetylcholinesterase in patients with subcortical ischemic vascular dementia. *Dementia and Geriatric Cognitive Disorders*, *16*(4), 200–207. https://doi.org/10.1159/000072803

Wang, C., Xu, J., Lou, W., & Zhao, S. (2014). Dynamic information flow analysis in Vascular Dementia patients during the performance of a visual oddball task. *Neuroscience Letters*, *580*, 108–113. https://doi.org/10.1016/j.neulet.2014.07.056

Wang, C., Xu, J., Zhao, S., & Lou, W. (2016). Graph theoretical analysis of EEG effective connectivity in vascular dementia patients during a visual oddball task. *Clinical Neurophysiology*, *127*(1), 324–334. https://doi.org/10.1016/j.clinph.2015.04.063

Wang, J., Zhang, H. Y., & Tang, X. C. (2009). Cholinergic deficiency involved in vascular dementia: Possible mechanism and strategy of treatment. *Acta Pharmacologica Sinica*, *30*(7), 879–888. https://doi.org/10.1038/aps.2009.82

Wardlaw, J. M., Smith, C., & Dichgans, M. (2019). Small vessel disease: mechanisms and clinical implications. *The Lancet Neurology*, *18*(7), 684–696. https://doi.org/10.1016/S1474-4422(19)30079-1

Wardlaw, J. M., Smith, E. E., Biessels, G. J., Cordonnier, C., Fazekas, F., Frayne, R., Lindley, R. I., O'Brien, J. T., Barkhof, F., Benavente, O. R., Black, S. E., Brayne, C., Breteler, M., Chabriat, H., DeCarli, C., de Leeuw, F. E., Doubal, F., Duering, M., Fox, N. C., … Dichgans, M. (2013). Neuroimaging standards for research into small vessel disease and its contribution to ageing and neurodegeneration. *The Lancet Neurology*, *12*(8), 822–838. https://doi.org/10.1016/S1474-4422(13)70124-8

Wattjes, M. P. (2011). Structural MRI. *International Psychogeriatrics*, *23*(S2), S13–S24. https://doi.org/10.1017/S1041610211000913

Wechsler, D. (1997). *Wechsler Memory Scale, Ed 3 (manual)*. Psychological Corporation. https://scholar.google.com/scholar?q=%281997%29+Wechsler+Memory+Scale%2C+Ed+3+%28manual%29+%28Psychological+Corporation%2C+San+Antonio%2C+TX%29.

Weiss, E., Kann, M., & Wang, Q. (2023). Neuromodulation of Neural Oscillations in Health and Disease. *Biology*, *12*(3), 371. https://doi.org/10.3390/biology12030371

Wiesman, A. I., Murman, D. L., Losh, R. A., Schantell, M., Christopher-Hayes, N. J., Johnson, H. J., Willett, M. P., Wolfson, S. L., Losh, K. L., Johnson, C. M., May, P. E., & Wilson, T. W. (2022). Spatially resolved neural slowing predicts impairment and amyloid burden in Alzheimer's disease. *Brain*, *2022*, 1–30. https://doi.org/10.1093/brain/awab430

Wirsching, J., Graßmann, S., Eichelmann, F., Harms, L. M., Schenk, M., Barth, E., Berndzen, A., Olalekan, M., Sarmini, L., Zuberer, H., & Aleksandrova, K. (2018). Development and reliability assessment of a new quality appraisal tool for cross-sectional studies using biomarker data (BIOCROSS) 11 Medical and Health Sciences 1117 Public Health and Health Services. *BMC Medical Research Methodology*, *18*(1), 1–8. https://doi.org/10.1186/s12874-018-0583-x

Wu, L., Chen, Y., & Zhou, J. (2014). A promising method to distinguish vascular dementia from alzheimer's disease with standardized low-resolution brain electromagnetic tomography and quantitative EEG. *Clinical EEG and Neuroscience*, *45*(3), 152–157. https://doi.org/10.1177/1550059413496779

Xu, J., Lou, W., Zhao, S., & Wang, C. (2015). Altered Directed Connectivity in Patients with Early Vascular Dementia During a Visual Oddball Task. *Brain Topography*, *28*(2), 330–339. https://doi.org/10.1007/s10548-014-0385-3

Xu, J., Zhao, S., Zhang, H., & Zheng, C. (2011). Decreased delta event-related synchronization in patients with early vascular dementia. *Clinical EEG and Neuroscience*, *42*(1), 53–58. https://doi.org/10.1177/155005941104200111

Yang, D. W., Kim, B. S., Park, J. K., Kim, S. Y., Kim, E. N., & Sohn, H. S. (2002). Analysis of cerebral blood flow of subcortical vascular dementia with single photon emission computed tomography: Adaptation of statistical parametric mapping. *Journal of the Neurological Sciences*, *203–204*, 199–205. https://doi.org/10.1016/S0022-510X(02)00291-5

Yang, T., Sun, Y., Lu, Z., Leak, R. K., & Zhang, F. (2017). The impact of cerebrovascular aging on vascular cognitive impairment and dementia. *Ageing Research Reviews*, *34*, 15–29. https://doi.org/10.1016/j.arr.2016.09.007

Yesavage, J. A., Brink, T. L., Rose, T. L., Lum, O., Huang, V., Adey, M., & Leirer, V. O. (1982). Development and validation of a geriatric depression screening scale: A preliminary report. *Journal of Psychiatric Research*, *17*(1), 37–49. https://doi.org/https://doi.org/10.1016/0022-3956(82)90033-4

Zalesky, A., Fornito, A., & Bullmore, E. T. (2010). Network-based statistic: Identifying differences in brain networks. *NeuroImage*, *53*(4), 1197–1207. https://doi.org/10.1016/j.neuroimage.2010.06.041

Zamrini, E., Maestu, F., Pekkonen, E., Funke, M., Makela, J., Riley, M., Bajo, R., Sudre, G., Fernandez, A., Castellanos, N., Del Pozo, F., Stam, C. J., van Dijk, B. W., Bagic, A., & Becker, J. T. (2011). Magnetoencephalography as a putative biomarker for Alzheimer's disease. *International Journal of Alzheimer's Disease*, *2011*, 280289. https://doi.org/10.4061/2011/280289

Zhu, Y. C., Dufouil, C., Tzourio, C., & Chabriat, H. (2011). Silent brain infarcts: A review of MRI diagnostic criteria. *Stroke*, *42*(4), 1140–1145. https://doi.org/10.1161/STROKEAHA.110.600114

Zimmerman, B., Rypma, B., Gratton, G., & Fabiani, M. (2021). Age-related changes in cerebrovascular health and their effects on neural function and cognition: A comprehensive review. *Psychophysiology*, *58*(7), 1–39. https://doi.org/10.1111/psyp.13796

Zlokovic, B. V. (2008). *Review The Blood-Brain Barrier in Health and Chronic Neurodegenerative Disorders*. *2*, 178–201. https://doi.org/10.1016/j.neuron.2008.01.003

List of author's publications

1. Torres-Simón, L. †, del Cerro, A. †, Yus, M., Bruña, R., Gil-Martinez, L., Dolado, A., Maestú, F., Arrazola-Garcia and Cuesta, P (2023). Comparison between tools for automatic segmentation of white matter hyperintensities of presumed vascular origin in aging: which one, how and why to choose the most suitable for your purpose? medRxiv. https://doi.org/10.1101/2023.03.30.23287946. This manuscript is under review in Human Brain Mapping

2. Torres-Simon, L., Cuesta, P., del Cerro-Leon, A., Chino, B., Orozco, L. H., Marsh, E. B., Gil, P. and Maestu, F. (2023). The effects of cerebrovascular damage on MEG power spectra on population with MCI. Frontiers in Human Neuroscience. //doi.org/10.3389/fnhum.2023.1068216

3. Torres-Simon, L., Doval, S., Nebreda, A., Llinas, S. J., Marsh. E. B., & Maestu, F. (2022) Understanding brain functioning in Vascular Cognitive Impairment and Dementia with EEG and MEG: a systematic review. Neuroimage: Clinical. https://doi.org/10.1016/j.nicl.2022.103040

4. Torres-Simon, L.†, Pusil, S.†, Chino-Vilca, B., López, M.E., Canuet, L., Bilbao, A., Maestu, F., & Paúl, N. (2022). Resting-state beta-band recovery network related to cognitive improvement after stroke. Frontiers in Clinical neurology. //doi.org/10.3389/fneur.2022.838170

5. Chino-Vilca, B.†, Rodriguez-Rojo, I.C.†, Torres-Simon, L., Cuesta, P., Carnes-Vendrell, A., Huerto, R., Tahan, R., & Maestu, F. (2022) Sex related Electrophysiological Signatures Associated with Cerebrospinal Fluid Biomarkers in Mild Cognitive Impairment. Clinical Neurophysiology. https://doi.org/10.1016/j.clinph.2022.08.007

6. Brenda Nadia Chino Vilca; Pablo Cuesta; Javier Pacios; Jaisalmer De Frutos-Lucas; Lucía Torres-Simon; Sandra Doval; Alberto Marcos; Ricardo Bruña; Fernando Maestú (2022) Episodic memory dysfunction and hypersynchrony in brain functional networks in cognitively intact subjects and MCI: a study of 379 individual. GeroScience. //doi.org/10.1007/s11357-022-00656-7

7. Villalobos, D., Torres-Simon, L., Pacios, J., Paul, N., & del Río, D. (2022) A systematic review of normative data for verbal fluency in different languages. Neuropsychology Reviews. //doi.org/10.1007/s11065-022-09549-0